Contents of issue 4 vol. XLV

http://rcin.org.pl

Polish Academy of Sciences

Institute of Fundamental Technological Research

Archives of Mechanics

Archiwum Mechaniki Stosowanej

volume 45 issue 4

Polish Scientific Publishers PWN

Warszawa 1993

http://rcin.org.pl

ARCHIVES OF MECHANICS IS DEVOTED TO
Theory of elasticity and plasticity • Theory of nonclassical continua • Physics of continuous media • Mechanics of discrete media • Nonlinear mechanics • Rheology • Fluid gas-mechanics • Rarefied gases • Thermodynamics

---

FOUNDERS

M.T. HUBER • W. NOWACKI • W. OLSZAK
W. WIERZBICKI

EDITORIAL ADVISORY COMMITTEE

W. SZCZEPIŃSKI — chairman • D.C. DRUCKER,
W. FISZDON • P. GERMAN • W. GUTKOWSKI
G. HERRMANN • T. IWIŃSKI • J. RYCHLEWSKI
I.N. SNEDDON • G. SZEFER • CZ. WOŹNIAK
H. ZORSKI

EDITORIAL COMMITTEE

M. SOKOŁOWSKI — editor • A. BORKOWSKI
W. KOSIŃSKI • M. NOWAK • W.K. NOWACKI
P. PERZYNA • H. PETRYK • J. SOKÓŁ-SUPEL
Z.A. WALENTA • B. WIERZBICKA — secretary
S. ZAHORSKI

Copyright 1993 by Polska Akademia Nauk, Warszawa, Poland
Printed in Poland, Editorial Office: Świętokrzyska 21,
00-049 Warszawa (Poland)

Arkuszy wydawniczych 8,25. Arkuszy drukarskich 7,5
Papier offset. kl. III 70 g. B1. Oddano do składania w kwietniu 1993 r.
Druk ukończono w grudniu 1993 r.
Skład i łamanie: CENTRUM Warszawa, ul. Husarii 12
Druk i oprawa: Drukarnia Braci Grodzickich, Żabieniec ul. Przelotowa 7

---

http://rcin.org.pl

Arch.Mech., 45, 4, pp. 387–403, Warszawa 1993

Propagation of waves in rotating magneto-thermoelastic media

J.N. SHARMA and D. CHAND (HAMIRPUR)

THE PAPER IS AIMED at presenting the distributions of deformation, temperature, perturbed magnetic field and stresses in vacuum as well as in the elastic medium due to a thermal shock, acting on the plane boundary; the solutions are derived by formulating a generalized thermoelasticity theory that combines both the theories developed by Lord and Shulman as well as by Green and Lindsay. The Laplace transform technique has been used to obtain the short time solutions. The theoretical results obtained have been verified numerically and are represented graphically for the case of carbon steel material.

1. Introduction

KALISKI and NOWACKI [1] studied the magneto-thermoelastic disturbances in a perfectly conducting elastic halfspace being in contact with vacuum, due to an applied thermal disturbance acting on the plane boundary, in the absence of coupling [2, 3] between temperature and strain fields. MASSALAS and DALMANGAS also considered the problems by taking into account the thermo-mechanical couplings. The problem [2] was extended to the generalized thermoelasticity theory developed by GREEN and LINDSAY [4] involving two relaxation times, and by CHATTERJEE and ROYCHOUDHURI [5]. SHARMA and CHAND [6, 7] studied the transient magnetic-thermoelastic waves in the context of generalized theories of thermoelasticity developed by LORD and SHULMAN (L–S) [8], and GREEN and LINDSAY (G–L) [4]. ROYCHOUDHURI and DEBNATH [9] and CHAND *et al.* [10] studied the magneto-thermoelastic waves in a rotating medium.

In the present paper the distributions of deformation, temperature, perturbed magnetic field, and stresses in vacuum as well as in the elastic medium due to a thermal shock, acting on the plane boundary, have been investigated by formulating a generalized theory of thermoelasticity [11] that combines both the theories developed in [4, 8]. The Laplace transform technique [12] is used to obtain the solutions. Since the "second sound" effects are short-lived, the small time approximations have been considered. The results obtained theoretically have been verified numerically and are represented graphically for the case of carbon steel [13].

2. Basic equations

The equations governing magneto-thermoelastic interactions in a rotating homogeneous isotropic solid, which combine the L-S and G-L theories, consist of the following equations

http://rcin.org.pl

a. Maxwell's equations

$$(2.1)\quad \nabla \times \mathbf{h} = 4\pi\mathbf{J}/c, \qquad \nabla \times \mathbf{E} = -\mu_0 \dot{\mathbf{h}}/c, \qquad \nabla \cdot \mathbf{h} = 0, \qquad \mathbf{E} = -\mu_0 (\dot{\mathbf{u}} \times \mathbf{H}_0)/c.$$

b. Strain-displacement relations

$$(2.2)\quad e_{ij} = \frac{1}{2}(u_{i,j} + u_{j,i}), \qquad i,j = 1,2,3.$$

c. Stress-strain-temperature relations

$$(2.3)\quad \sigma_{ij} = \lambda \delta_{ij} e_{kk} + 2\mu e_{ij} - \gamma (\theta + t_1 \dot{\theta}) \delta_{ij}.$$

d. Equation of motion

$$(2.4)\quad \mu \nabla^2 \mathbf{u} + (\lambda + \mu) \nabla (\nabla \cdot \mathbf{u}) + \frac{\mu_0}{4\pi}[(\nabla \times \mathbf{h}) \times \mathbf{H}_0] - \gamma \nabla (\theta + t_1 \dot{\theta}) = \rho[\ddot{\mathbf{u}} + \boldsymbol{\Omega} \times (\boldsymbol{\Omega} \times \mathbf{u}) + 2\boldsymbol{\Omega} \times \dot{\mathbf{u}}].$$

e. Energy equation

$$(2.5)\quad K \nabla^2 \theta = \rho C_v (\dot{\theta} + t_0 \ddot{\theta}) + \gamma T_0 \nabla \cdot (\dot{\mathbf{u}} + \delta_{ik} t_0 \ddot{\mathbf{u}}).$$

Here

θ	temperature change,
e_{ij}	components of the strain tensor,
σ_{ij}	components of the stress tensor,
$\mathbf{u} = (u_1, u_2, u_3)$	is the displacement vector,
ρ	density,
C_v	specific heat at constant volume,
$K = \lambda_T / C_e$	λ_T is the coefficient of heat conduction,
λ, μ	Lamé constants
C_e	specific heat at constant strain,
$\gamma =$	$(3\lambda + 2\mu)\alpha_t$,
α_t	coefficient of linear thermal expansion,
t_0, t_1	thermal relaxation times,
δ_{ij}	Kronecker's delta,
$\dot{u}$	du/dt,
$\mathbf{J}$	electric current density,
$\mathbf{h}$	perturbation of the magnetic field,
$\mathbf{H}_0$	initial magnetic field,
$\mathbf{E}$	electric field,
μ_0	magnetic permeability,
c	velocity of light,
$\boldsymbol{\Omega}$	angular velocity.

http://rcin.org.pl

For the L-S theory $t_1=0$, $\delta_{1k}=1$ and for the G-L theory $t_1>0$ and $\delta_{1k}=0$ ($k=1$ for L-S and 2 for G-L theory). The thermal relaxations t_0 and t_1 satisfy the inequalities [4]

$$t_1 \geqslant t_0 \geqslant 0 \tag{2.6}$$

for the G-L theory only.

3. The problem and its solution

We consider a homogeneous isotropic (thermally as well as electrically) conducting elastic medium at uniform initial temperature T_0, in contact with vacuum. We suppose that an initial magnetic field $\mathbf{H}_0$ is acting along the x_3-axis in both the media. Let the medium be rotating along the x_3-axis at a uniform angular speed Ω. Then for $\mathbf{H}_0=(0,0,H_3)$, $\mathbf{u}=(u,0,0)$, $\Omega=(0,0,\mathbf{\Omega})$ and $x_1=x$, Eqs. (2.1), (2.4) and (2.5) become

$$\mathbf{E}=\mu_0(0,\dot{u},0)/c, \qquad \dot{\mathbf{h}}=-c\left(0,0,\frac{\partial E_2}{\partial x}\right)/\mu_0, \qquad \mathbf{J}=c\left(0,-\frac{\partial h_3}{\partial x},0\right)/4\pi, \tag{3.1}$$

$$(\lambda+2\mu+a_0^2\rho)\frac{\partial^2 u}{\partial x^2}-\gamma\frac{\partial}{\partial x}(\theta+t_1\dot{\theta})=\rho(\ddot{u}+\Omega^2 u-2\Omega\dot{u}), \tag{3.2}$$

$$\rho C_v(\dot{\theta}+t_0\ddot{\theta})+\gamma T_0\left(\frac{\partial^2 u}{\partial x\,\partial t}+\delta_{1k}t_0\frac{\partial^3 u}{\partial x\,\partial t^2}\right)=K\frac{\partial^2\theta}{\partial x^2}, \tag{3.3}$$

where $a_0=(\mu_0 H_3^2/4\pi\rho)^{1/2}$ is the Alfven wave velocity. In vacuum, the system of equations of electrodynamics is expressed by

$$\left(\frac{\partial^2}{\partial x'^2}-\frac{1}{c^2}\frac{\partial^2}{\partial t^2}\right)h_3^0=0,$$

$$\left(\frac{\partial^2}{\partial x'^2}-\frac{1}{c^2}\frac{\partial^2}{\partial t^2}\right)E_2^0=0, \qquad \text{at} \qquad x'=-x. \tag{3.4}$$

The components of Maxwell's stress tensor in the elastic medium T_{11}, in vacuum T_{11}^0, and stress σ_{11} in the elastic medium are given by

$$T_{11}=-\mu_0 h_3 H_3/4\pi, \qquad T_{11}^0=-h_3^0 H_3/4\pi, \tag{3.5}$$

$$\sigma_{11}=(\lambda+2\mu)\frac{\partial u}{\partial x}-\gamma(\theta+t_1\dot{\theta}). \tag{3.6}$$

We assume that the medium is at rest and initially undisturbed.

The initial conditions can be written as

$$u=0=T, \qquad \frac{\partial u}{\partial t}=0 \qquad \text{at} \qquad t=0, \quad x\geqslant 0. \tag{3.7}$$

http://rcin.org.pl

We consider the boundary conditions

$$\sigma_{11}+T_{11}-T_{11}^0=0,$$

$$E_2=E_2^0, \tag{3.8}$$

$$\theta(0,t)=\theta_0 H(t), \quad \text{at} \quad x=x'=0,$$

where $H(t)$ is a Heaviside function of time.

We define the quantities

$$c_1^2=(\lambda+2\mu)/\rho, \quad a_0^2+c_1^2=c_0^2, \quad \eta=c_0 x/k, \quad \tau=c_0^2 t/k,$$

$$U=\rho c_0^3 u/\gamma T_0 k, \quad Z=\theta/T_0, \quad \varepsilon=\gamma^2 T_0/\rho^2 c_0^2 C_v, \quad k=K/\rho C_v, \tag{3.9}$$

$$\tau_0=\omega^* t_0, \quad \omega^*=\rho C_v c_0^2/K, \quad C_e=\rho C_v, \quad \tau_1=\omega^* t_1.$$

Using quantities (3.9) in Eqs. (3.2), (3.3) and (3.4), we obtain for $\eta, \eta'>0$

$$\frac{\partial^2 U}{\partial \eta^2}+2\Omega_0\frac{\partial U}{\partial \tau}-\frac{\partial^2 U}{\partial \tau^2}-\Omega_0^2 U=\frac{\partial Z}{\partial \eta}+\frac{\partial^2 Z}{\partial \eta^2}, \tag{3.10}$$

$$\frac{\partial^2 Z}{\partial \eta^2}-\frac{\partial Z}{\partial \tau}-\tau_0\frac{\partial^2 Z}{\partial \tau^2}=\varepsilon\left[\frac{\partial^2 U}{\partial \eta\,\partial \tau}+\delta_{1k}\tau_0\frac{\partial^3 U}{\partial \eta\,\partial \tau^2}\right], \tag{3.11}$$

$$\frac{\partial^2 h_3^0}{\partial \eta'^2}-\beta^2\frac{\partial^2 h_3^0}{\partial \tau^2}=0, \tag{3.12}$$

where

$$\Omega_0=k\Omega/c_0^2, \quad \eta'=-\eta, \quad \beta=c/c_0. \tag{3.13}$$

The initial conditions (3.7) are now given by

$$U(\eta,0)=0, \quad Z(\eta,0)=0, \quad \frac{\partial U}{\partial \tau}(\eta,0)=0. \tag{3.14}$$

The boundary conditions (3.8) and inequalities (2.6) become

$$\frac{\partial U}{\partial \eta}-Z-\tau_1\frac{\partial Z}{\partial \tau}+\beta_1 h_3^0=0,$$

$$\beta_2\frac{\partial^2 U}{\partial \tau^2}-\frac{\partial h_3^0}{\partial \eta'}=0, \tag{3.15}$$

$$Z(0,\tau)-\theta_0 H(t)/T_0=0, \quad \text{at} \quad \eta=\eta'=0,$$

and

$$\tau_1\geqslant\tau_0\geqslant 0, \tag{3.16}$$

for the G-L theory only.

http://rcin.org.pl

We consider a potential function ϕ defined by

$$U = \frac{\partial \phi}{\partial \eta}. \tag{3.17}$$

Using Eq. (3.17) in Eqs. (3.10) and (3.11) and then applying the Laplace transform with respect to time defined by

$$\bar{\psi}(s) = \int_0^\infty \psi(t) e^{st}\, dt, \tag{3.18}$$

we obtain for $\eta, \eta' > 0$,

$$(1+\tau_1 s)\,\bar{Z} = (D^2 - s^2 + 2\Omega_0 s - \Omega_0^2)\,\bar{\phi}, \tag{3.19}$$

$$[D^2 - s(1+\tau_0 s)]\,\bar{Z} = \varepsilon s(1+\delta_{1k}\tau_0 s)\, D^2 \bar{\phi}, \tag{3.20}$$

where $D = d/d\eta$.

Applying the Laplace transform to Eqs. (3.12) and (3.15), we get

$$\bar{h}_3^0 = A_3 e^{-\beta \eta' s}, \tag{3.21}$$

$$D^2\bar{\phi} - (1+\tau_1 s)\,\bar{Z} + \beta_1 \bar{h}_3^0 = 0,$$

$$\beta_2 s^2 D\bar{\phi} - D\bar{h}_3^0 = 0, \tag{3.22}$$

$$\bar{Z}(0,s) - \theta_0/sT_0 = 0, \quad \text{at} \quad \eta = \eta' = 0,$$

where

$$\bar{f}(s) = \int_0^\infty f(t)\, e^{-st}\, dt \quad \text{etc., and} \quad D = d/d\eta. \tag{3.23}$$

Eliminating $\bar{Z}$ from Eqs. (3.19) and (3.20), we obtain the general solution for $\bar{\phi}$ which vanishes at infinity, as

$$\bar{\phi}(\eta, s) = A_1 e^{-\lambda_1 \eta} + A_2 e^{-\lambda_2 \eta}, \quad \text{for} \quad \eta > 0, \tag{3.24}$$

where λ_1, λ_2 are the roots of the equation

$$\lambda^4 - [s(1+\varepsilon - 2\Omega_0) + s^2(1+\tau_0+\varepsilon\tau_1+\delta_{1k}\tau_0) + \Omega_0^2 + \varepsilon s^3 \delta_{1k}\tau_0\tau_1]\,\lambda^2 + s\Omega_0^2 + \Omega_0(\tau_0\Omega_0 - 2)\,s^2 + (1 - 2\Omega_0\tau_0)\,s^3 + \tau_0 s^4 = 0. \tag{3.25}$$

From Eqs. (3.19) and (3.24) we obtain

$$(1+\tau_1 s)\bar{Z} = A_1[\lambda_1^2 - s^2 + \Omega_0(2s - \Omega_0)]e^{-\lambda_1\eta} + A_2[\lambda_2^2 - s^2 + \Omega_0(2s-\Omega_0)]e^{-\lambda_2\eta}. \tag{3.26}$$

Using Eqs. (3.21), (3.24) and (3.26) in (3.23) and then solving and simplifying, we obtain for $\eta, \eta' > 0$

http://rcin.org.pl

(3.27) $$\bar{\phi}(\eta,s)=\theta_0(1+\tau_1 s)[\{\beta s^2-\beta\Omega_0(2s-\Omega_0)+\lambda_2\beta_1\beta_2 s\}\, e^{-\lambda_1\eta} - \{\beta s^2-\beta\Omega_0(2s-\Omega_0)+\lambda_1\beta_1\beta_2 s\}\, e^{-\lambda_2\eta}]/\Delta s^2 T_0,$$

(3.28) $$\bar{Z}(\eta,s)=\theta_0[\{\lambda_1^2-s^2+\Omega_0(2s-\Omega_0)\}\{\beta s^2-\beta\Omega_0(2s-\Omega_0)+\beta_1\beta_2 s\lambda_2\}\, e^{-\lambda_1\eta} - \{\lambda_2^2-s^2+\Omega_0(2s-\Omega_0)\}\{\beta s^2-\beta\Omega_0(2s-\Omega_0)+\beta_1\beta_2 s\lambda_1\}\, e^{-\lambda_2\eta}]/T_0 s^2\Delta,$$

(3.29) $$\bar{h}_3^0(\eta',s)=\theta_0(1+\tau_1 s)\beta_2(\lambda_1-\lambda_2)\{\beta s^2-\beta\Omega_0(2s-\Omega_0)\}\, e^{-\beta\eta' s}/\beta T_0\Delta s^2,$$

(3.30) $$\bar{U}(\eta,s)=\theta_0(1+\tau_1 s)[\lambda_2\{\beta s^2-\beta\Omega_0(2s-\Omega_0)+\beta_1\beta_2 s\lambda_1\}\, e^{-\lambda_2\eta} - \lambda_1\{\beta s^2-\beta\Omega_0(2s-\Omega_0)+\beta_1\beta_2 s\lambda_2\}\, e^{-\lambda_1\eta}]/T_0 s^2\Delta,$$

where

(3.31) $$\Delta=(\lambda_1-\lambda_2)[\beta_1\beta_2 s^2+\beta(\lambda_1-\lambda_2)s+\beta_1\beta_2\lambda_1\lambda_2+\beta_1\beta_2\Omega_0(2s-\Omega_0)].$$

4. Small time approximations

The dependence of λ_1 and λ_2 on s is very complicated and so inversion of the Laplace transform is difficult. These difficulties, however, are reduced if we use some approximate methods. Since the thermal effects are short-lived, the discussion is confined to small time approximations, i.e. we assume s to be large. A similar approach was made by SHARMA [14]. The roots λ_1 and λ_2 of Eq. (3.25) can be approximated by

(4.1) $$\lambda_{1,2}=s\nu_{1,2}^{-1}+B_{1,2}+D_{1,2}(s^{-1})+O(s^{-2}),$$

where

(4.2) $$\nu_{1,2}^{-1}=(K_2\pm\overset{1}{\Gamma^2})^{1/2}/\sqrt{2},$$

(4.3) $$B_{1,2}=(K_1\pm(K_1K_2-2+8\tau_0\Omega_0)/\Gamma^{1/2})/2\sqrt{2}\,(K_2\pm\Gamma^{1/2})^{1/2},$$

(4.4) $$D_{1,2}=[\pm(K_1^2+2K_2\Omega_0^2-4\tau_0\Omega_0+8\Omega_0)/\Gamma^{1/2}\mp(K_1K_2-2+8\tau_0\Omega_0)^2 /\Gamma^{3/2}-(K_1\pm(K_1K_2-2+8\tau_0\Omega_0)/\Gamma^{1/2})^2/2(K_2\pm\Gamma^{1/2})]/4\sqrt{2}\,(K_2\pm\Gamma^{1/2})^{1/2},$$

(4.5) $$\Gamma=K_2^2-4\tau_0,\quad K_1=1+\varepsilon-2\Omega_0,\quad K_2=1+\tau_0+\varepsilon\tau_1+\delta_{1k}\varepsilon\tau_0.$$

Again

$$\Gamma=(1+\varepsilon\tau_1-\tau_0)^2+4\varepsilon\tau_0\tau_1+\varepsilon\tau_0\delta_{1k}\{\varepsilon\tau_0+2(1+\tau_0+\varepsilon\tau_1)\}.$$

The wave propagating with speed v_1 will be elastic, that with speed v_2 will be thermal, and the third one travelling with velocity c_0 will be tha Alfven-acoustic wave [6].

http://rcin.org.pl

Using Eq. (4.1) in Eqs. (3.28)–(3.30), we obtain

$$\bar{Z}(\eta,s)=\theta_0\left[\left\{\frac{N_1P'}{s}+(N_1Q'+N_2P')/s^2\right\}e^{-\lambda_1\eta}-\left\{\frac{N_1'P'}{s}+(N_1'Q'+N_2'P')/s^2\right\}e^{-\lambda_2\eta}\right]/T_0 \tag{4.6}$$

(for L-S and G-L theories),

$$\bar{h}_3^0(\eta',s)=\theta_0\beta_2[\tau_1P+\{P+\tau_1(Q-2\Omega_0)\}]e^{-\beta\eta's}/T_0 \tag{4.7}$$

(for G-L theory),

$$\bar{h}_3^0(\eta',s)=\theta_0\beta_2\left[\frac{P}{s}+(Q-2\Omega_0\beta P)/s^2\right]e^{-\beta\eta's}/T_0, \tag{4.8}$$

(for L-S theory),

$$\bar{U}(\eta,s)=\theta_0[\{M_1P'\tau_1/s)+(M_1Q'+M_2P')/s^2\}e^{-\lambda_2\eta}-\{(M_1'P'\tau_1/s)+(M_1'Q'+M_2'P')/s^2\}e^{-\lambda_1\eta}]/T_0 \tag{4.9}$$

(for G-L theory),

$$\bar{U}(\eta,s)=\theta_0[\{M_1P'/s^2)+(M_1Q'+M_2P')/s^3\}e^{-\lambda_2\eta}-\{(M_1'P/s^2)+(M_1'Q'+M_2'P')/s^3\}e^{-\lambda_1\eta}]/T_0 \tag{4.10}$$

(for L-S theory),

and

$$\bar{T}_{11}^0(\eta',s)=-H_3\bar{h}_3^0(\eta',s)/4\pi \tag{4.11}$$

(for G-L theory),

$$\bar{T}_{11}^0(\eta',s)=-H_3\bar{h}_3^0(\eta',s)/4\pi \tag{4.12}$$

(for L-S theory),

$$\bar{\sigma}_{11}(\eta,s)=\theta_0\gamma[\{\beta_3^2R_1P'-N_1P')/s+(\beta_3^2(R_1Q'+R_2P')-N_1Q'-N_2P')/s^2\}e^{-\lambda_1\eta}-\{(\beta_3^2R_1'P'-N_1'P')/s+(\beta_3^2(R_1'Q'+R_2'P')-N_1'Q'-N_2'P')/s^2\}e^{-\lambda_2\eta}] \tag{4.13}$$

(for L-S theory),

http://rcin.org.pl

(4.14) $$\bar{\sigma}_{11}(\eta,s)=\theta_0\gamma[\{\tau_1(\beta_3^2R_1P'-N_1P')+((\beta_3^2R_1P'-N_1P')+\tau_1(\beta_3^2(R_1Q'+R_2P')-N_1Q'-N_2P'))/s\}e^{-\lambda_1\eta}-\{\tau_1(\beta_3^2R_1'P'-N_1'P')+((\beta_3^2R_1'P'-N_2'P')+\tau_1(\beta_3^2(R_1'Q'+R_2'P')-N_1'Q'-N_2'P'))/s\}e^{-\lambda_2\eta}]$$

(for G-L theory).

Now inverting the Laplace transform of Eqs. (4.6)–(4.14), we obtain

(4.15) $$Z(\eta,\tau)=\theta_0[\{N_1P'+(N_1Q'+N_2P')(\tau-\eta/\upsilon_1)\}H(\tau-\eta/\upsilon_1)e^{-B_1\eta}-\{N_1'P'+(N_1'Q'+N_2'P')(\tau-\eta/\upsilon_2)\}H(\tau-\eta/\upsilon_2)e^{-B_2\eta}]/T_0$$

(for L-S and G-L theories),

(4.16) $$h_3^0(\eta',\tau)=\beta_2\theta_0[\tau_1P\delta(\tau-\eta'\beta)+(P+\tau_1(Q-2\Omega_0)H(\tau-\eta'\beta)]/T_0$$

(for G-L theory),

(4.17) $$U(\eta,\tau)=\theta_0[\{\tau_1M_1P'+(M_1Q'+M_2P')(\tau-\eta/\upsilon_2)\}H(\tau-\eta/\upsilon_2)e^{-B_2\eta}-\{\tau_1M_1'P'+(M_1'Q'+M_2'P')(\tau-\eta/\upsilon_1)\}H(\tau-\eta/\upsilon_1)\}e^{-B_1\eta}]/T_0$$

(for G-L theory),

(4.18) $$U(\eta,\tau)=\theta_0[\{M_1P'(\tau-\eta/\upsilon_2)+(M_1Q'+M_2P')(\tau-\eta/\upsilon_2)^2\}H(\tau-\eta/\upsilon_2)e^{-B_2\eta}-\{M_1'P'(\tau-\eta/\upsilon_1)+(M_1'Q'+M_2'P')(\tau-\eta/\upsilon_1)^2\}H(\tau-\eta/\upsilon_1)e^{-B_1\eta}]/T_0$$

(for L-S theory),

and

(4.19) $$T_{11}^0(\eta',\tau)=-H_3h_3^0(\eta',\tau)/4\pi$$

(for G-L theory),

(4.20) $$T_{11}^0(\eta',\tau)=-H_3h_3^0(\eta',\tau)/4\pi$$

(for L-S theory),

(4.21) $$\sigma_{11}(\eta,\tau)=\gamma\theta_0[\{\beta_3^2R_1P'-N_1P')+(\beta_3^2(R_1Q'+R_2P')-N_1Q'-N_2P')\}\times H(\tau-\eta/\upsilon_1)e^{-B_1\eta}-\{(\beta_3^2R_1'P'-N_1'P')+(\beta_3^2(R_1'Q'+R_2'P')-N_1'Q'-N_2'P')(\tau-\eta/\upsilon_2)\}H(\tau-\eta/\upsilon_2)e^{-B_2\eta}]$$

(for L-S theory),

(4.22) $$\sigma_{11}(\eta,\tau)=\gamma\theta_0[\{\tau_1(\beta_3^2R_1P'-N_1P')\delta(\tau-\eta/\upsilon_1)+((\beta_3^2R_1P'-N_1P')+\tau_1(\beta_3^2(R_1Q'+R_2P')-N_1Q'-N_2P')H(\tau-\eta/\upsilon_1)\}e^{-B_1\eta}-\{\tau_1(\beta_3^2(R_1'P'-N_1'P')\times\delta(\tau-\eta/\upsilon_2)+(\tau_1(\beta_3^2(R_1'Q'+R_2'P')-N_1'Q'-N_2'P')+(\beta_3^2R_1'P'-N_1'P'))\times H(\tau-\eta/\upsilon_2)\}e^{-B_2\eta}]$$

(for G-L theory).

http://rcin.org.pl

Here the following notations have been used:

$$P = [\beta_1^4\beta_2^4\upsilon_1^4\upsilon_2^4+\beta^2\beta_1^2\beta_2^2(\upsilon_1+\upsilon_2)^2\upsilon_1^2\upsilon_2^2+2\beta\beta_1^3\beta_2^3\upsilon_1^2\upsilon_2^2(\upsilon_1+\upsilon_2) \tag{4.23}$$
$$-\beta\beta_1\beta_2\upsilon_1\upsilon_2(\upsilon_1+\upsilon_2)^3-\beta_1^4\beta_2^4\upsilon_1^3\upsilon_2^3+\beta_1^4\beta_2^4\upsilon_1^2\upsilon_2^2+\beta^4(\upsilon_1+\upsilon_2)^4$$
$$-3\beta\beta_1^2\beta_2^2\upsilon_1\upsilon_2(\upsilon_1+\upsilon_2)^2-\beta\beta_1^3\beta_2^3\upsilon_1^3\upsilon_2^3(\upsilon_1+\upsilon_2)]/\beta_1^5\beta_2^5\upsilon_1^4\upsilon_2^4,$$

$$Q=[2\beta^2\beta_1^2\beta_2^2\upsilon_1\upsilon_2(\upsilon_1+\upsilon_2)(B_1+B_2)-\beta_1^4\beta_2^4\upsilon_1^2\upsilon_2^2+2\Omega_0\beta_1^4\beta_2^4\upsilon_1^3\upsilon_2^3 \tag{4.24}$$
$$-\beta\beta_1^3\beta_2^3\upsilon_1^3\upsilon_3^3(B_1+B_2)+2\beta\beta_1^3\beta_2^3\upsilon_1\upsilon_2\{(\upsilon_1+\upsilon_2)(B_1\upsilon_1+B_2\upsilon_2)$$
$$+(B_1+B_2)\upsilon_1\upsilon_2\}+4\beta_1^4\beta_2^4\upsilon_1^2\upsilon_2^2\Omega_0-3\beta^3\beta_1\beta_2\upsilon_1\upsilon_2(\upsilon_1+\upsilon_2)^2(B_1+B_2)$$
$$-6\beta\beta_1^2\beta_2^2\upsilon_1\upsilon_2\Omega_0(\upsilon_1+\upsilon_2)^2+2\beta_1^4\beta_2^4\upsilon_1\upsilon_2(B_1\upsilon_1+B_2\upsilon_2)$$
$$-12\beta\beta_1^3\beta_2^3\upsilon_1^2\upsilon_2^2\Omega_0(\upsilon_1+\upsilon_2)-3\beta^2\beta_1^2\beta_2^2\{(\upsilon_1+\upsilon_2)^2(B_1\upsilon_1+B_2\upsilon_2)$$
$$+2\upsilon_1\upsilon_2(B_1+B_2)(\upsilon_1+\upsilon_2)\}+4\beta^4(\upsilon_1+\upsilon_2)^3(B_1+B_2)$$
$$+8\beta^3\beta_1\beta_2(\upsilon_1+\upsilon_2)^3]/\beta_1^5\beta_2^5\upsilon_1^3\upsilon_2^3,$$

$$P'=\upsilon_1\upsilon_2 P/(\upsilon_1-\upsilon_2),\quad Q'=\{\upsilon_1\upsilon_2 Q/(\upsilon_2-\upsilon_1)\}-\upsilon_1\upsilon_2(B_1-B_2)P/(\upsilon_2-\upsilon_1)^2,$$

$$L=(1-\upsilon_1^2)(1-\upsilon_2^2)/\upsilon_1^2\upsilon_1^2, \tag{4.25}$$

$$M=[2(B_2+\Omega_0\upsilon_2(1-\upsilon_1^2)+2\upsilon_1(B_1+\Omega_0\upsilon_1)(1-\upsilon_2^2)]/\upsilon_1^2\upsilon_2^2,$$

$$M_1=(\beta\upsilon_1+\beta_1\beta_2)/\upsilon_1\upsilon_2,\quad M_1'=(\beta\upsilon_2+\beta_1\beta_2)/\upsilon_1\upsilon_2,$$

$$M_2'=[B_1\upsilon_1(\beta\upsilon_2+\beta_1\beta_2)+\upsilon_2(B_2\beta_1\beta_2-2\beta\Omega_0)]/\upsilon_1\upsilon_2,$$

$$M_2=[B_2\upsilon_2(\beta\upsilon_1+\beta_1\beta_2)+\upsilon_1(B_1\beta_1\beta_2-2\beta\Omega_0)]/\upsilon_1\upsilon_2,$$

$$N_1=(1-\upsilon_1^2)(\beta\upsilon_2+\beta_1\beta_2)/\upsilon_1^2\upsilon_2,$$

$$N_1'=(1-\upsilon_2^2)(\beta\upsilon_1+\beta_1\beta_2)/\upsilon_1\upsilon_2^2,$$

$$N_2=[(2B_1+2\upsilon_1\Omega_0)(\beta\upsilon_2+\beta_1\beta_2)/\upsilon_1\upsilon_2]+(1-\upsilon_2^2)(B_2\beta_1\beta_2-2\beta\Omega_0)/\upsilon_2^2, \tag{4.26}$$

$$R_1=(\beta\upsilon_2+\beta_1\beta_2)/\upsilon_1^2\upsilon_2,\quad R_1'=(\beta\upsilon_1+\beta_1\beta_2)/\upsilon_1\upsilon_2^2,$$

$$N_2'=[(2B_2+2\upsilon_2\Omega_0)(\beta\upsilon_1+\beta_1\beta_1)/\upsilon_1\upsilon_2]+(1-\upsilon_1^2)(B_1\beta_1\beta_2-2\beta\Omega_0)/\upsilon_1^2,$$

$$R_2=[2B_1\upsilon_1(\beta\upsilon_2+\beta_1\beta_2)+\upsilon_2(B_2\beta_1\beta_2-2\beta\Omega_0)]/\upsilon_1^2\upsilon_2,$$

$$R_2'=[2B_2\upsilon_2(\beta\upsilon_1+\beta_1\beta_2)+\upsilon_1(B_1\beta_1\beta_2-2\beta\Omega_0)]/\upsilon_1\upsilon_2^2,$$

$$\beta_3=c_1/c_0.$$

http://rcin.org.pl

5. Long time solutions

The long time solutions can be obtained by expanding the roots λ_1^2, λ_2^2 of Eqs. (3.28) for small values of s in Taylor's series. The roots λ_1, λ_2 can be written in the form

$$\lambda_1=(1+\varepsilon)^{1/2}\sqrt{s}+O(s^{3/2}),$$

$$\lambda_2=(1+\varepsilon)^{1/2}s+O(s^2).$$

These expressions for the roots do not contain the thermal relaxation times up to the first order, which again confirms the fact that the "second sound" effects are short-lived. Hence short time solutions are more important than the long time solutions. However, the deformation, temperature, the perturbed magnetic field and stresses in vacuum as well as in the elastic medium can be obtained by using these values of λ_1 and λ_2 in various relevant equations as in the previous sections.

6. Discussion of the results

The short time solutions in the previous Sec. 4 show that they consist of three waves, namely, elastic, thermal and Alfven-acoustic waves travelling with velocities v_1, v_2 and c_0, respectively. The terms containing $H(\tau-\eta/v_1)$, $H(\tau-\eta/v_2)$ and $H(\tau-\eta'/\beta)$ represent the contribution of elastic, thermal and Alfven-acoustic waves in the vicinities of their wave fronts $\eta=v_1\tau$, $\eta=\tau v_2$ and $\eta'=\tau/\beta$. In this case the deformation is continuous in the L-S theory but is found to be discontinuous in G-L theory. The temperature, perturbed magnetic field and stresses in vacuum as well as in the elastic medium are all found to be discontinuous in both the theories.

The discontinuities are given by the formulae

$$(Z^+-Z^-)_{\eta=v_1\tau} = \theta_0 N_1 P' \exp(-B_1 v_1 \tau)/T_0,$$

$$(Z^+-Z^-)_{\eta=v_2\tau} = -\theta_0 N_2 P' \exp(-B_2 v_2 \tau)/T_0,$$

$$(h_3^{0+}-h_3^{0-})_{\eta'=\tau/\beta} = \theta_0 \beta_2 P/T_0,$$

$$(T_{11}^{0+}-T_{11}^{0-})_{\eta'=\tau/\beta} = -\theta_0 \beta_2 H_3 P/4\pi T_0,$$

$$(\sigma_{11}^{+}-\sigma_{11}^{-})_{\eta=v_1\tau} = \theta_0 \gamma (\beta_3^2 R_1 P' - N_1 P') \exp(-B_1 v_1 \tau),$$

$$(\sigma_{11}^{+}-\sigma_{11}^{-})_{\eta=v_2\tau} = -\theta_0 \gamma (\beta_3^2 R_1' P' - N_1' P') \exp(-B_2 v_2 \tau),$$

for L-S theory,

$$(U^+-U^-)_{\eta=v_1\tau} = -\theta_0 M_1 P' \tau_1 \exp(-B_1 v_1 \tau)/T_0,$$

$$(U^+-U^-)_{\eta=v_2\tau} = \theta_0 \tau_1 M_1' P' \exp(-B_2 v_2 \tau)/T_0,$$

http://rcin.org.pl

$$(Z^+ - Z^-)_{\eta=v_1\tau} = \theta_0 N_1 P' \exp(-B_1 v_1 \tau)/T_0,$$

$$(Z^+ - Z^-)_{\eta=v_2\tau} = -\theta_0 N_1' P' \exp(-B_2 v_2 \tau)/T_0,$$

$$(h_3^{0+} - h_3^{0-})_{\eta'=\tau/\beta} = \theta_0 \beta_2 [Q\tau_1 + P(1-\tau_1\Omega_0)]/T_0,$$

$$(T_{11}^{0+} - T_{11}^{0-})_{\eta'=\tau/\beta} = \theta_0 \beta H_3 [Q\tau_1 + P(1-\tau_1\Omega_0)/4\pi T_0,$$

$$(\sigma_{11}^+ - \sigma_{11}^-)_{\eta=v_1\tau} = \theta_0\gamma[\beta_3^2 R_1 P' - N_1 P' + \tau_1\{\beta_3^2(R_1 Q' + R_2 P') - N_1 Q' - N_2 P'\}] \times \exp(-B_1 v_1 \tau),$$

$$(\sigma_{11}^+ - \sigma_{11}^-)_{\eta=v_2\tau} = -\theta_0\gamma[\beta_3^2 R_1' P' - N_1' P' + \tau_1\{\beta_3^2(R_1' Q' + R_2' P') - N_1' Q' - N_2' P'\}] \times \exp(-B_2 v_2 \tau)$$

for G-L theory.

Clearly the discontinuities in deformation, temperature, and stress in the elastic medium decay exponentially, and the perturbed magnetic field and stress in vacuum vary linearly with time.

7. Particular cases

i. If the medium is non-rotating, i.e. $\Omega = 0$, then the results obtained reduce to those in [6, 10] for the L-S theory and for the G-L theory; the results can be deduced from the corresponding equations by putting $\Omega = 0$.

ii. If $\tau_1 = \tau_0 = 0$, then we have

$$K_1 = 1 + \varepsilon - 2\Omega_0, \quad K_2 = 1, \quad \Gamma = 1, \quad v_1 = 1, \quad v_2 \to \infty, \quad B_1 = (\varepsilon - 2\Omega_0)/2,$$

$$B_2 \to \infty, \quad D_1 = [\varepsilon(4-\varepsilon) + 2\Omega_0(\varepsilon - 2\Omega_0)]/8, \quad D_2 \to \infty.$$

It is observed that the deformation and temperature are found to be continuous at the elastic and thermal wavefronts in both the theories. The stress in the elastic medium is also found to be continuous at thermal wavefront in both the theories. The perturbed magnetic field and stress in vacuum at the acoustic wavefront and the stress in the elastic medium at the elastic wavefront, experience finite jumps in both the theories, given, for both the L-S and G-L theories, by

$$(h_3^{0+} - h_3^{0-})_{\eta'=\tau/\beta} = \theta_0 \beta_2 P/T_0,$$

$$(T_{11}^{0+} - T_{11}^{0-})_{\eta'=\tau/\beta} = -\theta \beta_2 H_3 P/4\pi T_0,$$

$$(\sigma_{11}^+ - \sigma_{11}^-)_{\eta=v_1\tau} = \theta_0 \gamma \beta \beta_3^2 P \exp[-(\varepsilon - 2\Omega_0)\tau/2].$$

iii. For $\tau_1 = \tau_0 = 0$ and $\Omega_0 = 0$, we have the case of the conventional coupled theory of thermoelasticity, and thus

$$K_1 = 1 + \varepsilon, \quad K_2 = 1, \quad \Gamma = 1, \quad v_1 = 1, \quad v_2 \to \infty, \quad B_1 = \varepsilon/2, \quad B_2 \to \infty,$$
$$D_1 = \varepsilon(4-\varepsilon)/8, \quad D_2 \to \infty.$$

http://rcin.org.pl

In this case the results obtained agree with those of case ii), except for the stress in the elastic medium which suffers a discontinuity at the elastic wavefront in both the theories, given by

$$(\sigma_{11}^{+}-\sigma_{11}^{-})_{\eta=v_1\tau}=\theta_0\gamma\beta\beta_3^2 P\exp(-\varepsilon\tau/2).$$

iv. If $\tau_1=\tau_0=0$, $\varepsilon=0$, $\Omega_0\neq 0$, then we have

$$3K_1=1-2\Omega_0,\quad K_2=1,\quad \Gamma=1,\quad v_1=1,\quad v_2\to\infty,\quad B_2=-\Omega_0,\quad B_2\to\infty,$$
$$D_1=-\Omega_0^2/4,\quad D_2\to\infty.$$

The results obtained here agree with case ii), except the fact that the stress in the elastic medium experiences finite jump at the elastic wavefront in both the theories, given by

$$(\sigma_{11}^{+}-\sigma_{11}^{-})_{\eta=v_1\tau}=\theta_0\gamma\beta\beta_3^2 P\exp(\Omega_0\tau).$$

v. If $\tau_1=\tau_0=0$, $\varepsilon=0$, $\Omega_0=0$, then we have

$$K_1=1,\quad K_2=1,\quad \Gamma=1,\quad v_1=1,\quad v_2\to\infty,\quad B_1=0,\quad B_2\to\infty,\quad D_1=0,\quad D_2\to\infty.$$

The results obtained here again agree with those of case ii) except the stress in the elastic medium, which experiences a finite jump at the elastic wavefronts in both the theories, given by $(\sigma_{11}^{+}-\sigma_{11}^{-})_{\eta=v_1\tau}=\theta_0\gamma\beta\beta_3^2 P$.

vi. In the absence of the magnetic field, i.e. $H_3=0$, then $\beta_1=\beta_2=0$, what means that there is no coupling between the electromagnetic and strain fields, than the stress in vacuum $T_{11}^0=0$. The result agrees with [5].

8. Numerical results and discussion

In this section the jumps obtained theoretically in the previous sections for deformation, temperature, the perturbed magnetic field and stresses in vacuum as well as in the elastic medium, are computed numerically for carbon steel material [13] for which the physical data are

$$\lambda=9.3\times10^{10}\ \text{N m}^{-2},\quad \mu=8.4\times10^{10}\ \text{N m}^{-2},$$
$$\rho=7.9\times10^{3}\ \text{kg m}^{-3},\quad T_0=293\cdot1\,^{\circ}\text{K},\quad \varepsilon=0.34,$$
$$C_e=6.4\times10^{2}\ \text{Jkg}^{-1}\,\text{deg}^{-1},\quad \Omega=8\ \text{r.p.s.}\quad \text{and}\quad H_3=1\ \text{gauss}.$$

The variations of jumps are plotted as functions of time for relaxation time $(\tau_1, \tau_0)=0$, 0.1, 0.5, for non-rotating and rotating medium in both L-S and G-L theories, as shown in Figures 1 to 5. It is found that, in general, the variations of jumps in the cases of perturbed magnetic field and stress in vacuum are linear in nature, whereas in the cases of deformation, temperature, and stress in the elastic medium, they decay exponentially with time.

http://rcin.org.pl

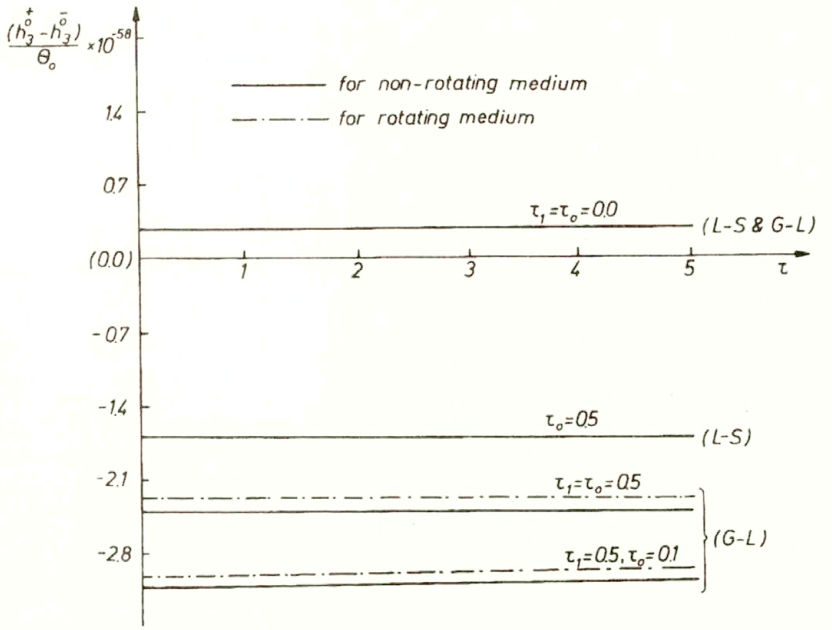

FIG. 1. The variation of jumps in perturbed magnetic field in vacuum with time for different relaxation times, at the wavefronts.

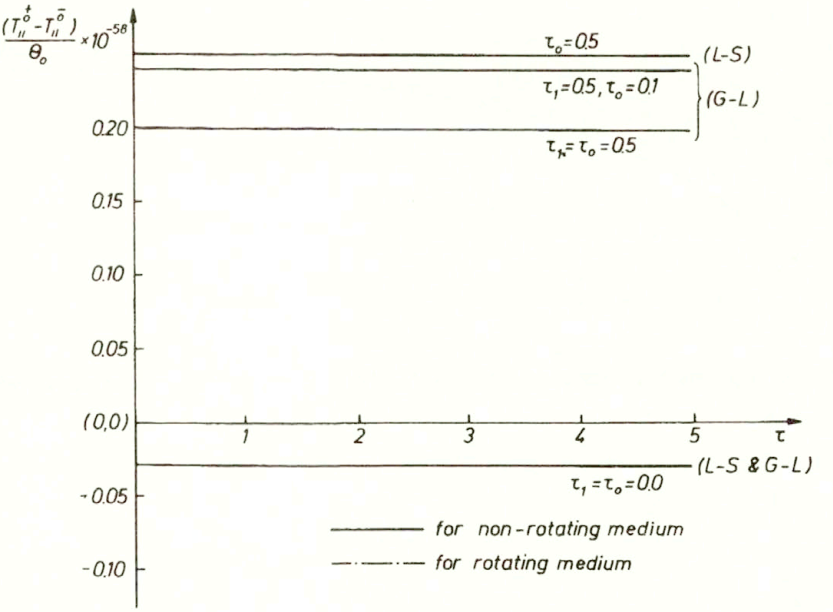

FIG. 2. The variation of jumps in stresses in vacuum with time for different relaxation times, at the wavefronts.

http://rcin.org.pl

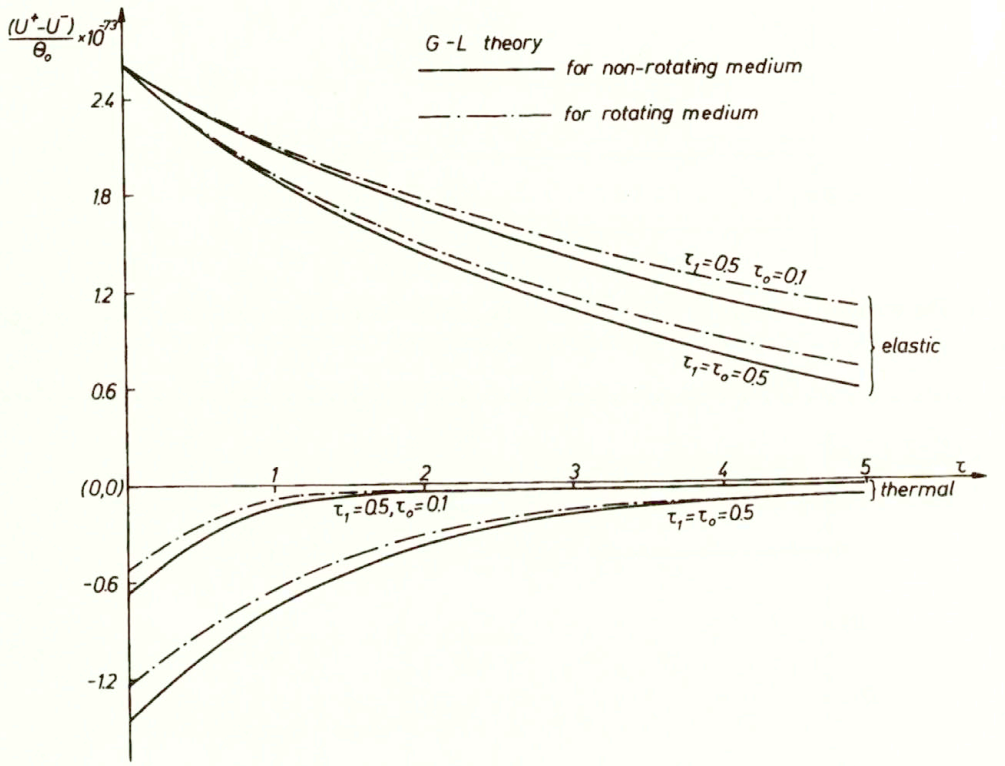

FIG. 3. The variation of jumps in deformation with time for different relaxation times, at the wavefronts.

http://rcin.org.pl

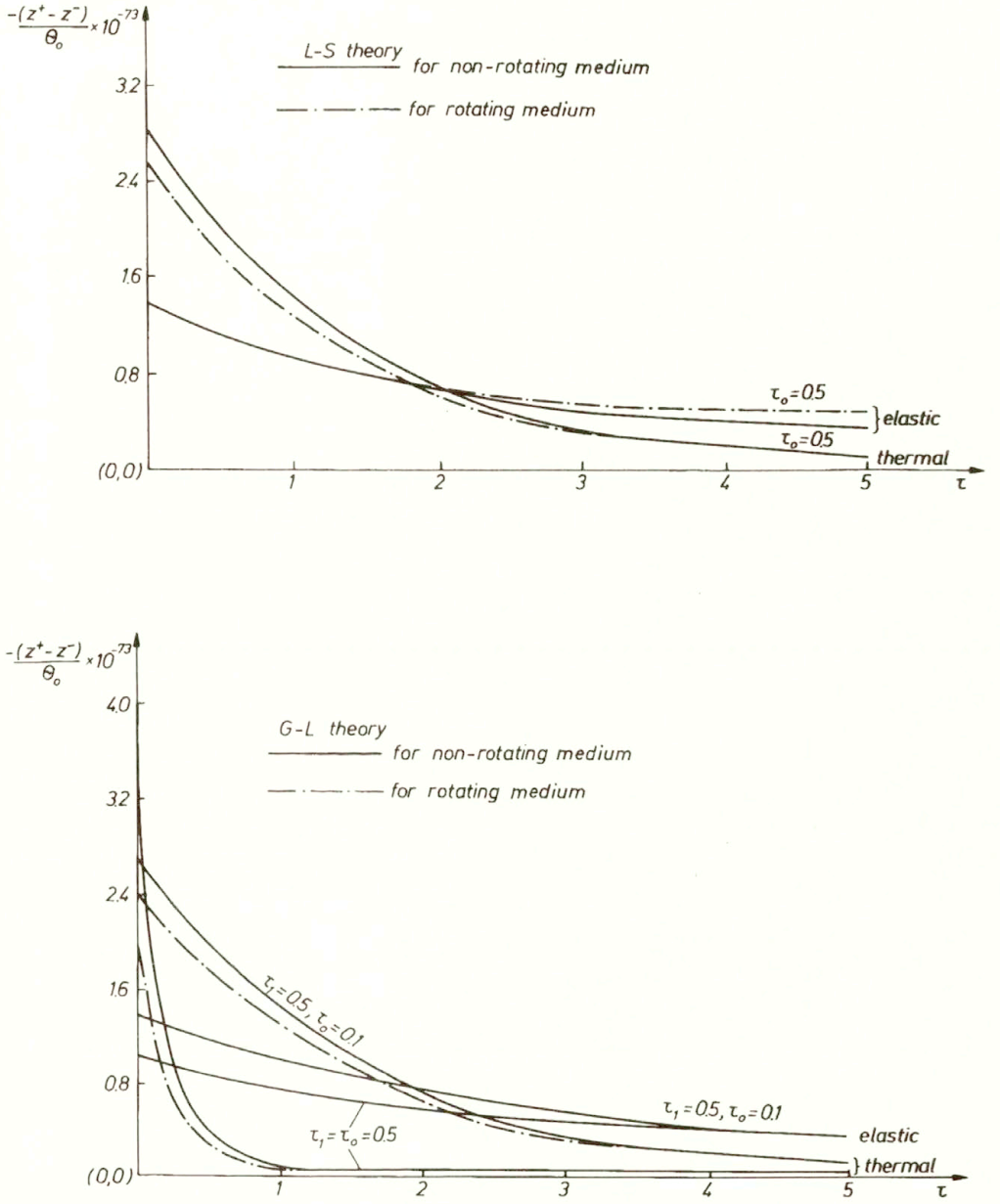

FIG. 4 a. The variation of jumps in temperature with time for different relaxation times, at the wavefronts.
b. The variation of jumps in temperature with time for different relaxation times, at the wavefronts.

http://rcin.org.pl

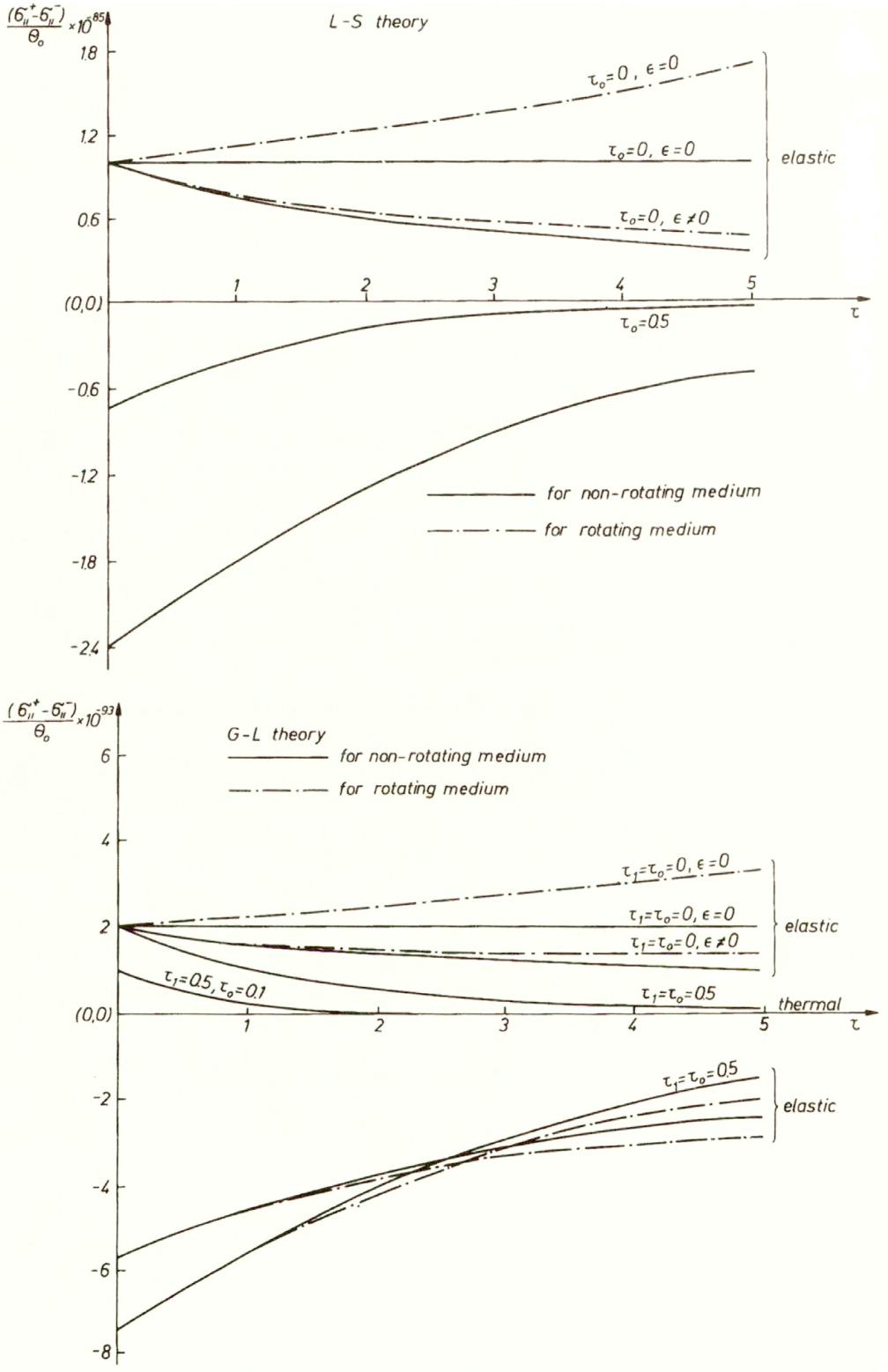

FIG. 5 a. The variation of jumps in stress in the elastic medium with time for different relaxation times, at the wavefronts. b. The variation of jumps in stress in the elastic medium with time for different relaxation times, at the wavefronts.

http://rcin.org.pl

References

1. S. KALISKI and W. NOWACKI, *Excitation of mechanical electromagnetic waves induced by a thermal shock*, Bull. Acad. Polon. Sci., Série Sci. Techn., **25**, 1, 1962.
2. C. MASSALAS and A. DALMANGAS, *Coupled magneto-thermoelastic problem in elastic half-space*, Lett. Appl. Engng. Sci., **21**, 171, 1983.
3. C. MASSALAS and A. DALMANGAS, *Coupled magneto-thermoelastic problem in elastic half-space having finite conductivity*, Lett. Appl. Engng.Sci., **21**, 199, 1983.
4. A.E. GREEN and K.A. LINDSAY, *Thermoelasticity*, J. Elasticity, **2**, 1, 1972.
5. G. CHATTERJEE and S.K. ROYCHOUDHURI, *The coupled magneto-thermoelastic problem in elastic half-space with two relaxation times*, Lett.Appl.Engng.Sci., **23**, 975, 1988.
6. J.N. SHARMA and DAYAL CHAND, *Transient generalized magneto-thermoelastic waves in a half-space*, Int. J. Engng.Sci., **26**, 951, 1988.
7. DAYAL CHAND and J.N. SHARMA, *Transient magneto-thermoelastic waves in a half-space with thermal relaxations*, Indian J. Pure appl. Math., **19**, 1227, 1988.
8. H.W. LORD and Y. SHULMAN, *A generalized dynamical theory of thermoelasticity*, J. Mech. Phys. Solids, **15**, 299, 1967.
9. S.K. ROYCHOUDHURI and LOKNATH DEBNATH, *Magneto-thermo-elastic plane waves in rotating media*, Int. J. Engng. Sci., **21**, 155, 1983.
10. DAYAL CHAND, J.N. SHARMA and S.P. SUD, *Transient generalized magneto-thermoelastic waves in a rotating half-space*, Int. J. Engng. Sci., **28**, 547, 1990.
11. N. NODA, T. FURUK-AWA and F. ASHIDA, *Generalized thermoelasticity in an infinite solid with a hole*, J. Thermal stresses, **12**, 385, 1989.
12. R.E. COLLINS, *Mathematical methods for physicists and engineers*, Reinhold, New York 1968.
13. B. MARUSZEWSKI, *Dynamic magneto-thermoelastic problem in circular cylinder. II. Thermal, magnetic and electric fields*, Int. J. Engng Sci., **19**, 1241, 1981.
14. J.N. SHARMA, *Some considerations on generalized thermoelasticity*, Int. J. Engng Sci., **25**, 1387, 1987.

DEPARTMENT OF APPLIED SCIENCES
REGIONAL ENGINEERING COLLEGE, HAMIRPUR, INDIA.

Received November 26, 1992.

http://rcin.org.pl

Arch.Mech., 45, 4, pp. 405–421, Warszawa 1993

Analysis of interaction of impulse-like pressure wave in a fluid with undeformable layer of porous material(*)

M. CIESZKO and J. KUBIK (POZNAŃ)

THE PROBLEM of interaction of a plane impulse-like pressure wave in fluid with an undeformable layer of porous material is analysed for the case of normal incidence of the wave. The method of analytical solution of the problem is proposed. This allowed us to discuss the influence of the viscous drag force of fluid in the porous layer and its pore structure parameters on the reflection and transmission of the incident wave. It was shown that the viscous drag force causes not only damping and dispersion of waves propagating in the porous layer but also affects the reflection and transmission of waves at both surfaces of the layer where the pore structure plays the fundamental role. The pore structure is the cause of the amplitude growth effect of the wave penetrating the porous layer.

1. Introduction

POROUS MATERIALS saturated with fluids (as the air, water, gas, crude oil) are encountered both in the nature (soils, oil-bearing rocks, bones, crops etc.) and in the technology (sintered powders, filters, construction ceramics, insulating and sound-absorbing materials). Increasing research interest has been lately observed in considering physical phenomena (microscopic) occuring in porous media and in their macroscopic description. Particularly, theoretical and experimental investigations of mechanical behaviour of fluid-saturated porous materials as well as their mechanical properties are developed (see [1, 2, 18]). Due to the complexity of deformation processes in such materials and multiparameter character of their description the investigations require especially prepared methods [9, 11, 19].

In extensively developed dynamical methods applied for examining porous materials it is important to know basic features of reflection and transmition phenomena of impuls waves interacting with bounded porous media. On one hand, samples in the form of layer are often used as elements of systems in the dynamical methods to determine the pore structure parameters and other material constants [8, 10, 12]; on the other hand, the analytical solution of a boundary problem makes it possible to formulate the conditions necessary for the tests to be performed. Furthemore, the obtained relationships are indispensable to interpret the measurements in an appropriate manner.

This paper is the first part of the analysis regarding interaction of an impulse-like pressure wave propagating in a fluid with a layer of porous material. It concerns the normal incidence of a plane wave on a rigid, fixed and permeable layer immersed in a fluid. The second part will be devoted to the case when a porous layer is deformable.

(*) The reported research was done under the grant No. 300149101.

http://rcin.org.pl

The aim is to obtain an analytical solution to the problem and to discuss the influence of the geometry of pores and the diffusion forces on the process of reflection and transmission of an impulse wave.

The considerations are based on the assumption that the motion of a fluid outside a porous layer is described by the Navier-Stokes equations, while the motion of fluid in the pores of undeformable layer is described by suitably reduced equations of the theory of deformable porous media [6, 7, 13 – 15]. In the framework of this theory the structure of the skeleton is characterized by two parameters: volumetric porosity and structural permeability. These two parameters enter the continuity and the motion equations of the pore fluid in an explicit way, and so do they in the compatibility conditions formulated as the continuity of the fluid mass flux and its effective pressure on both faces of the layer.

The analysis is given in two steps. First, the interaction of the plane harmonic wave with a porous layer is considered for which the explicit expressions describing acoustical fields in particular regions of the system are obtained. These expressions are employed at the second stage to construct a solution of the problem of interaction for an arbitrary profile of the plane incident wave. The solution has been obtained in the analytical form considering interaction of the wave with the layer as the superposition of interactions of wave harmonic components given by Fourier transform.

It is shown that the forces of viscous friction between fluid and skeleton cause not only damping and dispersion of the propagating waves, but also influence the phenomenon of reflection and transmission of waves on both faces of the layer, where the pore structure plays a fundamental role.

2. Interaction of an acoustic impulse wave with a layer of porous material; formulation of the problem

We analyse the problem of reflection and transmission of a plane pressure wave through an undeformable layer of porous material with the thickness b immersed in a fluid. The incident wave is perpendicular to the layer (Fig. 1). The fluid is assumed

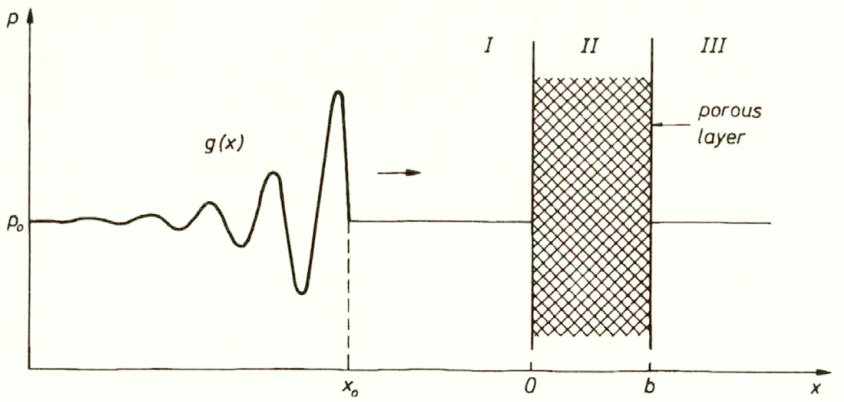

FIG. 1. Outline of the system: impulse wave — porous layer.

http://rcin.org.pl

to be barotropic, i.e. the effective pressure p^f in the fluid is a single-valued function of its effective density ρ^f ($p^f = p^f(\rho^f)$). Moreover, it is assumed that the viscosity of the fluid does not influence its macroscopic stress state (the stress deviators in the fluid, both outside and inside the layer, are neglected). The viscosity is accounted for in the interface force between the fluid and the porous skeleton.

Under the above assumptions, the propagation of disturbances with small amplitudes in the half-spaces $x<b$ (region I) and $x>b$ (region III) is described by linear one-dimensional equations

$$\frac{\partial v}{\partial t} + \frac{\partial p}{\partial x} = 0, \tag{2.1}$$

$$\frac{1}{a_0^2}\frac{\partial p}{\partial t} + \frac{\partial v}{\partial x} = 0,$$

$$p = (p^f - p_0^f)/p_0^f, \tag{2.2}$$

where v stands for the velocity of fluid particles and

$$a_0 = \left(\frac{dp^f}{d\rho^f}\right)^{\frac{1}{2}}\Bigg|_{\rho^f=\rho_0^f}$$

is the velocity of propagation of disturbances in the medium. Effective density and pressure in the undisturbed fluid are denoted by ρ_0^f and p_0^f, respectively.

The description of the fluid motion in the pores of the undeformable layer (region II) will be based on the so-called two-parameter theory of deformable porous body saturated with fluid [6, 7, 13–15], where the structure of pores is characterized by two parameters: volumetric porosity f_v and structural permeability λ ($\lambda \leqslant f_v$). The problem of the motion of barotropic fluid through the pores of an undeformable skeleton reduces to a specific case of this theory and the equations for propagation of disturbances with small amplitude take the form

$$\frac{\partial v}{\partial t} + \frac{\partial p}{\partial x} + \bar{k}v = 0, \tag{2.3}$$

$$\frac{1}{c_0^2}\frac{\partial p}{\partial t} + \frac{\partial v}{\partial x} = 0,$$

$$\bar{k} = \bar{k}'/(\lambda\rho_0^f), \tag{2.4}$$

where $\bar{k}'$ is a coefficient in a linear law of diffusion resistance and c_0 is the velocity of propagation of the wave front in the medium and is related to the velocity a_0 of the propagation of disturbances in the fluid itself (regions I and III) by means of the formula

$$c_0 = \sqrt{\varkappa}\, a_0, \qquad \varkappa = \lambda/f_v. \tag{2.5}$$

http://rcin.org.pl

The acoustic fields in particular regions of the system are coupled through the compatibility conditions on the contact surfaces. For small disturbances these conditions are: continuity of the effective pressure and of the fluid mass flux on the faces of the porous layer ([1])

In the case of barotropic fluid we obtain [5]

$$p \mid_{x=0^-} = p \mid_{x=0^+}, \tag{2.6}$$

$$v \mid_{x=0^-} = \lambda v \mid_{x=0^+}, \tag{2.7}$$

and

$$p \mid_{x=b^-} = p \mid_{x=b^+}, \tag{2.8}$$

$$\lambda v \mid_{x=b^-} = v \mid_{x=b^+}, \tag{2.9}$$

where α^-, α^+ denote the left-hand and the right-hand side limiting values of the magnitude.

To solve the problem, a state of the system at an initial instant of the process must be assumed. The initial condition is formulated as follows

$$p(x,t) \mid_{t=0^+} = \begin{cases} g(x) & \text{for } x<0, \\ 0 & \text{for } x>0. \end{cases} \tag{2.10}$$

Equations (2.1)–(2.4) together with the conditions (2.6)–(2.9) fully describe the phenomenon of the reflection and transition of an impulse wave through a porous layer. Their form shows that, apart from the parameters b and $\bar{k}$, characterizing the geometry of the system and the dissipative properties of the fluid in its viscous interaction with the walls of pores, an essential influence on the acoustic properties of the system is also exerted by the parameters of the pore structures of the layer. These parameters are explicitly seen in the continuity equation (2.4) and in the compatibility equations (2.7), (2.9). Interaction of the wave with the porous layer also depends on the form of an incident wave, given by the expression (2.10).

3. Solution of the problem

The acoustic fields in particular regions of the system, described by Eqs. (2.3), (2.4), may be represented by one of the muttually coupled quantities that characterize the motion of the fluid — its velocity or its pressure. The solution appears easier when these fields are represented by the velocities of fluid particles. This results from the possibility of replacing the compatibility conditions (2.6), (2.8) for pressure by the compatibility conditions for velocities. Opposite replacement does not apply.

([1])These types of continuity conditions are analogous to those required at sudden stepwise changes of cross-sections in the wave-guides transmitting disturbances [17].

http://rcin.org.pl

Making use of the continuity equations (2.2), (2.4), the motion equations (2.1), (2.3) take the form of wave equations

$$\frac{\partial^2 v}{\partial x^2} = \frac{1}{a_0^2}\frac{\partial^2 v}{\partial t^2}, \tag{3.1}$$

$$\frac{\partial^2 v}{\partial x^2} = \frac{1}{c_0^2}\left(\frac{\partial^2 v}{\partial t^2} + \bar{k}\frac{\partial v}{\partial t}\right). \tag{3.2}$$

The conditions (2.6), (2.8) lead to

$$\left.\frac{\partial v}{\partial x}\right|_{x=0^-} = \varkappa \left.\frac{\partial v}{\partial x}\right|_{x=0^+}, \tag{3.3}$$

$$\varkappa \left.\frac{\partial v}{\partial x}\right|_{x=b^-} = \left.\frac{\partial v}{\partial x}\right|_{x=b^+}. \tag{3.4}$$

However, the use of velocity fields appears inconvenient if we aim at observation of the interaction of the wave with the porous layer as a function of time. The reason for the difficulty is a discontinuity of the fluid velocity at both faces of the layer. From this point of view it is much more convenient to use the effective pressure field in the fluid which remains continuous on the layer faces. Thus, after solving the problem for the velocities of fluid particles, we shall again employ the continuity equations (2.2), (2.4), in order to express the acoustic field in terms of the pressure field in the fluid.

The initial-boundary problem of interaction of an impulse wave with a porous layer will be solved analytically in two steps. First, the interaction of a plane harmonic wave will be considered to obtain the explicit analytical expressions for the acoustic fields in the particular regions of the system. Thus the frequency characteristics will be determined. Secondly, an impulse wave falling on a porous layer will be dealt with. To this end, the incident wave will be decomposed into its harmonic components with a continuous distribution of spectrum and, next, the knowledge of the interaction of harmonic waves with porous layer, gained at the first step, will be employed to construct the solution for an arbitrary plane impulse wave.

3.1. Interaction of a harmonic wave

When a plane harmonic wave with the frequency f ($\omega = 2\pi f$) and an amplitude A_1 falls perpendicularly on a porous layer, the acoustic fields in the regions I and II consist of two waves moving in opposite directions, whereas the acoustic field in the region III is represented only by a wave leaving the layer. These waves are the sums of all the elementary waves suitably directed after consecutive reflections and transmissions of the incident wave on both faces of the porous layer.

The acoustic fields in the regions I and III being the solution of Eq. (3.1) can be expressed with the use of the functions

http://rcin.org.pl

$$v^{\mathrm{I}} = \mathrm{Re}\{(A_1 e^{-2\pi i\hat{k}x} - D_1 e^{2\pi i\hat{k}x})\, e^{i\omega t}\}, \tag{3.5}$$

$$v^{\mathrm{III}} = \mathrm{Re}\{A_3 e^{-2\pi i\hat{k}x}\, e^{i\omega t}\}. \tag{3.6}$$

The acoustic field in the region II, satisfying Eq. (3.2), is represented by

$$v^{\mathrm{II}} = \mathrm{Re}\{(A_2 e^{-2\pi ik'x} - D_2 e^{2\pi ik'x})\, e^{i\omega t}\}, \tag{3.7}$$

where A_α, D_α ($\alpha = 1, 2, 3$) denote the amplitudes of particular waves and Re ( ) stands for a real part of the complex expression. Wave numbers $\hat{k}$ and k' satisfy the following relationships:

$$\hat{k} = f/a_0, \qquad k'^2 = k^2\left(1 - i\frac{\sqrt{\varkappa}}{2\pi}\frac{k_0}{\hat{k}}\right), \tag{3.8}$$

where

$$k = f/c_0, \qquad k_0 = \bar{k}/c_0. \tag{3.9}$$

The expressions (3.5)–(3.7) contain four unknown amplitudes which must be determined from four compatibility conditions (2.7), (2.9), (3.3), (3.4).

Substituting Eqs. (3.5)–(3.7) into the appropriate compatibility conditions (2.7), (2.9), (3.3), (3.4), the following algebraic system of equations is obtained

$$\begin{aligned}
&A_1 - D_1 = \lambda(A_2 - D_2),\\
&A_1 + D_1 = \sqrt{\varkappa}\,K(A_2 + D_2),\\
&\lambda(A_2 e^{-2\pi i\eta K/\sqrt{\varkappa}} - D_2 e^{2\pi i\eta K/\sqrt{\varkappa}}) = A_3 e^{-2\pi i\eta},\\
&\sqrt{\varkappa}\,K(A_2 e^{-2\pi i\eta K/\sqrt{\varkappa}} + D_2 e^{2\pi i\eta K/\sqrt{\varkappa}}) = A_3 e^{-2\pi i\eta},
\end{aligned} \tag{3.10}$$

where

$$K = k'/k = \left(1 - i\frac{\sqrt{\varkappa}}{2\pi}\frac{\eta_0}{\eta}\right)^{\frac{1}{2}} \tag{3.11}$$

and $\eta_0 = b\,k_0$ is a dimensionless coefficient characterizing the dissipative properties of the fluid that saturates the porous layer. The magnitude $\eta = b\,\hat{k}$ can be interpreted as a dimensionless frequency of the incident wave.

The above equations make it possible to determine the ratios of the wave amplitudes propagating in the system to the amplitude of the incident wave as explicit functions of the quantities that characterize an internal structure of the pores, dissipative properties of the fluid and macroscopic geometry of the system for various frequencies of the incident wave. In particular, these equations enable us to determine the relationships between the reflection and the transmission coefficients of the harmonic wave falling on the porous layer and those parameters (see [4]).

http://rcin.org.pl

From Eqs. (3.10) we have

$$
\begin{aligned}
\bar{D}_1 &= \frac{1-\hat{K}^2}{1+\hat{K}^2-2i\hat{K}\operatorname{ctg}(z)}, \\
\bar{A}_2 &= (1+\hat{K})-(1-\hat{K})\bar{D}_1/2\varkappa f_v, \\
\bar{D}_2 &= (1+\hat{K})+(1-\hat{K})\bar{D}_1/2\varkappa f_v, \\
\bar{A}_3 &= e^{2\pi i\eta}(1-\bar{D}_1)\cos(z)-i\hat{K}(1+\bar{D}_1)\sin(z),
\end{aligned}
\tag{3.12}
$$

where

$$
(\bar{\ }) = (\ )/A_1, \qquad \hat{K} = \sqrt{\varkappa} f_v / K, \qquad z = 2\pi\eta K/\sqrt{\varkappa}.
$$

The expressions (3.5)–(3.7) together with Eqs. (3.12) fully describe the velocity fields of the fluid in particular regions brought about by the incident harmonic wave. From the conditions (2.7), (2.9) it follows that these fields are discontinuous on both faces of the layer.

To describe the problem by means of the pressure fields, continuous on both faces of the layer (see conditions (2.6), (2.8)), let us use the continuity conditions (2.2), (2.4). Then the pressure fields in particular regions, coupled with the velocity fields (3.5)–(3.7) will be given by the expressions

$$
p^{\mathrm{I}}(\tilde{x},\tilde{t}) = \operatorname{Re}\left\{\bar{A}_1\left(e^{2\pi i\eta(\tilde{t}-\tilde{x})} + \bar{D}_1 e^{2\pi i\eta(\tilde{t}+\tilde{x})}\right)\right\}, \tag{3.13}
$$

$$
p^{\mathrm{II}}(\tilde{x},\tilde{t}) = \operatorname{Re}\left\{\bar{A}_1\left(\tilde{A}_2 e^{-2\pi i\eta\left(\tilde{t}-\frac{K}{\sqrt{\varkappa}}\tilde{x}\right)} + \tilde{D}_2 e^{2\pi i\eta\left(\tilde{t}+\frac{K}{\sqrt{\varkappa}}\tilde{x}\right)}\right)\right\}, \tag{3.14}
$$

$$
p^{\mathrm{III}}(\tilde{x},\tilde{t}) = \operatorname{Re}\left\{\bar{A}_1\bar{A}_3 e^{2\pi i\eta(\tilde{t}-\tilde{x})}\right\}, \tag{3.15}
$$

where

$$
\bar{A}_1 = A_1 a_0 \rho_0^f / p_0^f
$$

is the dimensionless amplitude of the incident pressure wave in the fluid, and

$$
\tilde{A}_2 = \sqrt{\varkappa} K \bar{A}_2, \qquad \tilde{D}_2 = \sqrt{\varkappa} K \bar{D}_2 \tag{3.16}
$$

denote the amplitudes of the resultant pressure waves in a fluid saturating the porous layer related to the amplitude of the incident wave. In the relations (3.13)–(3.15) a dimensionless coordinate $\tilde{x}$ and a dimensionless time $\tilde{t}$ have been introduced. Suitable formulae are

$$
\tilde{x} = x/b, \qquad \tilde{t} = t/T = ta_0/b.
$$

http://rcin.org.pl

The spatial coordinate $\tilde{x}$ is a measure of the distance from the origin of the frame of reference expressed as a fraction of the thickness of the porous layer. The dimensionless time $\tilde{t}$ is a measure of time elapsed related to the time necessary for the wave in the bulk fluid to travel through a distance equal to the thickness of the layer.

Such a choice of independent variables is convenient both in the numerical calculations and in the diagrammatic illustration of the interaction of the wave and the porous layer.

3.2. Interaction of an impulse wave

Let us now make use of the knowledge of the response of the considered system to the harmonic wave and determine its response to an arbitrary impulse wave. The impulse wave travelling in the fluid towards a porous layer with the pressure distribution

$$p(\tilde{x}, \tilde{t}) = f(\tilde{t}-\tilde{x}), \qquad \tilde{x}<0,$$

satisfying the initial condition (2.10) will be decomposed into the harmonic components with the use of the Fourier transform [3].

We obtain

$$f(\tilde{t}-\tilde{x}) = \int_{-\infty}^{\infty} F(u)\, e^{2\pi i u(\tilde{t}-\tilde{x})}\, du, \tag{3.17}$$

where $F(u)$ is a spectrum of a function $f(z)$ defined as its Fourier transform

$$F(u) = \int_{-\infty}^{\infty} f(z)\, e^{-2\pi i z u}\, du. \tag{3.18}$$

Since $f(z)$ is a real function, its transform $F(u)$ becomes a Hermitian function satisfying the condition [3]

$$F^*(-u) = F(u),$$

where $F^*(\ )$ is a complex function coupled with the function $F(u)$. This means that the real part of the function $F(u)$ is an even function and its imaginary part is an odd function. Since $\exp(2\pi i u(t-\tilde{x}))$ is also a Hermitian function with respect to the variable u and a product of Hermitian functions remains a Hermitian function, the expansion (3.17) can be rearranged to become

$$f(\tilde{t}-\tilde{x}) = \int_{0}^{\infty} \mathrm{Re}\{2F(u)\, e^{2\pi i u(\tilde{t}-\tilde{x})}\}\, du. \tag{3.19}$$

The above expression can be interpreted as a decomposition of an arbitrary wave $f(\tilde{t}-\tilde{x})$ into the harmonic components and that is why $2F(u)$ appears to be a distribution density of the wave amplitude while $2F(u)du$ is an amplitude of a wave with a frequency contained in the range $\langle u, u+du\rangle$. The expression (3.19) makes it

http://rcin.org.pl

possible to consider the interaction of an impulse wave with a porous layer as a superposition of interactions of the particular harmonic components of its expansion.

Assuming that

$$u = \eta, \qquad \overline{A}_1 = 2F(\eta)\, d\eta,$$

$$p^{\alpha} = d\tilde{p}^{\alpha} \qquad (\alpha = \mathrm{I}, \mathrm{II}, \mathrm{III})$$

the pressure fields in the fluid corresponding to the harmonic components of the impulse wave are given by the formulae (3.13)–(3.15), while its resultant fields in the particular regions can be obtained by integrating these formulae over the whole frequency ranges for which the harmonic components exist, i.e. over $\eta \in [0; \infty)$.

Bearing in mind that all functions appearing in Eqs. (3.13)–(3.15) which depend on the frequency η are Hermitian functions, the expressions for the resultant fields take the form

$$\tilde{p}^{\mathrm{I}}(\tilde{x}, \tilde{t}) = \int_{-\infty}^{\infty} F(\eta)\left(e^{2\pi i\eta(\tilde{t}-\tilde{x})} + \overline{D}_1 e^{2\pi i\eta(\tilde{t}+\tilde{x})}\right) d\eta \tag{3.20}$$

for $\tilde{x} \leqslant 0$,

$$\tilde{p}^{\mathrm{II}}(\tilde{x}, \tilde{t}) = \int_{-\infty}^{\infty} F(\eta)\left(\tilde{A}_2 e^{-2\pi i\eta\left(\tilde{t}-\frac{K}{\sqrt{\varkappa}}\tilde{x}\right)} + \tilde{D}_2 e^{2\pi i\eta\left(\tilde{t}+\frac{K}{\sqrt{\varkappa}}\tilde{x}\right)}\right) d\eta \tag{3.21}$$

for $0 \leqslant \tilde{x} \leqslant 1$, and

$$\tilde{p}^{\mathrm{III}}(\tilde{x}, \tilde{t}) = \int_{-\infty}^{+\infty} F(\eta)\, \overline{A}_3 e^{2\pi i\eta(\tilde{t}-\tilde{x})}\, d\eta \tag{3.22}$$

for $\tilde{x} \geqslant 1$.

The formulae (3.20)–(3.22) satisfy the appropriate equations of the fluid dynamics (2.1)–(2.4) and the compatibility conditions (2.6)–(2.9) given on both faces of the porous layer.

Although the considerations are limited to the waves of an impulse type, the above expressions constitute a general form of solution for the perpendicular incidence of an arbitrary plane pressure wave on the rigid immovable layer of porous material immersed in the fluid.

The solution (3.20)–(3.22) for a plane harmonic wave of the frequency η' and the amplitude $\overline{A}_1$, whose spectrum (the Fourier transform) is represented by the Dirac delta

$$F(\eta) = \overline{A}_1 \delta(\eta - \eta'),$$

reduces to the form given by the formulae (3.13)–(3.15).

In the case in which a wave impinging on a porous layer constitutes a pressure impulse of the Dirac delta type with a unit area, its spectrum is a constant function equal to unity over the whole frequency range: $F(\eta) = 1$. Then the solution (3.20)–(3.22) takes the form which is called an impulse response of the system.

http://rcin.org.pl

4. Influence of the diffusion drag forces and the structure of pores on the reflection and transmission of an impulse wave

An explicit functional form of the solution (3.20)–(3.22) in the general form is very difficult to obtain. Main reason is the existence of viscous behaviour (diffusion resistance) of a fluid flowing through a porous layer; the walls of pores case a dissipation of mechanical energy. Moreover, the phase velocities of harmonic components depend on their frequency [16, 19]. This leads to a nonlinear relationship between the frequency η and the exponents of functions in the expression (3.21) that discribes the fluid pressure field in the porous layer. As a result, the wave profile during its travel through the porous layer undergoes certain deformations caused by damping and dispersion of the wave.

Remembering Eq. (3.11), these functions can be shown as a product of three terms characterizing those two phenomena. We have

$$e^{2\pi i\eta(\tilde{t}\pm K/\sqrt{\varkappa}\,\tilde{x})} = e^{\pm\eta_0\tilde{x}/2}\, e^{\mp\pi i\eta(K-1)^2\,\tilde{x}/\sqrt{\varkappa}}\, e^{2\pi i\eta(\tilde{t}\pm\tilde{x}/\sqrt{\varkappa})}. \tag{4.1}$$

The first term on the right-hand side of Eq. (4.1) characterizes damping, the second is responsible for a dispersion of a wave corresponding to its harmonic component represented by the third term.

In view of the decomposition (4.1), the fluid pressure field (3.21) in the porous layer takes the form

$$\tilde{p}^{\mathrm{II}}(\tilde{x},\tilde{t}) = e^{-\eta_0\tilde{x}/2}\int_{-\infty}^{\infty}\left(F(\eta)\,\tilde{A}_2 e^{\pi i\eta(K-1)^2\,\tilde{x}/\sqrt{\varkappa}}\right)e^{2\pi i\eta(\tilde{t}-\tilde{x}/\sqrt{\varkappa})}\,d\eta + e^{\eta_0\tilde{x}/2}\int_{-\infty}^{\infty}\left(F(\eta)\,\tilde{D}_2 e^{-\pi i\eta(K-1)^2\,\tilde{x}/\sqrt{\varkappa}}\right)e^{2\pi i\eta(\tilde{t}+\tilde{x}/\sqrt{\varkappa})}\,d\eta. \tag{4.2}$$

Viscous interaction of the fluid with the walls of pores causes not only damping and dispersion of waves propagating in the layer but also influences the course of reflection and penetration of waves on both faces of the porous layer. All the three effects together with the structure of the pores determine the values of the ratios of amplitudes $\overline{D}_1$, $\tilde{A}_2$, $\tilde{D}_2$, $\overline{A}_3$ of the harmonic components of the fluid pressure wave in particular regions ([2]).

An influence of viscous interaction and the structure of pores on the reflection and transmission of waves is particularly pronounced when a wave impinges on a porous half-space. In this case the acoustic field in the porous half-space is formed only by a wave penetrating through its surface and therefore the ratios of the amplitudes of harmonic components do not depend on the dispersion and damping taking place inside the porous medium.

([2]) Detailed analysis of the dependence of the reflection and transmission coefficients of harmonic waves through porous layer (closely connected with their amplitudes) on the dissipative properties of the fluid and the structure parameters of the porous layer is made in [4] for a broad range of frequencies of incident waves.

http://rcin.org.pl

4.1. Interaction of a wave with a porous half-space

Solution of interaction of an impulse wave with a porous half-space is a special case of the expressions (3.20) and (4.2) describing the pressure fields in the fluid alone in the region $\tilde{x} \leqslant 0$ and in the fluid saturating the pores of the layer. All that remains to be done is to enlarge the thickness of the porous layer up to infinity.

For $b \to \infty$ $(k_0 \neq 0)$ from Eqs. (3.20) and (4.2) it follows

$$\tilde{p}^{\mathrm{I}}(\tilde{x}, \tilde{t}) = \int_{-\infty}^{\infty} F(\eta)\left(e^{2\pi i\eta(\tilde{t}-\tilde{x})} + \hat{D}_1 e^{2\pi i\eta(\tilde{t}+\tilde{x})}\right) d\eta, \tag{4.3}$$

$$\tilde{p}^{\mathrm{II}}(\tilde{x}, \tilde{t}) = e^{-\eta_0 \tilde{x}/2} \int_{-\infty}^{\infty} F(\eta)\, \hat{A}_2 e^{\pi i\eta(K-1)^2 \tilde{x}/\sqrt{\varkappa}} e^{2\pi i\eta(\tilde{t}-\tilde{x}/\sqrt{\varkappa})}\, d\eta, \tag{4.4}$$

where

$$\hat{D}_1 = \frac{K-\sqrt{\varkappa} f_v}{K+\sqrt{\varkappa} f_v}, \qquad \hat{A}_2 = \frac{2K}{K+\sqrt{\varkappa} f_v} \tag{4.5}$$

and the dimensionless quantities $\tilde{x}$, $\tilde{t}$, η, η_0 are defined as

$$\tilde{x} = x/b_0, \qquad \tilde{t} = ta_0/b_0, \qquad \eta = b_0 k, \qquad \eta_0 = b_0 k_0.$$

The dimension b_0 is a certain constant reference length.

The squared modulus of the ratio $\hat{D}_1$ of the amplitudes given by the formula

$$\beta = |\hat{D}_1|^2 = \frac{(P-\sqrt{\varkappa} f_v)^2 + Q^2}{(P+\sqrt{\varkappa} f_v)^2 + Q^2}, \tag{4.6}$$

where

$$P = \mathrm{Re}(K) = \sqrt{\left(1+\sqrt{1+(\bar{k}/2\pi f)^2}\right)\Big/ 2},$$
$$Q = \mathrm{Im}(K) = -\sqrt{\left(-1+\sqrt{1+(\bar{k}/2\pi f)^2}\right)\Big/ 2} \tag{4.7}$$

represents the ratio of the amount of energy of the harmonic wave (or its harmonic component) reflected from the surface of the porous medium to the energy of the incident wave. This quantity is called the coefficient of reflection and enables us to define the role played by the diffusion forces and the structure of pores in the course of the phenomenon considered.

Dependence of the coefficient β on the dimensionless frequency $2\pi f/\bar{k}$ for two different pore structures is shown diagrammatically in Fig. 2. This coefficient is seen

http://rcin.org.pl

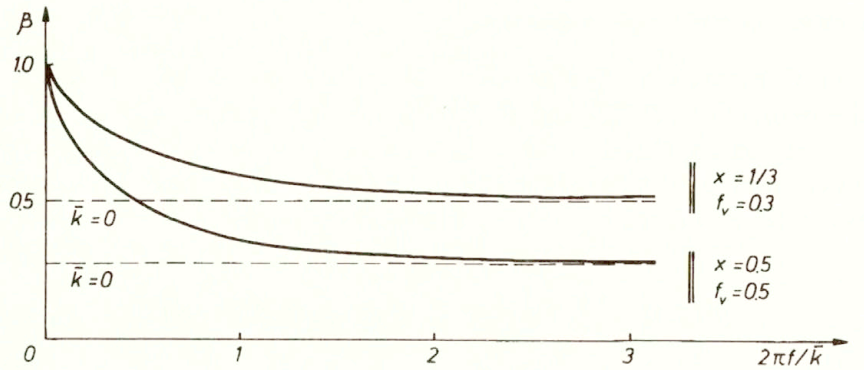

FIG. 2. Diagrams of the reflection coefficient β vs. dimensionless frequency $2\pi f/\bar{k}$ (for an acoustic plaster filled with air [20] $2\pi f/\bar{k}=1$ corresponds to $f=400$ Hz).

to be the largest for low frequency and gradually decreases with the increase of frequency to arrive asymptotically at the value

$$\beta_0 = \left(\frac{1-\sqrt{\varkappa} f_v}{1+\sqrt{\varkappa} f_v}\right)^2, \tag{4.8}$$

which is fully defined by the parameters of the pore structure.

The quantity β_0 is the reflection coefficient in the case of filling the half-space with an inviscid fluid ($\bar{k}=0$). This means that the influence of viscous friction on the reflection of the wave is considerable for lower frequencies

$$2\pi f/\bar{k} < 1, \quad (2\pi\eta/(\sqrt{\varkappa}\eta_0) < 1)$$

and fades away in the range of higher frequencies

$$2\pi f/\bar{k} \gg 1, \quad (2\pi\eta/(\sqrt{\varkappa}\eta_0) \gg 1), \tag{4.9}$$

where an essential role is played by the structure of pores, while the coefficient of reflection can be considered constant.

Bearing in mind that both the amplitude ratios $\hat{D}_1$ and $\hat{A}_2$ and an exponent of the function characterizing the dispersion of the waves depend on the viscous friction through the magnitude K, the conclusions with respect to the viscous friction can be directly referred to these magnitudes. This means that the amplitude ratios $\hat{D}_1$ and $\hat{A}_2$ are constant and the dispersion of waves fades away ($\exp(\pi i (K-1)^2 \eta \tilde{x}/\sqrt{x}) \to 1$) in the range of higher frequencies of harmonic components of their spectra.

In the case in which the main part of the spectrum of the wave impinging on a porous half-space corresponds to the frequency range satisfying the condition (4.9), an influence of the viscous friction on the reflection and transmission of the wave as well as its dispersion can be ignored. Then the expressions (4.3), (4.4) describing the

http://rcin.org.pl

fluid pressure fields in both regions assume, after inversion of the transforms, an explicit functional form. We obtain

$$\hat{p}^{\mathrm{I}}(\tilde{x},\tilde{t}) = f(\tilde{t}-\tilde{x}) + \beta_0^{1/2} f(\tilde{t}+\tilde{x}) \tag{4.10}$$

for $\tilde{x} \leqslant 0$ and

$$\hat{p}^{\mathrm{II}}(\tilde{x},\tilde{t}) = (1+\beta_0^{1/2})\, e^{-\eta_0 \tilde{x}/2} f(\tilde{t}-\tilde{x}/\sqrt{\varkappa}) \tag{4.11}$$

for $\tilde{x} \geqslant 0$.

From the expressions (4.10), (4.11) it follows that the amplitude of a wave penetrating the porous medium considerably increases as compared with the amplitude of an incident wave, although its global energy is smaller by the energy of the reflected wave. At the same time, the effect of wave concentration is the larger (apparently paradoxically), the greater is the part of the incident wave energy reflected from the surface of the porous medium.

The appearance of the concentration is caused by two reasons: a stepwise increase in the fluid mass transfer upon penetrating the wave into the porous medium, resulting from the continuity of the mass flux on its surface (see formula (2.7)) and a smaller velocity of penetration of disturbances in the fluid that fills the pores as compared with this velocity in the fluid alone (see formula (2.5)). Both reasons are closely connected with the pore structure parameters; the first one with the structural permeability parameter λ, the other with the parameter $\varkappa = \lambda/f_v$.

4.2. Interaction of a wave with a porous layer

Confining the considerations to the waves whose main part of the spectrum is present in the frequency range satisfying the condition (4.9) it is possible to obtain the explicit functional forms of the solution for the interaction of an impulse wave with the porous layer. The following approximations hold here true:

$$\hat{K} \simeq \sqrt{\varkappa} f_v,$$
$$z = 2\pi\eta K/\sqrt{\varkappa} \simeq -i\eta_0/2 + 2\pi\eta/\sqrt{\varkappa}. \tag{4.12}$$

With the use of them, the influence of the viscous friction on reflection and transmission of the wave on both faces of the porous layer as well as the dispersion of the wave within the layer can be eliminated.

Making use of Eqs. (4.12), the amplitude ratio $\overline{D}_1$ given by the formula $(3.12)_1$, takes the form

$$\overline{D}_1 = \beta_0^{-1/2}\left(1 - \frac{1-\beta_0}{1-\beta_0 d^2 e^{4\pi i\eta/\sqrt{\varkappa}}}\right),$$

where

$$d = \exp(-\eta_0/2).$$

http://rcin.org.pl

On expanding the expression

$$\frac{1}{1-\beta_0 d^2 e^{4\pi i\eta/\sqrt{\varkappa}}},$$

$$(\,|\,\beta_0 d^2 e^{4\pi i\eta/\sqrt{\varkappa}}\,|\,=\beta_0 d^2<1)$$

into a series, we get

$$\overline{D}_1=\beta^{1/2}\left[1-\frac{1-\beta_0}{\beta_0}\sum_{n=1}^{\infty}(\beta_0 d^2)^n\, e^{4\pi i n/\sqrt{\varkappa}}\right]. \tag{4.13}$$

Such a form of the amplitude ratio $\overline{D}_1$ and the approximations (4.12) make it possible to inverse the Fourier transforms in the expressions (3.20), (4.2), (3.22) in a straightforward manner. We arrive at

$$\tilde{p}^{\mathrm{I}}(\tilde{x},\tilde{t})=f(\tilde{t}-\tilde{x})+\beta^{1/2}f(\tilde{t}+\tilde{x})-\frac{1-\beta_0}{\beta_0^{1/2}}\sum_{n=1}^{\infty}(\beta_0 d^2)^n f(\tilde{t}+\tilde{x}-2n/\sqrt{\varkappa}).$$

$$\tilde{p}^{\mathrm{II}}(\tilde{x},\tilde{t})(1+\beta_0^{1/2})\left\{d^{\tilde{x}}\left[f(\tilde{t}-\tilde{x}/\sqrt{\varkappa})+\sum_{n=1}^{\infty}(\beta_0 d^2)^n f(\tilde{t}-(\tilde{x}+2n)/\sqrt{\varkappa})\right]\right. \tag{4.14}$$

$$\left.-\frac{d^{\tilde{x}}}{\beta_0^{1/2}}\sum_{n=1}^{\infty}(\beta_0 d^2)^n f(\tilde{t}+(\tilde{x}-2n)/\sqrt{\varkappa})\right\},$$

$$\tilde{p}^{\mathrm{III}}(\tilde{x},\tilde{t})=\frac{1-\beta_0}{\beta_0^{1/2}}\sum_{n=1}^{\infty}(\beta_0^{1/2}d)^{2n-1}f(\tilde{t}-(\tilde{x}-1)-(2n-1)/\sqrt{\varkappa}).$$

The pressure fields (4.14) in the case of an inviscid fluid ($\tilde{k}=0\to d=1$) constitute an exact solution to the problem of interaction of a wave with a porous layer. Their forms indicate that the decisive factor in the studied phenomenon are the pore structure parameters of the layer that determine the value of the coefficient β_0.

The phenomenon of reflection and transmission of the impulse wave (through a porous layer immersed in a fluid), whose initial profile is given by the function (Fig. 1)

$$f(\tilde{x},\tilde{t})\,|_{\tilde{t}=0}=e^{\tau(\tilde{x}-\tilde{x}_0)}\,(H(\tilde{x}-\tilde{x}_0)-1)\sin 2\pi\eta^0(\tilde{x}-\tilde{x}_0),$$

is depicted in Fig. 3. $H(\tilde{x})$ is the Heaviside function, η^0 and τ are the dimensionless frequency and the dimensionless coefficient of spatial fading of the wave, $\tilde{x}_0$ is the coordinate of the wave-front. The illustrative example refers to a dispersionless (but damped) interaction of the wave, the fluid pressure field of which is described by Eq. (4.14).

http://rcin.org.pl

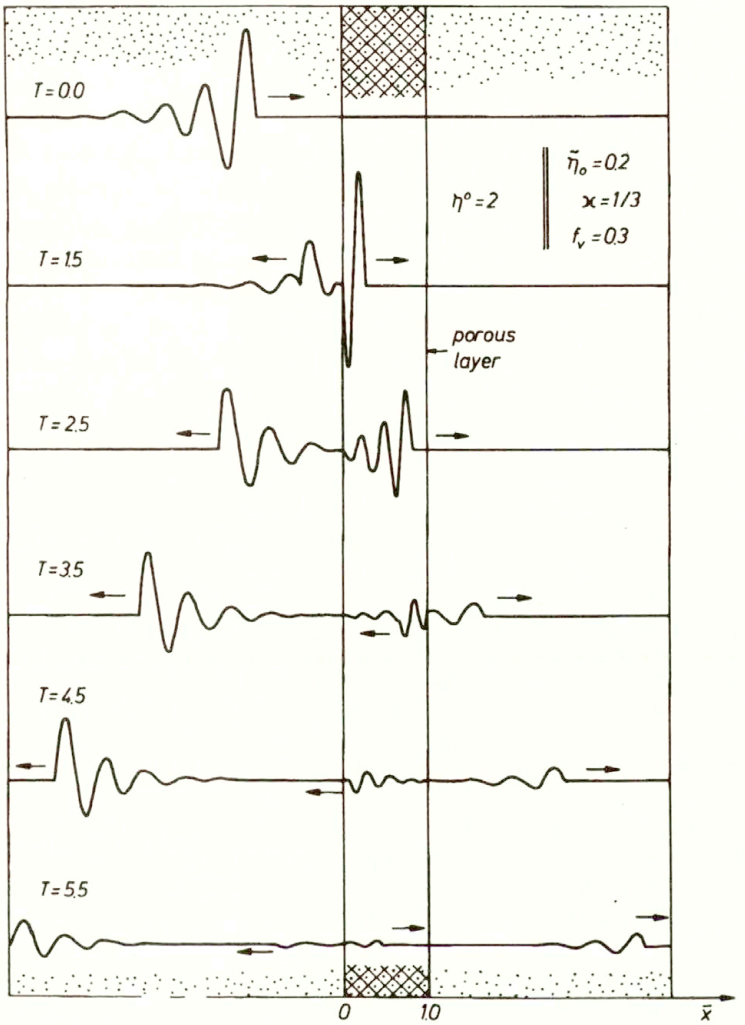

FIG. 3. Example of reflection and transmission of an impulse wave through a porous layer.

5. Final remarks

The paper deals with the interaction of a plane impulse wave propagating in a fluid in which an undeformable porous layer is immersed. Analytical solution is obtained with explicit forms of expressions for the pressure distributions in the particular regions of the considered system. Influence of the viscous forces in the pore walls and the parameters of the pore structure on the reflection and penetration of the wave is discussed.

http://rcin.org.pl

The obtained results appear important both from the cognitive and practical points of view. They can be useful in the design of the dynamic methods for the determination of internal parameters of a porous medium, for instance by use of the ultrasonic devices (when the main part of the wave spectrum is in the range of high frequencies). Interpretation of the experimentally obtained data may also be easier. Moreover, an analysis of reflection and penetration of an impulse audible waves through a porous layer when the main part of the spectrum is in the range of lower frequencies is made possible and seems to be interesting from the point of view of noise control.

The method proposed in the paper can be extended to cover the case of a deformable porous layer. The next paper will be devoted to this issue.

References

1. J. BEAR, M.Y. CORAPCIOGLU, *Fundamentals of transport phenomena in porous media*, Martinus Nijhoff, 1984.
2. T. BOURBIE, O. COUSSY, B. ZINSZNER, *Acoustics of porous media*, Gulf Publ. Company, Houston 1987.
3. R. BRACEWELL, *The Fourier transform and its applications* (in Polish), WNT, Warszawa 1968.
4. M. CIESZKO, *Acoustical properties of porous layer-undeformable halfspace system at normal incidence of harmonic wave*, Arch. Acoustics, **17**, 2, 261–267, 1992.
5. M. CIESZKO, J. KUBIK, *On the compatibility conditions in the fluid-fluid saturated porous solid contact problems*, Arch. Mech., **45**, 1, 77–91, 1993.
6. W. DERSKI, *Equations of motion for a fluid-saturated porous solid*, Bull. Acad. Polon. Sci., Série Sci. Techn., **26**, 1, 11–16, 1978.
7. W. DERSKI, S.J. KOWALSKI, *On the motion and mass continuity equations in a fluid-saturated porous medium*, Studia Geotech. et Mech., 2, 3–12, 1980.
8. D.L. JOHNSON, *Recent developments in the acoustic properties of porous media*, [in:] Frontiers in Physical Acoustics, XCIII Corso, Soc. Italiana di Fisica Bologna, 1986.
9. M. KACZMAREK, J. KUBIK, *Determination of material constants for classical physical and kinematic components of a fluid-saturated porous medium* (in Polish), Rozpr. Inż., **33**, 3, 589–609, 1985.
10. M. KACZMAREK, J. KUBIK, *Dynamic methods to determine material characteristics of saturated permeable media. I. Determination of elastic constants* (in Polish), IFTR Report, 16, 1993.
11. H.B. KINSBURY, *Determination of material parameters of poroelastic media*, [in:] Fundamentals of Transport Phenomena in Porous Media. [Ed.] J. BEAR, M. CORAPCIOGLU, Martinus Ninhoff, 579–615, 1984.
12. J. KUBIK, M. KACZMAREK, *Dynamic methods to determine material characteristics of saturated permeable media. II. Determination of parameters of pore structure* (in Polish), IFTR Reports, 17, 1993.
13. J. KUBIK, *Mechanics of deformable porous media with anisotropic permeability* (in Polish), IFTR Reports, **29**, 1981.
14. J. KUBIK, *A macroscopic description of geometrical pore structure of porous solids*, Int. J. Engng. Sci., **24**, 6, 971–980, 1986.
15. J. KUBIK, M. CIESZKO, *On internal forces in liquid-saturated porous medium*, Rozpr. Inż., **35**, 1, 55–70, 1987.
16. J. KUBIK, M. KACZMAREK, *Influence of pore structure on the propagation of harmonic waves in a permeable medium filled with a fluid* (in Polish), Rozpr. Inż., **36**, 3, 419–440, 1988.
17. E. SKUDRZYK, *Foundation of acoustics*, Springer, Vienna 1983.
18. J.E. WHITE, *Application of seismic waves*, Elsevier, 1983.

http://rcin.org.pl

19. C.H. YEW, P.N. JOGI, K.E. GRAY, *Estimation of the mechanical properties of fluid-saturated rocks using the measured wave motions*, J. Energy Res. Techn., **101**, 112–116, 1979.
20. C. ZWIKKER, C.W. KOSTEN, *Sound absorbing materials*, Elsevier, Amsterdam 1949.

POLISH ACADEMY OF SCIENCES
INSTITUTE OF FUNDAMENTAL TECHNOLOGICAL RESEARCH.

Received April 8, 1993.

http://rcin.org.pl

Arch.Mech., 45, 4, pp. 423–437, Warszawa 1993

A theory of viscoplastic shells including damage

M. KLEIBER (WARSZAWA) and F.G. KOLLMANN (DARMSTADT)

IN THIS PAPER we first extend the inelastic constitutive model of Bodner and Partom to include some damage effects. For this purpose the inelastic strain rate tensor is decomposed additively into a deviatoric and a volumetric term. Furthermore a non-associative flow rule is assumed. Then a parameter β can be defined which measures the ratio of the rate of the plastic dilactancy over the effective deviatoric inelastic strain rate. For this parameter we adopt an evolution equation first proposed by Gurson in the context of rate-independent plasticity. Finally, we suggest an evolution equation for the void volume fraction. We apply the inelastic constitutive model to a general inelastic shell theory presented by Kollmann and Mukherjee. We use a mixed variational principle which contains velocities and strain rates as variables to be varied independently. For axisymmetric shells a mixed Finite Shell Element is presented. We give some numerical results for a cylindrical shell made of pure titanium and loaded by internal pressure.

1. Introduction

WHILE THE THEORY of elastic shells is well established [1–3], inelastic shell theory is still a vivid research area. Inelasticity is understood in this paper as a rate-dependent behavior. KOLLMANN and MUKHERJEE [4] have proposed a general theory of inelastic shells under small deformations. They presuppose that the inelastic part of the deformation is governed by a unified constitutive model using internal variables. KOLLMANN and BERGMANN [5] have developed a finite element model for axisymmetric shells starting from the theory of Kollmann and Mukherjee. They use HART'S [6] inelastic constitutive model. In a further paper KOLLMANN, CORDTS and HACKENBERG [7] give a FEM formulation, using the inelastic constitutive model of BODNER and PARTOM (BPM) [5].

Significant achievements have been obtained to model the development of damage in combination with inelastic deformations. Most of the known results have been obtained under the assumption of rate-independent plasticity [9–12]. In this context the model of GURSON [6] is often used as a point of departure. Extensions covering some viscoplastic material models are now available as well [13, 14].

In this paper we first extend the theory of Bodner and Partom to include in it some damage effects. Then we show the application of the theory obtained to finite element modelling of shells starting from the formulation of Kollmann and Bergmann. Finally, we give some numerical results.

2. Bodner–Partom model with damage

First, we give a brief overview of the original BPM for small strains. We start from the additive decomposition of the total strain rate $\dot{\varepsilon}$ into an elastic part $\dot{\varepsilon}^e$ and an inelastic part $\dot{\varepsilon}^n$

http://rcin.org.pl

$$\dot{\boldsymbol{\varepsilon}} = \dot{\boldsymbol{\varepsilon}}^e + \dot{\boldsymbol{\varepsilon}}^n . \tag{2.1}$$

Bodner and Partom assume the inelastic flow rule for the isotropic material as

$$\dot{\boldsymbol{\varepsilon}}^n = \lambda \mathbf{s}, \tag{2.2}$$

where $\mathbf{s}$ is the stress deviator and λ is a scalar parameter. We define the following invariants

$$I_2(\dot{\boldsymbol{\varepsilon}}^n) := \frac{1}{2}\dot{\boldsymbol{\varepsilon}}^n : \dot{\boldsymbol{\varepsilon}}^n, \tag{2.3}$$

$$J_2 := \frac{1}{2}\mathbf{s} : \mathbf{s}, \tag{2.4}$$

where the colon (:) denotes the standard inner product of second order tensors.

From Eqs. (2.2), (2.3) and (2.4) follows the relation

$$\lambda^2 = \frac{I_2(\dot{\boldsymbol{\varepsilon}}^n)}{J_2}. \tag{2.5}$$

Bodner and Partom assume

$$I_2(\dot{\boldsymbol{\varepsilon}}^n) = f(J_2), \tag{2.6}$$

where the scalar function $f(J_2)$ is defined as

$$f(J_2) := D_0^2 \exp\left[-\left(\frac{A_2}{J_2}\right)^n\right]. \tag{2.7}$$

In Eq. (2.7) the quantities D_0 and n are material parameters and A_2 is defined as

$$A_2 := \frac{Z^2}{3}\left(\frac{n+1}{n}\right)^{1/n}. \tag{2.8}$$

The quantity Z is an internal variable which depends on the plastic work W_p

$$\dot{Z} = Z_1 + (Z_0 - Z_1)\exp\left(-\frac{mW_p}{Z_0}\right), \tag{2.9}$$

where m, Z_0 and Z_1 are again material parameters. Inserting Eq. (2.8) into Eq. (2.7) we obtain

$$f(J_2) = D_0^2 \exp\left[-\frac{n+1}{n}\left(\frac{Z^2}{3J_2}\right)^n\right]. \tag{2.10}$$

For the subsequent analysis it is convenient to replace $I_2(\dot{\boldsymbol{\varepsilon}}^n)$ by the effective inelastic strain rate

$$\dot{\bar{\varepsilon}}^n := \sqrt{\frac{2}{3}\dot{\boldsymbol{\varepsilon}}^n : \dot{\boldsymbol{\varepsilon}}^n} \tag{2.11}$$

http://rcin.org.pl

and J_2 by the effective deviatoric stress

$$\bar{\sigma} := \sqrt{\frac{3}{2}\mathbf{s}:\mathbf{s}}. \tag{2.12}$$

From Eqs. (2.11), (2.12) and (2.5) follows the relation

$$\lambda^2 = \frac{9}{4}\frac{(\dot{\bar{\varepsilon}}^n)^2}{\bar{\sigma}^2}. \tag{2.13}$$

Equations (2.6) and (2.11) give

$$(\dot{\bar{\varepsilon}}^n)^2 = \frac{4}{3} f(J_2). \tag{2.14}$$

Finally, Eqs. (2.10) and (2.12) result in

$$f(J_2) = D_0^2 \exp\left[-\frac{n+1}{n}\left(\frac{Z}{\bar{\sigma}}\right)^{2n}\right] := g^2(\bar{\sigma}). \tag{2.15}$$

With Eqs. (2.13), (2.14) and (2.15) the flow rule (2.2) takes the form

$$\dot{\boldsymbol{\varepsilon}}^n = \sqrt{3}\frac{D_0}{\bar{\sigma}}\sqrt{\exp\left[-\frac{n+1}{n}\left(\frac{Z}{\bar{\sigma}}\right)^{2n}\right]}\,\mathbf{s}. \tag{2.16}$$

Next, we compute the dissipated plastic work during the time increment $\Delta t = t_2 - t_1$.

By the definition

$$W_p = \int_{t_1}^{t_2} \boldsymbol{\sigma}:\dot{\boldsymbol{\varepsilon}}^n\,dt = \int_{t_1}^{t_2} \mathbf{s}:\dot{\boldsymbol{\varepsilon}}^n\,dt.$$

By considering the flow rule (2.2) and Eq. (2.13) we obtain

$$W_p = \int_{t_1}^{t_2} \bar{\sigma}\,\dot{\bar{\varepsilon}}^n\,dt \tag{2.17}$$

and by Eq. (2.14)

$$W_p = \int_{t_1}^{t_2} \frac{2}{\sqrt{3}}\, g(\bar{\sigma})\,\bar{\sigma}\,dt, \tag{2.18}$$

where the function $g(\bar{\sigma})$ is defined in Eq. (2.15).

To include damage into the BPM we first assume that the inelastic strain rate is non-deviatoric, i.e.

$$\dot{\boldsymbol{\varepsilon}}^n = \dot{\mathbf{e}}^n + \frac{1}{3}\operatorname{tr}\dot{\boldsymbol{\varepsilon}}^n\,\mathbf{1}, \tag{2.19}$$

http://rcin.org.pl

where $\dot{\boldsymbol{\varepsilon}}^n$ denotes the deviatoric part of $\dot{\boldsymbol{\varepsilon}}^n$, tr is the trace operator and $\mathbf{1}$ is the second order unit tensor. We presuppose that damage is caused by the nucleation and growth of voids and that compressibility of the plastic strains is the macroscopic consequence of the existence of voids. To include the effect of voids into our model we assume the following non-associative flow rule

$$\dot{\boldsymbol{\varepsilon}}^n = \lambda(\mathbf{s}+\beta\bar{\sigma}\,\mathbf{1}). \tag{2.20}$$

In Eq. (2.20) β is a parameter to be discussed below. Setting $\beta=0$ the inelastic flow rule of the undamaged material is recovered. Taking the trace of Eq. (2.20) leads to

$$\operatorname{tr}\dot{\boldsymbol{\varepsilon}}^n = 3\,\lambda\beta\bar{\sigma}. \tag{2.21}$$

A comparison of Eqs. (2.19), (2.20) and (2.21) reveals that

$$\dot{\boldsymbol{e}}^n = \lambda\,\mathbf{s}. \tag{2.22}$$

Defining the equivalent inelastic deviatoric strain rate $\dot{\bar{\varepsilon}}^n$ analogously to Eq. (2.11) we find from Eq. (2.13), replacing $\dot{\bar{\varepsilon}}^n$ by $\dot{\bar{e}}^n$, the following relation

$$\dot{\bar{e}}^n = \frac{2}{3}\lambda\bar{\sigma}. \tag{2.23}$$

Eliminating $\lambda\bar{\sigma}$ in Eqs. (2.21) and (2.23) we obtain

$$\beta = \frac{2}{9}\frac{\operatorname{tr}\dot{\boldsymbol{\varepsilon}}^n}{\dot{\bar{e}}^n}. \tag{2.24}$$

The parameter β is thus a measure of the ratio of the plastic dilatancy over the effective deviatoric inelastic strain rate.

To capture the effects of voids in the simplest possible way we assume that the only additional parameter entering our model is the void volume fraction ξ. In rate independent plasticity [9–12] the following equation describing the relation between the parameter β and the void volume fraction has been proposed

$$\beta = \frac{\xi}{3}\sinh\left(\frac{\operatorname{tr}\boldsymbol{\sigma}}{2\,\sigma_B}\right), \tag{2.25}$$

where σ_B is the current yield stress of the void-free base material. Since some studies [11] indicate that Eq. (2.25) underestimates the parameter β, we use in our work the approximation $\sigma_B = \bar{\sigma}/2$ so that Eq. (2.25) takes the form

$$\beta = \frac{\xi}{3}\sinh\left(\frac{\operatorname{tr}\boldsymbol{\sigma}}{\bar{\sigma}}\right). \tag{2.26}$$

Next, we compute the effective inelastic strain rate. From Eqs. (2.11) and (2.20) follows the relation

http://rcin.org.pl

(2.27) $$\dot{\bar{\varepsilon}}^n = \sqrt{\frac{4}{9} + 2\beta^2}\,\lambda\bar{\sigma}.$$

Define

(2.28) $$\kappa := \sqrt{1 + \frac{9}{2}\beta^2}.$$

Equations (2.27) and (2.28) give

(2.29) $$\dot{\bar{\varepsilon}}^n = \frac{2}{3}\kappa\lambda\bar{\sigma}.$$

However, for the model (2.13) without damage we have

$$\dot{\bar{\varepsilon}}^n = \frac{2}{3}\lambda\bar{\sigma}.$$

This motivates to replace the function $f(J_2)$ in Eq. (2.14) by a modified function $\hat{f}(\bar{\sigma}, \xi)$. Here $\bar{\sigma}$ denotes the effective stress of the material containing voids. This effective stress is related with the effective stress of the undamaged base material by

(2.30) $$\bar{\sigma} = (1-\xi)\bar{\sigma}_B.$$

Now we replace $\bar{\sigma}$ in Eq. (2.15) by $\bar{\sigma}_B$ according to Eq. (2.30) and obtain

(2.31) $$\hat{f}(\bar{\sigma}, \xi) := D_0^2 \exp\left[-\frac{n+1}{n}\left(\frac{(1-\xi)Z}{\bar{\sigma}}\right)^{2n}\right] = \hat{g}^2(\bar{\sigma}, \xi).$$

Equation (2.14) of the undamaged model is modified to become

(2.32) $$(\dot{\bar{\varepsilon}}^n)^2 = \frac{4}{3}\hat{f}(\bar{\sigma}, \xi).$$

From Eq. (2.29) we then obtain

(2.33) $$\lambda = \sqrt{3}\,\frac{\sqrt{\hat{f}(\bar{\sigma}, \xi)}}{\kappa\bar{\sigma}} = \sqrt{3}\,\frac{\hat{g}(\bar{\sigma}, \xi)}{\kappa\bar{\sigma}}.$$

Now the extended inelastic flow rule Eq. (2.20) takes the form

(2.34) $$\dot{\boldsymbol{\varepsilon}}^n = \sqrt{3}\,\frac{\hat{g}(\bar{\sigma}, \xi)}{\kappa\bar{\sigma}}(\mathbf{s} + \beta\bar{\sigma}\mathbf{1}).$$

Finally, an evolution equation for the void volume fraction ξ is needed. We assume

(2.35) $$\dot{\xi} = (1-\xi)\,\mathrm{tr}\,\dot{\boldsymbol{\varepsilon}}^n + B\dot{\bar{\varepsilon}}^n.$$

http://rcin.org.pl

The first term describes the growth of existing voids whereas strain-controlled nucleation of new voids is controlled by the second term. The parameter B takes a non-zero value only if the current value of the accumulated effective plastic strain

$$\bar{\varepsilon}^n = \int_0^t \dot{\bar{\varepsilon}}^n \, dt$$

exceeds its maximum value attained so far. By using Eqs. (2.21), (2,29) and (2.28), we obtain from Eq. (2.35) the relation

$$\dot{\xi} = \sqrt{3}\left[\frac{\sqrt{2}}{\kappa}\sqrt{\kappa^2-1}\,(1-\xi)+\frac{2}{3}B\right]\hat{g}(\bar{\sigma},\xi). \tag{2.36}$$

The BPM extended to cover the effects of damage is summarized in Box 1.

Box 1. Bodner–Partom model with damage

$$\dot{\boldsymbol{\varepsilon}}^n = \sqrt{3}\,\frac{\hat{g}(\bar{\sigma},\xi)}{\kappa\bar{\sigma}}(\bar{\mathbf{s}} + \beta\bar{\sigma}\mathbf{1})$$

$$\dot{\xi} = \sqrt{3}\left[\frac{\sqrt{2}}{\kappa}\sqrt{\kappa^2-1}\,(1-\xi)+\frac{2}{3}B\right]\hat{g}(\bar{\sigma},\xi)$$

$$\beta = \frac{\xi}{3}\sin h\left(\frac{\operatorname{tr}\boldsymbol{\sigma}}{\bar{\sigma}}\right)$$

$$\kappa = \sqrt{1+\frac{9}{2}\beta^2}$$

$$\hat{g}(\bar{\sigma},\xi) = D_0\sqrt{\exp\left[-\frac{n+1}{n}\left(\frac{(1-\xi)Z}{\bar{\sigma}}\right)^{2n}\right]}$$

$$\dot{Z} = Z_1 + (Z_0 - Z_1)\exp\left(-\frac{mW_p}{Z_0}\right)$$

$$W_p = \int_{t_1}^{t_2}\frac{2}{\sqrt{3}}\,\hat{g}(\bar{\sigma},\xi)\,\bar{\sigma}\,dt$$

B, D_0, Z_0, Z_1, m and n are material parameters

3. Inelastic shell theory

A shell $\mathscr{B}$ is the Cartesian product of a two-dimensional surface $\mathscr{S} \subset \mathscr{E}_3$ with a closed interval $[-h/2, h/2] \subset \mathfrak{R}$

http://rcin.org.pl

$$\mathscr{B} = \mathscr{S} \times [-h/2, h/2] \subset \mathscr{E}_3, \tag{3.1}$$

where $\mathscr{E}_3$ is the three-dimensional Euclidean space. The parameter h is the shell thickness. For simplicity we presuppose h = const. We introduce curvilinear coordinates Θ^α ($\alpha = 1,2$) on $\mathscr{S}$. In the following Greek indexes always range from 1 to 2 while Latin indexes range from 1 to 3. The two-dimensional surface $\mathscr{S}$ is the shell midsurface (SMS). On the SMS covariant and contravariant base vectors $\mathbf{a}_\alpha$ and $\mathbf{a}^\alpha$ can be defined in the standard manner. The first and second fundamental tensors on $\mathscr{S}$ are denoted as $\mathbf{a}$ and $\mathbf{b}$, respectively, and b is the determinant of $\mathbf{b}$. The covariant base vectors $\mathbf{g}$ of the shell $\mathscr{B}$ are given as

$$\begin{aligned} \mathbf{g}_\alpha &= \mu \mathbf{a}_\alpha, \\ \mathbf{g}_3 &= \mathbf{a}_3. \end{aligned} \tag{3.2}$$

Here

$$\mathbf{a}_3 := \frac{\mathbf{a}_1 \times \mathbf{a}_2}{\| \mathbf{a}_1 \times \mathbf{a}_2 \|} \tag{3.3}$$

is the unit normal vector on the SMS $\mathscr{S}$ and

$$\boldsymbol{\mu} := \mathbf{I} - \zeta \mathbf{b} \tag{3.4}$$

is the shifter tensor. In Eq. (3.4) $\mathbf{I}$ denotes the identity tensor on $\mathscr{S}$ and $\zeta \in [-h/2, h/2]$ is a normal coordinate. The determinant μ of the shifter tensor is

$$\mu = 1 - \zeta \operatorname{tr} \mathbf{b} + \zeta^2 b. \tag{3.5}$$

Following KOLLMANN and MUKHERJEE [4] we assume that the displacement vector $\mathbf{u}^*$ of the shell $\mathscr{B}$ (quantities with a star (e.g. $\mathbf{u}^*$) are defined on the shell $\mathscr{B}$ while unstarred quantities (e.g. $\mathbf{u}$) are defined on the SMS $\mathscr{S}$) can be presented as

$$\mathbf{u}^* := \mathbf{u} + \zeta \boldsymbol{\delta}, \tag{3.6}$$

where $\mathbf{u}$ is the displacement vector of the SMS $\mathscr{S}$ and $\boldsymbol{\delta}$ is the difference vector which describes the rotation of the normal vector $\mathbf{a}_3$ of the undeformed SMS during deformation. In this work it is assumed that the difference vector $\boldsymbol{\delta}$ is independent of the displacement vector $\mathbf{u}$ and, therefore, our formulation can account for transverse shear strains.

Denoting the strain tensor of the shell $\mathscr{B}$ by $\boldsymbol{\varepsilon}^*$ we take from [4] the following representations

$$\begin{aligned} \mu \varepsilon^*_{\alpha\beta} &= e_{\alpha\beta} + \zeta \kappa_{\alpha\beta}, \\ \mu \varepsilon^*_{\alpha 3} &= \gamma_\alpha + \zeta \rho_\alpha, \\ \varepsilon^*_{33} &= \gamma_3. \end{aligned} \tag{3.7}$$

http://rcin.org.pl

Here $e_{\alpha\beta}$, $\kappa_{\alpha\beta}$, γ_α, ρ_α and γ_3 are strain-like quantities defined on $\mathscr{S}$. In [4] also strain-displacement relations are given.

For inelastic analysis the additive decomposition (2.1) — with all quantities starred — is used. Following the approach of classical elastic shell theory the plane stress hypothesis ($\sigma^*_{33} = 0$) and the assumption $\dot{\varepsilon}^*_{33} = 0$ are introduced. Then the following relations hold [4]

$$\begin{aligned} \dot{\varepsilon}^*_{33} &= \frac{1}{\lambda+2G}\left[-\lambda\,\dot{\varepsilon}^{*\alpha}_{\alpha} + 2G\,\dot{\varepsilon}^{*n}_{33}\right], \\ \lambda\,\dot{\varepsilon}^{*k}_{k} &= \lambda'\left[\dot{\varepsilon}^{*\alpha}_{\alpha} + \dot{\varepsilon}^{*n}_{33}\right], \\ \dot{\varepsilon}^{*e}_{33} &= -\,\dot{\varepsilon}^{*n}_{33}. \end{aligned} \tag{3.8}$$

Here λ and G are the Lamé constants and λ' is the modified Lamé constant for plane stress.

Following [4] the lines of principal curvature are used as coordinate lines on the SMS $\mathscr{S}$ and physical components (denoted by $<\cdot>$) referred to these coordinates are introduced. For matrix notation we introduce a generalized displacement vector

$$\mathbf{v}^T := [\mathbf{u}^T, \boldsymbol{\delta}^T] \tag{3.9}$$

and a generalized strain vector

$$\boldsymbol{\gamma}^T := [e_{<11>}, e_{<22>}, e_{<12>}, \kappa_{<11>}, \kappa_{<22>}, \kappa_{<12>}, \gamma_{<1>}, \gamma_{<2>}, \rho_{<1>}, \rho_{<2>}], \tag{3.10}$$

where the superscrit T denotes matrix transposition. The general strain-displacement relation can be written as

$$\boldsymbol{\gamma} = \mathbf{L}_{\gamma v}\,\mathbf{v}, \tag{3.11}$$

where $\mathbf{L}_{\gamma v}$ is a linear operator. Component representations of this operator are given in [4]. Further, a general elasticity matrix is defined

$$\mathbf{D}_{\gamma\gamma} := \begin{bmatrix} \mathbf{D}_{ee} & \mathbf{D}_{e\varkappa} & \mathbf{O}_{3\times 4} \\ \mathbf{D}_{\varkappa e} & \mathbf{D}_{\varkappa\varkappa} & \mathbf{O}_{3\times 4} \\ \mathbf{O}_{4\times 3} & \mathbf{O}_{4\times 3} & \mathbf{D}_{\varphi\varphi} \end{bmatrix}. \tag{3.12}$$

All components of $\mathbf{D}_{\gamma\gamma}$ are derived in [4].

The inelastic strain rates contribute the following rates of inelastic pseudo-forces and pseudo-moments

$$\begin{aligned} \dot{N}^n_{<ij>} &= 2G \int_{-h/2}^{h/2} \dot{\varepsilon}^{*n}_{<ij>}\, d\zeta, \\ \dot{M}^n_{<ij>} &= 2G \int_{-h/2}^{h/2} \dot{\varepsilon}^{*n}_{<ij>}\, \zeta\, d\zeta. \end{aligned} \tag{3.13}$$

http://rcin.org.pl

They can be combined to form a vector of generalized inelastic pseudo-force rates

$$[\dot{\mathbf{F}}^{n}]^T := \{[\dot{N}^{n}_{<\alpha\beta>}]^T, \dot{N}^{n}_{<33>}, [\dot{M}^{n}_{<\alpha\beta>}]^T \dot{M}^{n}_{<33>}, [\dot{N}^{n}_{<\alpha 3>}]^T, [\dot{M}^{n}_{<\alpha 3>}]^T\}\}, \tag{3.14}$$

where e.g. $[\dot{N}^{n}_{<\alpha\beta>}]^T$ and $[\dot{N}^{n}_{<\alpha 3>}]^T$ are arranged as $e^T_{<\alpha\beta>}$ and $\gamma^T_{<\alpha>}$, respectively, in Eq. (3.10).

Finally, boundary conditions must be specified. The boundary $\partial\mathscr{B}$ of the shell can be decomposed as

$$\partial\mathscr{B} = \mathscr{S}^+ \cup \mathscr{S}^- \cup \mathscr{S}^c, \tag{3.15}$$

where $\mathscr{S}^+ = \{\mathscr{S}^+ \subset \partial\mathscr{B} : \zeta = h/2\}$ and $\mathscr{S}^- = \{\mathscr{S}^- \subset \partial\mathscr{B} : \zeta = -h/2\}$ are the lateral surfaces of $\mathscr{B}$ and $\mathscr{S}^c$ is the edge. We consider only the case, when tractions are prescribed on $\mathscr{S}^+$ and $\mathscr{S}^-$ and displacements on $\mathscr{S}^c$. In this case the tractions can be considered in a generalized load vector $\dot{\mathbf{F}}_L$. Details of this load vector can be found in [4] and [5].

The deformation of the inelastic shell is governed by the following variational principle [4]

$$\delta \int_{\mathscr{S}} \left[\frac{1}{2} \dot{\gamma}^T \mathbf{D}_{\gamma\gamma} \dot{\gamma} - 2\dot{\gamma}^T \mathbf{D}_{\gamma\gamma} \mathbf{L}_{\gamma\upsilon} \dot{\upsilon} + \dot{\mathbf{F}}_L \dot{\upsilon} + [\dot{\mathbf{F}}^{n}]^T \mathbf{L}^{n}_{\gamma\upsilon} \dot{\upsilon} \right] d\mathscr{S} = 0, \tag{3.16}$$

where $\mathbf{L}^{N}_{\gamma\upsilon}$ is a linear operator defined by KOLLMANN and BERGMANN [5] and dS is the area element on the shell SMS $\mathscr{S}$.

The variational principle contains only displacement rates and strain rates and not stress rates. This is a major advantage in inelastic shell analysis since the assumption (3.6) is reasonable that the displacements are distributed linearly over the shell thickness. As a consequence of this basic kinematic assumption, also the strains are distributed linearly over the shell thickness (compare Eqs. $(3.7)_1$ and $(3.7)_3$), where quadratic terms in ζ are neglected. A reasoning for this approximation is given by Kollmann and Mukherjee. However, unlike the elastic shell analysis, the distribution of the stresses and their rates over the shell thickness is not known *a priori* in inelastic analysis. Rather, it changes in time and space and is a part of the solution sought. For this reason it is not possible to compute from stress resultants and moments — which arise naturally in any shell theory including stresses — the stresses in arbitrary points of the shell $\mathscr{B}$.

4. Mixed finite element model

We shall derive the discrete version of the variational principle (3.16). For this purpose we introduce different shape functions N and $\overline{N}$ for displacement rates and strain rates, respectively. We denote the nodal values of the velocities and strain rates by $\hat{\dot{\upsilon}}$ and $\hat{\dot{\gamma}}$, respectively. Then the discrete approximations of the velocities and strain rates are given as

$$\dot{\upsilon} = N\hat{\dot{\upsilon}},$$

http://rcin.org.pl

(4.1)
$$\dot{\boldsymbol{\gamma}} = \overline{N}\,\hat{\dot{\boldsymbol{\gamma}}},$$

Using standard techniques we obtain the following mixed FEM from Eq. (3.16)

(4.2)
$$\begin{aligned} \mathbf{K}_{\gamma\gamma}\,\hat{\dot{\boldsymbol{\gamma}}} - \mathbf{K}_{\gamma v}\,\hat{\dot{\mathbf{v}}} &= \mathbf{0}, \\ -\mathbf{K}_{\gamma v}^{T}\,\hat{\dot{\boldsymbol{\gamma}}} &= -\dot{\mathbf{P}}_{L} - \dot{\mathbf{P}}_{N}. \end{aligned}$$

The terms in Eqs. (4.2) have the following representations.

(4.3)
$$\mathbf{K}_{\gamma\gamma} := \int_{\mathscr{S}} \overline{\mathbf{N}}^{T}\,\mathbf{D}_{\gamma\gamma}\,\overline{\mathbf{N}}\,d\mathscr{S},$$

(4.4)
$$\mathbf{K}_{\gamma v} := \int_{\mathscr{S}} \overline{\mathbf{N}}^{T}\,\mathbf{D}_{\gamma\gamma}\,\mathbf{L}_{\gamma v}\,\mathbf{N}\,d\mathscr{S},$$

(4.5)
$$\dot{\mathbf{P}}_{L} := \int_{\mathscr{S}} \mathbf{N}^{T}\,\dot{\mathbf{F}}_{L}\,d\mathscr{S},$$

(4.6)
$$\dot{\mathbf{P}}_{N} := \int_{\mathscr{S}} \mathbf{N}^{T}\,(\mathbf{L}_{\gamma v}^{n})^{T}\,\dot{\mathbf{F}}^{n}\,d\mathscr{S}.$$

In this study we confine ourselves to axisymmetric shells and use a conical element according to Fig. 1 which has been originally proposed for a displacement formulation by ZIENKIEWICZ *et al.* [15]. KOLLMANN, CORDTS and HACKENBERG [7] have shown by numerical experiments that the mixed model Eqs. (4.2) gives satisfactory results only if the order of approximation of the strain field is equal or greater than that of the displacement field. In the present work we use first order approximations for both fields.

Denote the arc length on the conical element by s, its mean radius by R, its length by L and the angle of aperture as α. Introduce a dimensionless coordinate η by the transformation

(4.7)
$$s = L\left(\frac{\eta}{2} + \frac{R}{L\sin\alpha}\right)$$

with $\eta \in [-1, 1]$. Then the shape functions for our mixed element are

(4.8)
$$\begin{aligned} N_1(\eta) = \overline{N}_1(\eta) &= \frac{1}{2}(1+\eta), \\ N_2(\eta) = \overline{N}_2(\eta) &= \frac{1}{2}(1-\eta). \end{aligned}$$

Details of the numerical implementation of the model are omitted here for the sake of brevity. We only mention the following points. Evaluation of the Bodner–Partom

http://rcin.org.pl

model with damage requires the knowledge of stresses. The stresses are computed from the Hooke's generalized law with elastic strains ε^e obtained from (2.1). The rates of the inelastic pseudo-forces and pseudo-moments (3.13), are computed by numerical integration over the shell thickness. The Gauss rule with five quadrature points is used. For time integration of the inelastic constitutive model (see Box 1) an implicit algorithm developed by CORDTS and KOLLMANN [13] is employed. A more detailed description of the implementation can be found in [2].

5. Numerical results

Our numerical results are obtained for commercially pure titanium [8] at room temperature. The material data are given in Table 1. The parameter values for E, υ, Z_0, Z_1, D_0, n and m, which describe the BPM without damage, are taken from [5]. For titanium no data for either the initial value ξ_0 of the void volume fraction or for the parameter B controlling nucleation of new voids are available in the literature. Therefore, our computations should be considered as numerical experiments rather than realistic simulations.

Table 1. Material data of Bodner–Partom model with damage for high purity titanium.

Quantity	Unit	Value
E	MPa	117 940
υ	–	0.34
Z_0	MPa	1150
Z_1	MPa	1400
D_0	s^{-1}	10 000
n	–	1
m	–	100
B	–	5
ξ_0	–	0.01

For our numerical test we consider a cylindrical shell with diameter $d = 500$ mm, length $l = 1000$ mm and thickness $h = 10$ mm. Both edges of the shell are simply supported with no displacements of the boundaries. The shell is symmetric with respect to the plane $z = 0$ (z is the axial coordinate of cylindrical coordinate system). One half of the shell is discretized by 70 finite elements of equal length. The shell is loaded by internal pressure with the following history. The pressure increases linearly from 0 to 13 MPa within 1 s. Then it is held constant over 9 s and finally it decreases linearly within 1 s to 0 MPa.

http://rcin.org.pl

Figure 1 shows the distribution of the deflection w over the axis of the shell at the end of the hold time ($t = 10$ s) with and without damage. Clearly in the middle segment of the shell ($0 \leqslant z \leqslant 200$ mm) a pure membrane deformation prevails. In the rest of the shell bending effects are dominant. The strong influence of damage effects can be clearly seen.

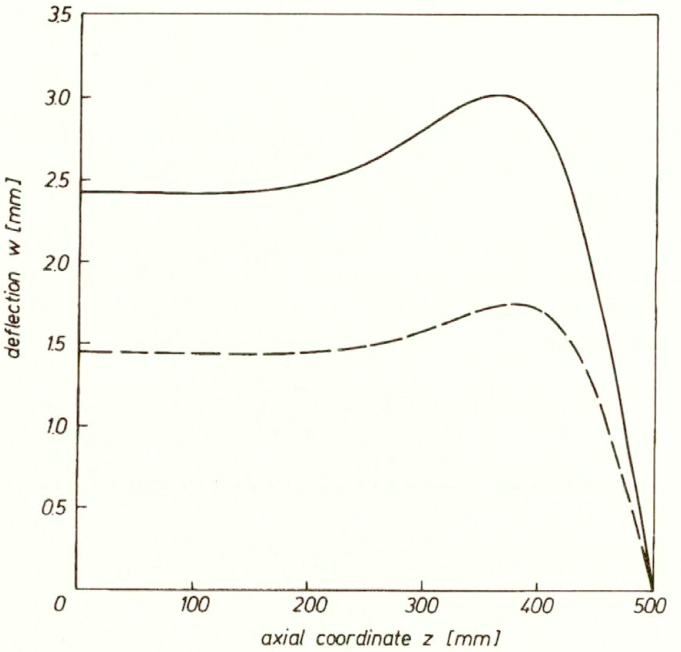

FIG. 1. Deflection of cylindrical shell under pressure (——— with damage, – – – – without damage).

Figure 2 presents the history of the effective inelastic strain rate $\dot{\bar{\varepsilon}}^{in}$ tensor at a point of the shell ($z = 408.9$ mm) where bending effects are dominant. In both cases (with and without damage) a sharp increase of $\dot{\bar{\varepsilon}}^{in}$ during the loading phase can be observed. However the peak values are different ($\dot{\bar{\varepsilon}}^{in}_{\text{damaged}} = 4.57 \cdot 10^{-3}\ s^{-1}$, $\dot{\bar{\varepsilon}}^{in}_{\text{undamaged}} = 3.67 \cdot 10^{-3}\ s^{-1}$). During the hold phase $\dot{\bar{\varepsilon}}^{in}$ drops off sharply first. The drop-off rate is larger for the undamaged material. The equivalent inelastic strain rate $\dot{\bar{\varepsilon}}^{in}$ is significantly smaller for the undamaged material at the end of the hold time. During the unloading phase $\dot{\bar{\varepsilon}}^{in}$ drops to zero for the damaged and undamaged material.

In Fig. 3 the distribution of the axial stress σ_{zz} at different time instants over the normal coordinate ζ ($-h/2 \leqslant \zeta \leqslant M/2$) at the section $z = 408.9$ mm is given for the damaged material. In this section again bending effects prevail. The curved stress distributions show the influence of the material nonlinearity since for elastic materials

http://rcin.org.pl

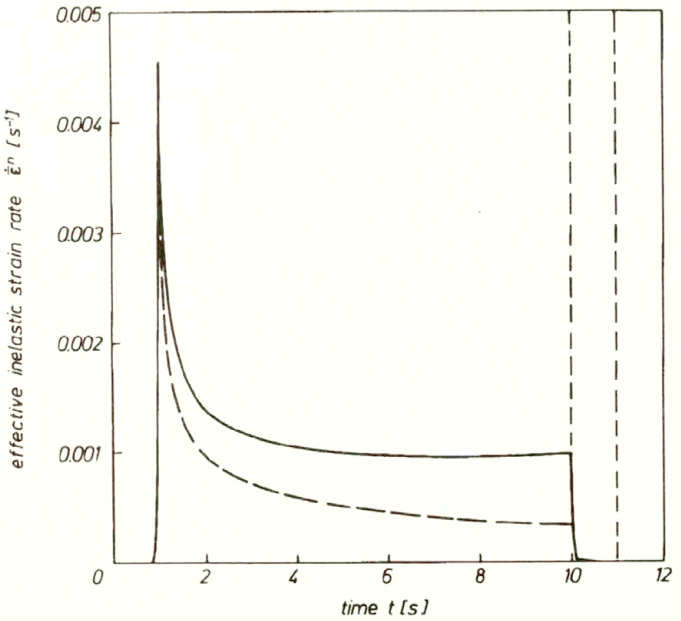

FIG. 2. History of inelastic strain rate at point (z = 408.9 mm, r = 254.8 mm), legend as in Fig. 1.

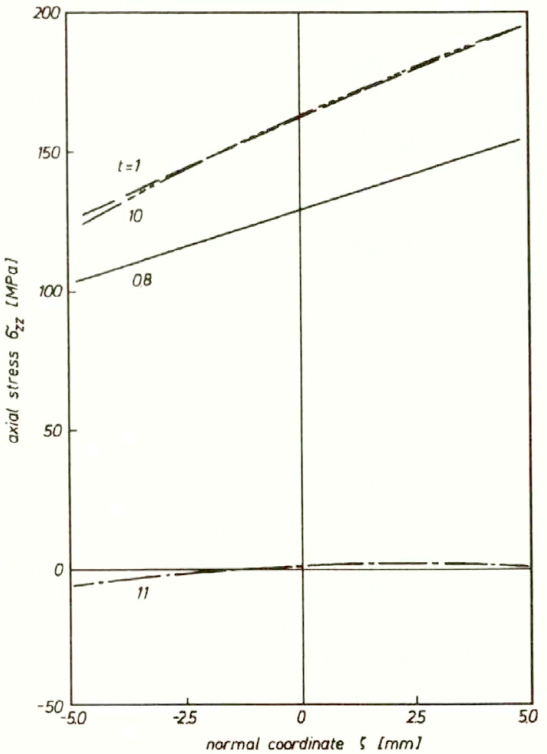

FIG. 3. Distribution of axial stress over shell thickness in section z = 408.9 mm for damaged material.

http://rcin.org.pl

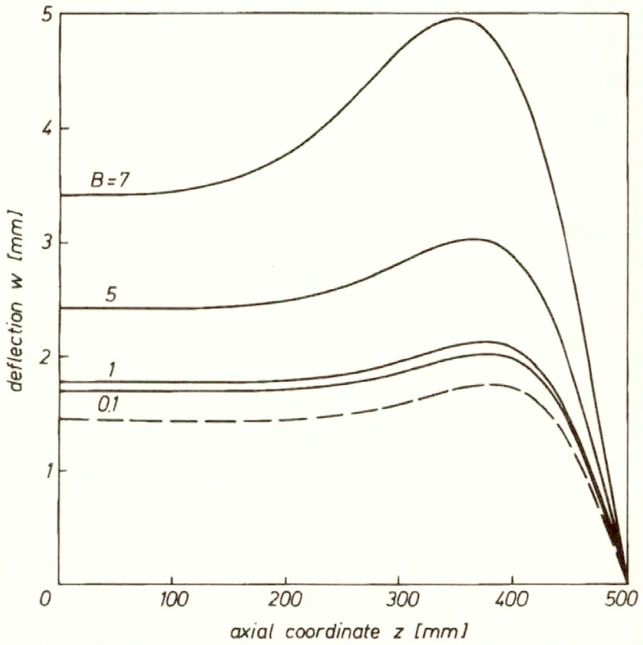

FIG. 4. Influence of the void nucleation parameter B on the deflection of the shell ($t = 10$ s).

the stress distributions would be linear. During the hold time ($1\ s \leqslant t \leqslant 10$ s) a slight redistribution of the axial stress can be observed. For $t = 11$ s, where the shell is completely unloaded, a residual stress field σ_{zz} is observed.

Finally, in Fig. 4 we present a sensitivity analysis showing the influence of the parameter B controlling nucleation of new voids on the deflection of the shell. It can be seen that with increasing values of B the deflection grows substantially. Therefore, it has to be emphasized that for any realistic analysis this parameter has to be identified very carefully.

6. Conclusions

In this paper we first presented an extension of the BPM to include some damage effects. The methodology suggested in Sec. 2 can be used to extend other uniform viscoplastic models to include damage effects. Next, we briefly discussed an inelastic shell theory originally proposed by MUKHERJEE and KOLLMANN [4]. For this theory we gave a mixed finite element formulation and presented some numerical results for a cylindrical shell under variable internal pressure. It may be observed that the full merits of viscoplastic model with damage can only be seen for a finite shell element model capturing geometrical nonlinearity. Such a model is presently under development.

http://rcin.org.pl

References

1. P.M. NAGHDI, *The theory of plates and shells* [in:] Encyclopedia of Physics, S. FLÜGGE, C. TRUESDELL [Eds.], Vol. VI a/2, Berlin, Heidelberg, New York 1972.
2. Y. BASAR, W. KRÄTZIG, *Mechanik der Flächentragwerke*, Friedr. Vieweg u. Sohn, Braunschweig – Wiesbaden 1985.
3. W. PIETRASZKIEWICZ, *Introduction to the non-linear theory of shells*, Ruhr – Universität, Bochum 1977.
4. F.G. KOLLMANN, S. MUKHERJEE, *A general, geometrically linear theory of inelastic thin shells*, Acta Mech., **57**, 41 – 67, 1985.
5. F.G. KOLLMANN, V. BERGMANN, *Numerical analysis of viscoplastic axisymmetric shells based on a hybrid strain finite element*, Comp. Mech., 7, 89 – 105, 1990.
6. E.W. HART, *Constitutive relations for the non-elastic deformation of metals*, Trans. ASME, J. Engng. Mat. Technol., **98**, 193 – 202, 1976.
7. F.G. KOLLMANN, D. CORDTS, H – P. HACKENBERG, *A family of mixed and hybrid finite elements for the numerical analysis of viscoplastic shells of revolution* [in:] Nonlinear Computational Mechanics, P. WRIGGERS, W. WAGNER [Eds.] Springer, Berlin, Heidelberg, New York, 360 – 374, 1991.
8. S.R. BODNER, Y. PARTOM, *Constitutive equations for elastic-viscoplastic strain-hardening materials*, Trans. ASME, J. Appl. Mech., **42**, 385 – 389, 1975.
9. A.L. GURSON, *Continuum theory of ductile rupture by void nucleation and growth, Part I. Yield criteria and flow rules for porous ductile materials*, Trans. ASME, J. Engn. Mat. Technol., **99**, 2, 2 – 15, 1977.
10. A. NEEDLEMAN, J.R. RICE, *Limits to ductility set by plastic flow localization* [in:] Mechanics of Sheet Metal Forming, D.P. KOSTINEN, N.M. WANG [Eds.], Plenum, 237 – 266, 1978.
11. V. TVERGAARD, A. NEEDLEMAN, *Analysis of the cup-cone fracture in a round tensile bar*, Acta Metall., **32**, 157 – 169, 1984.
12. M. KLEIBER, *Numerical study on necking-type bifurcation in void-containing elastic-plastic material*, Int. J. Sol. Struct., **20**, 191 – 210, 1984.
13. J. LEMONDS, A. NEEDLEMAN, *Finite element analysis of shear localization in rate and temperature dependent solids*, Mechanics of Materials, **5**, 339 – 361, 1986.
14. M. KLEIBER, *Computational coupled non-associative thermo-plasticity*, Comp. Meths. Appl. Mech. Engng., **90**, 943 – 967, 1991.
15. O.C. ZIENKIEWICZ, J. BAUER, E. ONATE, *A simple and efficient element for axisymmetric shells*, Int. J. Num. Meth. Engng., **11**, 1545 – 1558, 1977.
16. D. CORDTS, F.G. KOLLMANN, *An implicit time integration scheme for inelastic constitutive equations with internal state variables*, Int. J. Num. Engng., **23**, 533 – 544, 1986.

POLISH ACADEMY OF SCIENCES
INSTITUTE OF FUNDAMENTAL TECHNOLOGICAL RESEARCH
and
TECHNISCHE HOCHSCHULE DARMSTADT
FACHGEBIET MASCHINENELEMENTE UND MASCHINENAKUSTIK, DARMSTADT, GERMANY.

Received July 12, 1993.

http://rcin.org.pl

Arch.Mech., 45, 4, pp. 439–455, Warszawa 1993

Bounds on energy in discrete deformable systems

A. GAWĘCKI (POZNAŃ)

SEVERAL BOUNDING theorems concerning the elastic and complementary energies in deformable systems are derived in the paper. Considerations have been carried out in the frame of geometrically linear theory, using FEM-oriented discrete description. All deformations due to physically nonlinear properties of the material are treated as effects of the presence of distortions imposed on the linear elastic structure. A comprehensive example of elastic-plastic and slackened structures illustrates the theory.

1. Introduction

THE MAIN AIM of the paper is to evaluate the elastic energy of deformable systems subjected to given loads or prescribed displacements. The distortional approach has been applied in considerations. The essence of this approach consists in the assumption that all deformations due to nonlinearity of the material (plasticity, nonlinear elasticity, effects of gaps, viscosity, cracking) or non-mechanical effects (temperature, shrinkage, material defects, manufacturing imperfections) are caused by the presence of distortions imposed on the linear elastic structure. All considerations are carried out in the frame of the geometrically linear theory. Nevertheless, the results obtained here are valid for a relatively wide class of important problems of deformable system mechanics. The main idea of the work was already presented in 1989 [1]. A numerical example, enclosed in Sec. 5, illustrates the theoretical considerations.

Let us assume that elastic coefficients of the material remain constant and are independent of distortions. Current mechanical state of the system can then be described by the following system of relations:

$$\begin{aligned} &\mathbf{C}\mathbf{u} = \boldsymbol{\varepsilon} = \boldsymbol{\varepsilon}_E + \boldsymbol{\varepsilon}_R, \\ &\mathbf{C}^T\boldsymbol{\sigma} = \mathbf{p}, \\ &\boldsymbol{\sigma} = \mathbf{E}\boldsymbol{\varepsilon}_E. \end{aligned} \tag{1.1}$$

In Eqs. (1.1) the FEM-oriented matrix description, applied by G. MAIER [2] and A. BORKOWSKI [3], is used. Here $\mathbf{p}$, $\mathbf{u}$, $\boldsymbol{\sigma}$ and $\boldsymbol{\varepsilon}$ denote vectors which represent components of loads, displacements, stresses and strains, respectively. $\mathbf{C}$ is the matrix of geometric compatibility and $\mathbf{E}$ represents the strictly positive definite, square and symmetric matrix of elasticity. The strain vector $\boldsymbol{\varepsilon}$ is divided into two parts, namely elastic $\boldsymbol{\varepsilon}_E$ and distortional $\boldsymbol{\varepsilon}_R$ ones. Superscript T denotes the matrix transpose.

http://rcin.org.pl

It should be pointed out here that in the FEM-oriented description both the surface and body forces are treated as loads acting at nodes of finite elements. Therefore, after discretization, they are indistinguishable and a relationship with the classical continuum approach requires some additional considerations. Nevertheless, the results obtained in the present paper are valid for suitable discretized shells, plates or skeletal structures and also for three-dimensional bodies.

The vectors of state variables are functions of time t, $0 \leqslant t \leqslant t^*$. We assume that a structure is initially stress-free in its virgin state (i.e. $\boldsymbol{\sigma}(0) \equiv \mathbf{0}$, and consequently: $\mathbf{p}(0) \equiv \mathbf{0}, \mathbf{u}(0) \equiv \mathbf{0}. \boldsymbol{\varepsilon}(0) \equiv \mathbf{0}$). In Eqs. (1.1) all the vectors of state variables correspond to $t = t^*$ (i.e. $\mathbf{p} = \mathbf{p}(t^*)$, $\mathbf{u} = \mathbf{u}(t^*)$, $\boldsymbol{\sigma} = \boldsymbol{\sigma}(t^*)$, $\boldsymbol{\varepsilon} = \boldsymbol{\varepsilon}(t^*)$), but the path of loading is unspecified.

From Eqs. (1.1) one can derive the following relationship:

$$\mathbf{p} = \mathbf{K}\mathbf{u} - \mathbf{C}^T\mathbf{E}\boldsymbol{\varepsilon}_R, \qquad \mathbf{K} = \mathbf{C}^T\mathbf{E}\mathbf{C}, \tag{1.2}$$

where $\mathbf{K}$ is the strictly positive definite stiffness matrix of the purely linear elastic structure. Relations (1.1) and (1.2) lead to the following formulae (cf. J.A. KÖNIG [4]):

$$\begin{aligned}
&\mathbf{u} = \mathbf{u}_e + \mathbf{u}_r, \quad && \mathbf{u}_e = \mathbf{K}^{-1}\mathbf{p}, && \mathbf{u}_r = \mathbf{K}^{-1}\mathbf{C}^T\mathbf{E}\boldsymbol{\varepsilon}_R,\\
&\boldsymbol{\sigma} = \boldsymbol{\sigma}_e + \boldsymbol{\sigma}_r, \quad && \boldsymbol{\sigma}_e = \mathbf{E}\mathbf{C}\mathbf{K}^{-1}\mathbf{p}, && \boldsymbol{\sigma}_r = \mathbf{Z}\boldsymbol{\varepsilon}_R,\\
&\mathbf{Z} = \mathbf{E}\mathbf{C}\mathbf{K}^{-1}\mathbf{C}^T\mathbf{E} - \mathbf{E}, && && \boldsymbol{\varepsilon} = \mathbf{C}\mathbf{u} = \boldsymbol{\varepsilon}_e + \boldsymbol{\varepsilon}_r,\\
&\boldsymbol{\varepsilon}_e = \mathbf{C}\mathbf{u}_e = \mathbf{E}^{-1}\boldsymbol{\sigma}_e = -\mathbf{E}^{-1}\boldsymbol{\sigma}_r + \boldsymbol{\varepsilon}_E, \quad && && \boldsymbol{\varepsilon}_r = \mathbf{C}\mathbf{u}_r = \mathbf{E}^{-1}\boldsymbol{\sigma}_r + \boldsymbol{\varepsilon}_R.
\end{aligned} \tag{1.3}$$

In Eqs. (1.3) conventional decompositions of displacement, stress and strain vectors are introduced. Subscript e relates to the linear elastic system without distortion, subjected to load $\mathbf{p}$, and subscript r indicates all the quantities due to the presence of distortions. $\mathbf{Z}$ is the square, singular, symmetric and semi-negative definite matrix of the distortion influence, [2, 3]. It is easily shown that

$$\mathbf{Z}\mathbf{C} \equiv \mathbf{0} \quad \text{and} \quad \mathbf{C}^T\mathbf{Z} \equiv \mathbf{0}. \tag{1.4}$$

Equations $(1.4)_1$ expresses the fact that a kinematically compatible distortion field (i.e. $\boldsymbol{\varepsilon}_R = \mathbf{C}\mathbf{u}_r$) does not induce any additional stress state:

$$\boldsymbol{\sigma}_r = \mathbf{Z}\boldsymbol{\varepsilon}_R = \mathbf{Z}\mathbf{C}\mathbf{u}_r \equiv \mathbf{0}, \tag{1.5}$$

and from Eq. $(1.4)_2$ it follows that the distortional stresses $\boldsymbol{\sigma}_r$ are in equilibrium with the zero-value load, namely

$$\mathbf{p}_r = \mathbf{C}^T\boldsymbol{\sigma}_r = \mathbf{C}^T\mathbf{Z}\boldsymbol{\varepsilon}_r \equiv \mathbf{0}. \tag{1.6}$$

http://rcin.org.pl

2. Fundamental energetic relations

Let us consider two identical linear elastic systems subjected to two different systems of loads and distortions. From the symmetry of elasticity matrix ($\mathbf{E}=\mathbf{E}^T$) we obtain the identity:

$$\boldsymbol{\sigma}_1^T\boldsymbol{\varepsilon}_{E2}=\boldsymbol{\varepsilon}_{E1}^T\mathbf{E}^T\boldsymbol{\varepsilon}_{E2}\equiv\boldsymbol{\varepsilon}_{E2}^T\mathbf{E}\boldsymbol{\varepsilon}_{E1}=\boldsymbol{\sigma}_2^T\boldsymbol{\varepsilon}_{E1}, \tag{2.1}$$

where subscripts 1 and 2 correspond to the states induced by the loads $\mathbf{p}_1$, $\mathbf{p}_2$ and distortions $\boldsymbol{\varepsilon}_{R1}$, $\boldsymbol{\varepsilon}_{R2}$, respectively.

Assuming that $\mathbf{p}_i$, $\boldsymbol{\sigma}_i$ ($i=1, 2$) are statically admissible and $\mathbf{u}_j$, $\boldsymbol{\varepsilon}_j$ ($j=1, 2$) are kinematically admissible, the virtual work principle can be used:

$$\mathbf{p}_i^T\mathbf{u}_j=\boldsymbol{\sigma}_i^T\boldsymbol{\varepsilon}_j \qquad (i, j=1, 2). \tag{2.2}$$

Substituting Eqs. (2.2) and $(1.1)_1$ into identity (2.1) one can obtain the reciprocal principle for the case of the presence of distortions:

$$\mathbf{p}_1^T\mathbf{u}_2-\boldsymbol{\sigma}_1^T\boldsymbol{\varepsilon}_{R2}=\mathbf{p}_2^T\mathbf{u}_1-\boldsymbol{\sigma}_2^T\boldsymbol{\varepsilon}_{R1}. \tag{2.3}$$

The form of Eq. (2.3) corresponds to the reciprocal principle used in thermoelasticity [5, 6]. In the absence of distortions ($\boldsymbol{\varepsilon}_{R1}=\boldsymbol{\varepsilon}_{R2}=\mathbf{0}$), relation (2.3) becomes the well-known E. BETTI's principle [7]. In particular, when $\boldsymbol{\varepsilon}_{R1}=\mathbf{0}$, and $\mathbf{p}_2=\mathbf{0}$, Eq. (2.3) represents the G. COLONNETI's theorem [8].

Since the elasticity matrix $\mathbf{E}$ is strictly positive definite, the following inequality is also valid:

$$(\boldsymbol{\varepsilon}_{E1}-\boldsymbol{\varepsilon}_{E2})^T\mathbf{E}(\boldsymbol{\varepsilon}_{E1}-\boldsymbol{\varepsilon}_{E2})\geqslant 0, \tag{2.4}$$

where the equality sign occurs only if $\boldsymbol{\varepsilon}_{E1}=\boldsymbol{\varepsilon}_{E2}$.

Making use of Eqs. (1.1), (2.2) and (2.4) we arrive at

$$(\mathbf{p}_1-\mathbf{p}_2)^T(\mathbf{u}_1-\mathbf{u}_2)-(\boldsymbol{\sigma}_1-\boldsymbol{\sigma}_2)^T(\boldsymbol{\varepsilon}_{R1}-\boldsymbol{\varepsilon}_{R2})\geqslant 0. \tag{2.5}$$

Relation (2.5) results from the definition of elasticity matrix $\mathbf{E}$, from the equilibrium equations and the geometric compatibility conditions only, and therefore the range of its validity is very wide.

The total elastic energy W_E of the body is non-negative definite and can be expressed as

$$W_E=\frac{1}{2}\boldsymbol{\sigma}^T\boldsymbol{\varepsilon}_E=\frac{1}{2}\boldsymbol{\sigma}^T(\mathbf{C}\mathbf{u}-\boldsymbol{\varepsilon}_R)=\frac{1}{2}(\mathbf{p}^T\mathbf{u}-\boldsymbol{\sigma}^T\boldsymbol{\varepsilon}_R)\geqslant 0. \tag{2.6}$$

Let us consider the difference between the elastic energy of two systems of loads and distortions

$$\Delta W_E=W_{E2}-W_{E1}=\frac{1}{2}(\mathbf{p}_2^T\mathbf{u}_2-\mathbf{p}_1^T\mathbf{u}_1-\boldsymbol{\sigma}_2^T\boldsymbol{\varepsilon}_{R2}+\boldsymbol{\sigma}_1^T\boldsymbol{\varepsilon}_{R1}). \tag{2.7}$$

http://rcin.org.pl

Using the reciprocal principle (2.3), Eq. (2.7) can be rewritten in the following two equivalent forms:

$$\Delta W_E = -\frac{1}{2}(\mathbf{p}_1-\mathbf{p}_2)^T(\mathbf{u}_1+\mathbf{u}_2)+\frac{1}{2}(\boldsymbol{\sigma}_1-\boldsymbol{\sigma}_2)^T(\boldsymbol{\varepsilon}_{R1}+\boldsymbol{\varepsilon}_{R2}),$$

$$\Delta W_E = -\frac{1}{2}(\mathbf{p}_1+\mathbf{p}_2)^T(\mathbf{u}_1-\mathbf{u}_2)+\frac{1}{2}(\boldsymbol{\sigma}_1+\boldsymbol{\sigma}_2)^T(\boldsymbol{\varepsilon}_{R1}-\boldsymbol{\varepsilon}_{R2}). \tag{2.8}$$

The difference of elastic energy ΔW_E can be evaluated from Eqs. (2.8) and relation (2.5). As a result, we obtain the following fundamental inequalities:

$$\begin{aligned}
\Delta W_E &\geqslant -(\mathbf{p}_1-\mathbf{p}_2)^T\mathbf{u}_1+(\boldsymbol{\sigma}_1-\boldsymbol{\sigma}_2)^T\boldsymbol{\varepsilon}_{R1},\\
\Delta W_E &\leqslant -(\mathbf{p}_1-\mathbf{p}_2)^T\mathbf{u}_2+(\boldsymbol{\sigma}_1-\boldsymbol{\sigma}_2)^T\boldsymbol{\varepsilon}_{R2},\\
\Delta W_E &\geqslant -\mathbf{p}_1^T(\mathbf{u}_1-\mathbf{u}_2)+\boldsymbol{\sigma}_1^T(\boldsymbol{\varepsilon}_{R1}-\boldsymbol{\varepsilon}_{R2}),\\
\Delta W_E &\leqslant -\mathbf{p}_2^T(\mathbf{u}_1-\mathbf{u}_2)+\boldsymbol{\sigma}_2^T(\boldsymbol{\varepsilon}_{R1}-\boldsymbol{\varepsilon}_{R2}).
\end{aligned} \tag{2.9}$$

It is worthwhile to note that all the relations derived above remain valid also when $\mathbf{p}_i$, $\mathbf{u}_i$, $\boldsymbol{\sigma}_i$, $\boldsymbol{\varepsilon}_{Ei}$ and $\boldsymbol{\varepsilon}_{Ri}$ are replaced by their velocities (rates). Relations (2.9) represent the most important result of this work.

3. Bounding theorems for elastic energy

3.1. A concept of reference structure

The specific form of relations (2.9) allows us to compare the elastic energy for two structures of identical geometry, subjected to different load, displacement and/or distortion systems. The boundary conditions of both structures should be identical because the geometric compatibility matrix $\mathbf{C}$ has been assumed to be the same. However, the problem of boundary conditions becomes not so important, if we introduce the concept of *slackened structures* (cf. [9–12]). It allows us to compare the structure of different boundary conditions by means of a suitable choice of the clearance surface. The theory of slackened structures, exhaustively described in [12], allows for the presence of gaps (clearances) at structural connections. This approach takes into account elastic, plastic and locking effects, induced by variations of the so-called clearance strains, $\boldsymbol{\varepsilon}_L$. Since the theoretical description is FEM-oriented, the locking effects can be also treated as a material property. The theory of such systems includes all the essential features of time-independent materials.

It is assumed that subscript 1 denotes a so-called *reference structure*. Subscript 2 is reserved for a given structure which will be the subject of the analysis.

Further considerations are restricted to two kinds of the reference structure. The first one corresponds to the linear elastic system without distortions, i.e. $\boldsymbol{\varepsilon}_{R1} \equiv \mathbf{0}$. Then

http://rcin.org.pl

$$(\sigma_1 - \sigma_2)^T \varepsilon_{R1} \equiv 0, \tag{3.1}$$

independently of the stress state in structure "2". The second type of reference structure corresponds to the holonomic elastic-perfectly plastic model. This model describes the path-independent class of plastic behaviour by means of a suitable constructed nonlinear elastic constitutive relation. It is known that the holonomic theory gives the true solutions in cases when the HAAR–KÁRMÁN's principle [13] holds. One should be aware of the fact that applicability of this principle depends partly on the loading, partly on the configuration of the system and partly on the material, [14]. The sufficient condition, which should be satisfied for the Haar–Kármán's model, can be expressed as

$$\int_0^{\sigma} \varepsilon_{P1}^T \, d\sigma_1 = \int_0^{t^*} \varepsilon_{P1}^T(t) \cdot \dot{\sigma}_1(t) \, dt = 0, \tag{3.2}$$

where ε_{P1} is the plastic strain vector and dot denotes the differentiation with respect to time. Condition (3.2) is satisfied for "restricted statically stress states", specified by P.G. HODGE [15]. There are two essential cases in which Eq. (3.2) surely occurs:

1. Stress remains constant after the stress point first reaches the yield (limit) surface. In this case $d\sigma_1 = \mathbf{0}$.

2. Stress point moves along a separate flat portion of the yield limit surface. Then, assuming the associated flow rule, $d\sigma_1$ and ε_{P1} are found to be orthogonal and their scalar product is equal to zero.

Relation (3.2) implies a simple expression for the plastic dissipation $D_1(t^*) = D_1$, namely

$$D_1(t^*) = \int_0^{t^*} \dot{\varepsilon}_{P1}^T(t) \cdot \sigma_1(t) \, dt = \sigma_1^T \varepsilon_{P1} - \int_0^{t^*} \varepsilon_{P1}^T(t) \cdot \dot{\sigma}_1(t) \, dt = \sigma_1^T \varepsilon_{P1}. \tag{3.3}$$

For holonomic models the following inequality holds:

$$(\sigma_1 - \sigma_1^*)^T \varepsilon_{P1} \geqslant 0. \tag{3.4}$$

Relation (3.4) results from the convexity of yield (limit) condition and from the associated flow law. In (3.4) σ_1^* denotes any stress state that does not violate the yield (limit) condition.

It is worth to notice that the stress state obtained by means of the holonomic theory is identical with those of general plastic flow theory in particular cases of proportional loading, in the absence of local unloading.

The comparison of elastic energy of systems 1 and 2 will be carried out for the cases of the same loads or the same displacements and/or the same distortion systems. It allows us to construct several bounding theorems related to the elastic and complementary energies of deformable systems. The bounding theorems cover a wider class of problems than the variational principles. In general, they determine the upper or lower bounds on the functional or function under considerations.

http://rcin.org.pl

However, the true solution does not necessarily correspond to the lower or upper bound, specified in the bounding theorem. Obviously, all extremum theorems are also bounding theorems but, in this case, the true solution corresponds to the stationary point of the functional.

3.2. Linear-elastic reference structure

In practical applications the most interesting is the case of equal loads, i.e. $\mathbf{p}_1=\mathbf{p}_2=\mathbf{p}$. Then, from Eqs. $(2.9)_{1,2}$ and (3.1) it follows that

$$0 \leqslant \Delta W_E \leqslant (\boldsymbol{\sigma}_1-\boldsymbol{\sigma}_2)^T \boldsymbol{\varepsilon}_{R2}. \tag{3.5}$$

Hence, we can formulate the following theorem:

THEOREM 1. *The elastic energy of a linear elastic structure with distortions cannot be less than the elastic energy of an identically loaded linear elastic structure without distortions.*

Theorem 1 is of a very general character. Its meaning is intuitively acceptable for elastic-cracking materials and is well-known in damage mechanics.

On the other hand, from Eqs. (2.1) and (2.8) we obtain

$$\Delta W_E = \frac{1}{2}(\boldsymbol{\sigma}_1-\boldsymbol{\sigma}_2)^T \boldsymbol{\varepsilon}_{R2} = -\frac{1}{2}\boldsymbol{\sigma}_{r2}\boldsymbol{\varepsilon}_{R2} = -\frac{1}{2}\boldsymbol{\varepsilon}_{R2}^T \mathbf{Z}\boldsymbol{\varepsilon}_{R2} \geqslant 0. \tag{3.6}$$

ΔW_E is expressed by the semi-positive definite quadratic form and therefore it does not depend on the sign of particular components of $\boldsymbol{\varepsilon}_{R2}$ ($\mathbf{Z}$ is the semi-negative definitive matrix).

In particular, the state of $\mathbf{p}=\mathbf{0}$ corresponds to $\boldsymbol{\sigma}_1 \equiv \mathbf{0}$, $\boldsymbol{\sigma}_2 = \boldsymbol{\sigma}_{r2}$, $W_{E1} = 0$ and, according to Eq. (3.6), $W_{E2} = -\frac{1}{2}\boldsymbol{\varepsilon}_{R2}^T \mathbf{Z}\boldsymbol{\varepsilon}_{R2} \geqslant 0$. The result obtained here represents a "hidden" elastic energy W_r (i.e. $\Delta W_E = W_r$), stored after unloading in an elastic-perfectly plastic structure, due to the presence of kinematically non-admissible plastic deformations (cf. [16]). This observation provides a simple interpretation of relation (3.6) which expresses the essence of Theorem 1. Namely, the non-negative value of ΔW_E can be treated as the stored elastic energy calculated for the unloaded elastic-perfectly plastic model in which the permanent plastic deformations are equal to the current distortions of system 2.

From the reciprocal principle (2.3) and relations (2.9) we can determine the difference between the *conventional works* ($W=\mathbf{p}^T\mathbf{u}$) done by loads (cf. Sec. 4):

$$\Delta W = \mathbf{p}^T(\mathbf{u}_2-\mathbf{u}_1) = \boldsymbol{\sigma}_1^T\boldsymbol{\varepsilon}_{R2} \geqslant \boldsymbol{\sigma}_2^T\boldsymbol{\varepsilon}_{R2}. \tag{3.7}$$

This difference can be treated as a measure of the *relative compliance* of two systems.

It should be mentioned here that slackened systems in the absence of plastic deformations are path-independent ones if the clearance region is convex (cf. [12]).

http://rcin.org.pl

Thus, the relative compliance ΔW is non-negative definite for slackened-elastic ($\boldsymbol{\varepsilon}_{R2} = \boldsymbol{\varepsilon}_{L2}$) and other holonomic models, e.g.: elastic-perfectly plastic ($\boldsymbol{\varepsilon}_{R2} = \boldsymbol{\varepsilon}_{P2}$) and slackened-elastic-perfectly plastic ($\boldsymbol{\varepsilon}_{R2} = \boldsymbol{\varepsilon}_{L2} + \boldsymbol{\varepsilon}_{P2}$). In all these cases $\boldsymbol{\sigma}_2^T \boldsymbol{\varepsilon}_{R2} \geqslant 0$.

It is worth to notice that the case of nonlinear elastic structure requires a suitable choice of elastic coefficients of the reference structure. Considerations connected with this problem will be presented in a separate paper.

The second particular case, which can be rather interesting from the theoretical point of view, corresponds to equal displacements ($\mathbf{u}_1 = \mathbf{u}_2 = \mathbf{u}$) when all the displacement vector components are controlled. In this case the joint displacements of system 2 are identical with those of the reference structure. Then relations (2.9) give

$$-\boldsymbol{\sigma}_1^T \boldsymbol{\varepsilon}_{R2} \leqslant \Delta W_E \leqslant -\boldsymbol{\sigma}_2^T \boldsymbol{\varepsilon}_{R2}, \tag{3.8}$$

and using the reciprocal principle (2.3) we conclude that

$$(\mathbf{p}_2 - \mathbf{p}_1)^T \mathbf{u} = -\boldsymbol{\sigma}_1^T \boldsymbol{\varepsilon}_{R2} \leqslant -\boldsymbol{\sigma}_2^T \boldsymbol{\varepsilon}_{R2}. \tag{3.9}$$

It is clear that for all the holonomic models $\Delta W_E \leqslant 0$ and $(\mathbf{p}_2 - \mathbf{p}_1)^T \mathbf{u} \leqslant 0$.

Consider now the particular case of zero-value displacements ($\mathbf{u} \equiv \mathbf{0}$). In this case $W_{E1} = 0$ and, because the elastic energy is always positive definite, $W_{E2} = \Delta W_E > 0$, unless the distortions of the system are kinematically admissible. Then $W_{E2} = \Delta W_E = 0$. So, we conclude that the elastic energy of the system with distortions can be sometimes larger than that of the system without distortions.

3.3. Linear elastic-perfectly plastic reference structure; holonomic model

In this case $\boldsymbol{\varepsilon}_{R1} = \boldsymbol{\varepsilon}_{P1}$, where and $\boldsymbol{\varepsilon}_{P1}$ denotes the plastic strains in the reference structure. Assuming the convexity of yield region and normality rule, the following requirement for the holonomic model is valid (cf. (3.4)):

$$(\boldsymbol{\sigma}_1 - \boldsymbol{\sigma}_2)^T \boldsymbol{\varepsilon}_{P1} \geqslant 0, \tag{3.10}$$

where $\boldsymbol{\sigma}_2$ *must* satisfy the yield (limit) condition of the reference structure.

In the case of equal loads ($\mathbf{p}_1 = \mathbf{p}_2 = \mathbf{p}$) from relations (2.9) we obtain

$$0 \leqslant (\boldsymbol{\sigma}_1 - \boldsymbol{\sigma}_2)^T \boldsymbol{\varepsilon}_{P1} \leqslant \Delta W_E \leqslant (\boldsymbol{\sigma}_1 - \boldsymbol{\sigma}_2)^T \boldsymbol{\varepsilon}_{R2}, \tag{3.11}$$

where the role of system 2 plays a model of linear elastic structure with arbitrary distortions $\boldsymbol{\varepsilon}_{R2}$. Inequality (3.11), when applied to the elastic-plastic systems, allows us to formulate the following theorem:

THEOREM 2. *The elastic energy of an elastic-perfectly plastic structure cannot be less than that of its holonomic model subjected to the same load.*

From inequality (3.11) it follows, however, a more general theorem, namely:

THEOREM 3. *If stress states do not violate the given constraints in the stress space, the elastic energy of any elastic structure with arbitrary distortions cannot be less than that of the holonomic model of elastic-perfectly plastic structure, subjected to the same load.*

http://rcin.org.pl

The constraints placed on the stress states correspond, of course, to the yield condition of system 1. As the system 2 we can assume, however, a body which does not exhibit any plastic deformations. It can be, for example, the elastic-cracking body structure whose cracking condition is identical with the yield condition of the reference structure, [17].

To the author's knowledge the case of equal displacements ($\mathbf{u}_1 = \mathbf{u}_2 = \mathbf{u}$) does not provide essentially new results and it will be not considered here.

4. Energy in systems made of time-independent material

Let us consider the deformation process of a system, assuming that in the natural (virgin) state for time $t=0$, the stresses are equal to zero. Introduce the concept of *conventional work* for time $t=t^*$, defined as follows:

$$W = \int_0^{t^*} \dot{W}(t)\,dt = \mathbf{p}^T\mathbf{u} = W_\varepsilon + W_\sigma, \tag{4.1}$$

where

$$W_\varepsilon = \int_0^{t^*} \mathbf{p}^T(t)\dot{\mathbf{u}}(t)\,dt, \qquad W_\sigma = \int_0^{t^*} \dot{\mathbf{p}}^T(t)\,\mathbf{u}(t)\,dt. \tag{4.2}$$

W_ε denotes here the strain energy and W_σ is the complementary (stress) energy when the load is controlled. Using the strain decomposition $(1.1)_1$ and virtual work equation, relations (4.2) can be rewritten in the form

$$\begin{aligned} W_\varepsilon &= \int_0^{t^*} \boldsymbol{\sigma}^T(t)\dot{\boldsymbol{\varepsilon}}(t)\,dt = \int_0^{t^*} \boldsymbol{\sigma}^T(t)\,\dot{\boldsymbol{\varepsilon}}_E(t)\,dt + \int_0^{t^*} \boldsymbol{\sigma}^T(t)\,\dot{\boldsymbol{\varepsilon}}_R(t)\,dt, \\ W_\sigma &= \int_0^{t^*} \dot{\boldsymbol{\sigma}}^T(t)\boldsymbol{\varepsilon}(t)\,dt = \int_0^{t^*} \dot{\boldsymbol{\sigma}}^T(t)\,\boldsymbol{\varepsilon}_E(t)\,dt + \int_0^{t^*} \dot{\boldsymbol{\sigma}}^T(t)\,\boldsymbol{\varepsilon}_R(t)\,dt, \end{aligned} \tag{4.3}$$

where $\boldsymbol{\varepsilon}_R$ denotes the total distortion strain vector. Taking into account the symmetry of elasticity matrix $\mathbf{E}$, it is easily seen that the first terms in Eqs. (4.3) represent the elastic energy of the system,

$$\int_0^{t^*} \boldsymbol{\sigma}^T(t)\,\dot{\boldsymbol{\varepsilon}}_E(t)\,dt = \int_0^{t^*} \dot{\boldsymbol{\sigma}}^T(t)\,\boldsymbol{\varepsilon}_E(t)\,dt = \frac{1}{2}\,\boldsymbol{\sigma}^T\boldsymbol{\varepsilon}_E = W_E(t^*) = W_E. \tag{4.4}$$

Thus

$$W_\varepsilon = W_E + W_{R\varepsilon}, \qquad W_\sigma = W_E + W_{R\sigma}, \tag{4.5}$$

where

$$W_{R\varepsilon} = \int_0^{t^*} \boldsymbol{\sigma}^T(t)\,\dot{\boldsymbol{\varepsilon}}_R(t)\,dt, \qquad W_{R\sigma} = \int_0^{t^*} \dot{\boldsymbol{\sigma}}^T(t)\,\boldsymbol{\varepsilon}_R(t)\,dt. \tag{4.6}$$

http://rcin.org.pl

$W_{R\varepsilon}$ and $W_{R\sigma}$ denote the stress and strain energies, respectively, induced by the presence of distortions. For a given final mechanical state of the structure, their sum takes the simple form

$$W_R = W_{R\varepsilon} + W_{R\sigma} = \boldsymbol{\sigma}^T \boldsymbol{\varepsilon}_R , \tag{4.7}$$

and

$$W = \mathbf{p}^T \mathbf{u} = 2W_E + W_{R\varepsilon} + W_{R\sigma} = 2W_E + W_R . \tag{4.8}$$

Let us assume the general case of slackened system made of a linear elastic-plastic material (cf. [12]). In this case the total distortion vector can be decomposed into two parts,

$$\boldsymbol{\varepsilon}_R = \boldsymbol{\varepsilon}_L + \boldsymbol{\varepsilon}_P . \tag{4.9}$$

Then W_ε and W_σ can be expressed as follows ($\boldsymbol{\sigma}^T(t)\,\dot{\boldsymbol{\varepsilon}}_L(t) \equiv 0$):

$$\begin{aligned} W_\varepsilon &= \int_0^{t^*} \boldsymbol{\sigma}^T(t)\,[\dot{\boldsymbol{\varepsilon}}_L(t) + \dot{\boldsymbol{\varepsilon}}_E(t) + \dot{\boldsymbol{\varepsilon}}_P(t)]\,dt = W_E + \int_0^{t^*} \boldsymbol{\sigma}^T(t)\,\dot{\boldsymbol{\varepsilon}}_P(t)\,dt , \\ W_\sigma &= \int_0^{t^*} \dot{\boldsymbol{\sigma}}^T(t)\,[\boldsymbol{\varepsilon}_L(t) + \boldsymbol{\varepsilon}_E(t) + \boldsymbol{\varepsilon}_P(t)]\,dt = W_E + \boldsymbol{\sigma}^T(\boldsymbol{\varepsilon}_L + \boldsymbol{\varepsilon}_P) - \int_0^{t^*} \boldsymbol{\sigma}^T(t)\,\dot{\boldsymbol{\varepsilon}}_P(t)\,dt . \end{aligned} \tag{4.10}$$

Convexity of the yield (limit) condition and the normality rule give

$$\int_0^{t^*} [\boldsymbol{\sigma}(t) - \boldsymbol{\sigma}(t^*)]^T\,\dot{\boldsymbol{\varepsilon}}_P(t)\,dt = D(t^*) - \boldsymbol{\sigma}^T \boldsymbol{\varepsilon}_P = -\int_0^{t^*} \dot{\boldsymbol{\sigma}}^T(t)\,\boldsymbol{\varepsilon}_P(t)\,dt \geqslant 0, \tag{4.11}$$

where $D(t^*)$ denotes the non-negative definite total plastic dissipation, computed in the interval $\langle 0, t^* \rangle$:

$$D(t^*) = D = \int_0^{t^*} \boldsymbol{\sigma}^T(t)\,\dot{\boldsymbol{\varepsilon}}_P(t)\,dt . \tag{4.12}$$

Since the clearance "dissipation" in slackened systems is equal to zero, one can obtain the following equality:

$$\int_0^{t^*} \boldsymbol{\sigma}^T(t)\,\dot{\boldsymbol{\varepsilon}}_L(t)\,dt = \boldsymbol{\sigma}^T \boldsymbol{\varepsilon}_L - \int_0^{t^*} \dot{\boldsymbol{\sigma}}^T(t)\,\boldsymbol{\varepsilon}_L(t)\,dt = \int_0^{t^*} [\boldsymbol{\varepsilon}_L(t^*) - \boldsymbol{\varepsilon}_L(t)]^T\,\dot{\boldsymbol{\sigma}}(t)\,dt \equiv 0. \tag{4.13}$$

On the other hand, from convexity of the clearance region it follows that $\boldsymbol{\sigma}^T \boldsymbol{\varepsilon}_L \geqslant 0$. Hence, using Eq. (4.13), we have

$$\boldsymbol{\sigma}^T \boldsymbol{\varepsilon}_L = \int_0^{t^*} \dot{\boldsymbol{\sigma}}^T(t)\,\boldsymbol{\varepsilon}_L(t)\,dt \geqslant 0. \tag{4.14}$$

http://rcin.org.pl

Thus, for slackened-elastic-perfectly plastic systems, from inequalities (4.11) and (4.14) it follows:

$$\int_0^{t^*} \dot{\boldsymbol{\sigma}}^T(t)\,[\boldsymbol{\varepsilon}_L(t)-\boldsymbol{\varepsilon}_P(t)]\,dt \geqslant 0, \tag{4.15}$$

or

$$\boldsymbol{\sigma}^T(\boldsymbol{\varepsilon}_L-\boldsymbol{\varepsilon}_P)+D \geqslant 0. \tag{4.15'}$$

Assume now that structure 1 is the holonomic elastic-perfectly-plastic and structure 2 corresponds to the general model of the slackened system made of an elastic-perfectly plastic material. According to inequality (3.11), relating to the case of equal loads ($\mathbf{p}_1=\mathbf{p}_2=\mathbf{p}$), we have

$$0 \leqslant \Delta W_E \leqslant (\boldsymbol{\sigma}_1-\boldsymbol{\sigma}_2)^T(\boldsymbol{\varepsilon}_{L2}+\boldsymbol{\varepsilon}_{P2}). \tag{4.16}$$

Relation (4.16) will be used to evaluate the complementary energy of both systems. From Eq. $(4.10)_2$ we obtain

$$\begin{aligned} W_{\sigma 1} &= W_{E1}, \\ W_{\sigma 2} &= W_{E2}+\boldsymbol{\sigma}_2^T(\boldsymbol{\varepsilon}_{L2}+\boldsymbol{\varepsilon}_{P2})-D_2, \end{aligned} \tag{4.17}$$

hence

$$W_{\sigma 1}-W_{\sigma 2} = -\Delta W_E+D_2-\boldsymbol{\sigma}_2^T(\boldsymbol{\varepsilon}_{L2}+\boldsymbol{\varepsilon}_{P2}). \tag{4.18}$$

Taking into account inequality (4.16) we find the following estimation of the complementary energy:

$$D_2-\boldsymbol{\sigma}_1^T(\boldsymbol{\varepsilon}_{L2}+\boldsymbol{\varepsilon}_{P2}) \leqslant W_{\sigma 1}-W_{\sigma 2} \leqslant D_2-\boldsymbol{\sigma}_2^T(\boldsymbol{\varepsilon}_{L2}+\boldsymbol{\varepsilon}_{P2}). \tag{4.19}$$

Let us consider two particular cases.

CASE 1

Structure 2 is assumed to be holonomic slackened-elastic-perfectly plastic ($D_2=\boldsymbol{\sigma}_2^T\boldsymbol{\varepsilon}_{P2}$). Then $D_2-\boldsymbol{\sigma}_2^T(\boldsymbol{\varepsilon}_{L2}+\boldsymbol{\varepsilon}_{P2})=\boldsymbol{\sigma}_2^T\boldsymbol{\varepsilon}_{L2} \leqslant 0$, and according to (4.19), we arrive at

$$W_{\sigma 1} \leqslant W_{\sigma 2}. \tag{4.20}$$

It corresponds to the theorem:

THEOREM 4. *The complementary energy of holonomic elastic-perfectly plastic structure is a lower bound on the complementary energy of identically loaded, holonomic slackened-elastic-perfectly plastic structure.*

CASE 2

Structure 2 is assumed to be elastic-perfectly plastic ($\boldsymbol{\varepsilon}_{L2} \equiv \mathbf{0}$). In this case the left-hand side in (4.19), using HILL'S principle [18], can be expressed as

http://rcin.org.pl

$$D_2-\boldsymbol{\sigma}_1^T\boldsymbol{\varepsilon}_{P_2}=\int_0^{t^*}\boldsymbol{\sigma}_2^T(t)\,\dot{\boldsymbol{\varepsilon}}_{P_2}(t)\cdot dt-\boldsymbol{\sigma}_1^T(t^*)\,\boldsymbol{\varepsilon}_{P_2}(t^*)=\int_0^{t^*}[\boldsymbol{\sigma}_2(t)-\boldsymbol{\sigma}_1(t^*)]^T\,\dot{\boldsymbol{\varepsilon}}_{P_2}(t)\,dt\geqslant 0.$$

Then, according to (4.19), $W_{\sigma 1}\geqslant W_{\sigma 2}$, that corresponds to HODGE's theorem [15]: "The complementary energy of any restricted statically admissible state is an upper bound on the complementary energy of the actual solution".

Similar considerations for $\mathbf{p}_1=\mathbf{p}_2=\mathbf{p}$ can be carried out assuming that structures 1 and 2 are elastic without distortions and the slackened-elastic ones, respectively. In this case we obtain

$$W_{\sigma 1}-W_{\sigma 2}=-DW_E-\boldsymbol{\sigma}_2^T\boldsymbol{\varepsilon}_{L_2}\leqslant 0. \tag{4.22}$$

Estimation (4.22) follows from (3.5), where $\Delta W_E\geqslant 0$, and from the inequality $\boldsymbol{\sigma}_2^T\boldsymbol{\varepsilon}_{L_2}\geqslant 0$. The result obtained here corresponds to the statement that the complementary energy (i.e. elastic energy of elastic structure) is a lower bound on the complementary energy of slackened-elastic structure, subjected to the same load.

The next problem is connected with the energy of residual stresses that remains after unloading. Let us consider elastic-perfectly plastic structures subjected to the same load $\mathbf{p}_0$. Assume that structure 1 had been proportionally loaded up to $\mathbf{p}_0$ without local plastic unloading, whereas the state of $\mathbf{p}=\mathbf{p}_0$ in structure 2 had been reached on an unspecified path of load. The elastic energy for $\mathbf{p}=\mathbf{p}_0$ can be expressed as follows

$$W_{E1}=W_{r1}+W^*,\qquad W_{E2}=W_{r2}+W^*, \tag{4.23}$$

where W_{r1} and W_{r2} represent the residual "hidden" elastic energies in structure 1 and structure 2, respectively. W^* denotes the recovered elastic energy which is the same for both structures. Using Eqs. (4.23) and Theorem 2 we find

$$\Delta W_E=W_{E2}-W_{E1}=W_{r2}-W_{r1}\geqslant 0. \tag{4.24}$$

Thus, we can state that the elastic energy stored in system 1, that behaves holonomically up to $\mathbf{p}=\mathbf{p}_0$, is a lower bound on the plastic energy stored in structure "2", that reaches the state of $\mathbf{p}=\mathbf{p}_0$ on an arbitrary loading path. The problem described has been also considered in [19]. However, the final conclusion of this work is strictly opposed to that presented here due to an improper interpretation of Hill's principle. The authors of [19] claim that the elastic energy stored in system 1 is an *upper* bound for W_r. Unfortunately, both the examples presented in this work are related to the holonomic behaviour before the prescribed load level $\mathbf{p}_0$ is reached, and therefore they cannot confirm the validity of conclusion drawn by the authors. The problem of elastic energy stored in the elastic-perfectly plastic system after unloading is numerically illustrated in Sec. 5. It should be added that the problem of unloading of

http://rcin.org.pl

slackened systems in the presence of plastic deformations appears to be much morecomplicated and will be considered in separate papers.

Finally, let us summarize some results related to the strain and stress energies in standard situations. Consider first the case of elastic-perfectly plastic structures ($\boldsymbol{\varepsilon}_L \equiv \mathbf{0}$). From Eq. (4.11) and from the non-negativity of plastic dissipation we obtain

$$\boldsymbol{\sigma}^T\boldsymbol{\varepsilon}_P \leqslant \int_0^{t^*} \boldsymbol{\sigma}^T(t)\,\dot{\boldsymbol{\varepsilon}}_P(t)\,dt = D = W_{R\varepsilon}, \qquad W_{R\varepsilon} \geqslant 0, \tag{4.25}$$

$$W_{R\sigma} = \int_0^{t^*} \dot{\boldsymbol{\sigma}}^T(t)\,\boldsymbol{\varepsilon}_P(t)\,dt \leqslant 0. \tag{4.26}$$

Therefore, in a general case of elastic-perfectly plastic system

$$W_\varepsilon \geqslant W_E \quad \text{and} \quad W_\sigma \leqslant W_E. \tag{4.27}$$

If $d\boldsymbol{\sigma}^T\boldsymbol{\varepsilon}_P = 0$, what occurs also for the holonomic model, we have

$$W_\varepsilon \geqslant W_E \quad \text{and} \quad W_\sigma = W_E. \tag{4.28}$$

In the case of slackened-elastic systems

$$W_\varepsilon = W_E \quad \text{and} \quad W_\sigma = W_E + \boldsymbol{\sigma}^T\boldsymbol{\varepsilon}_L \geqslant W_E. \tag{4.29}$$

5. Numerical example

Consider a two-span continuous beam shown in Fig. 1. The ideal I-cross-section of the beam is constant with the moment of inertia $J = 1000\ \text{cm}^4$ and depth $h = 16$ cm.

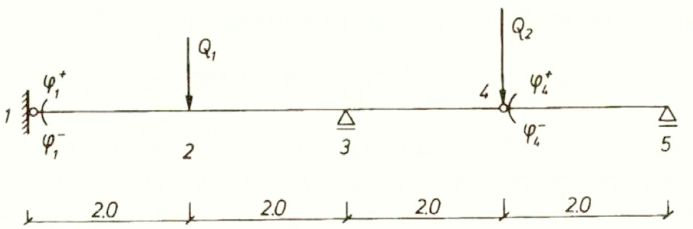

FIG. 1. Beam layout, loads and rotation constraints at points 1 and 4.

Two kinds of the material of the beam are assumed, namely: the linear elastic body of infinite strength, and the linear elastic-perfectly plastic body with the yield stress $\sigma_Y = 240$ Mpa; the corresponding fully plastic bending moment $M_Y = 30$ kNm. Young's modulus for both the materials is assumed to be the same: $E = 200$ GPa. In addition, at points 1 and 4 the presence of the so-called clearance hinges, i.e. hinges with rotation constraints, is permitted. In other words, the angle of free rotation (ϕ_i;

http://rcin.org.pl

$i = 1, 4$) at these points can vary between the limits: $-\phi_1^- \leqslant \phi_1 \leqslant \phi_1^+$, $-\phi_4^- \leqslant \phi_4 \leqslant \phi_4^+$, where $\phi_1^- = \phi_1^+ = 0.01$ rad, $\phi_4^- = \phi_4^+ = 0.02$ rad. The cases where clearance hinges are introduced correspond to the systems which are slackened. If all the limit rotations ($-\phi_i^- = \phi_i^+ = 0$) are equal to zero, the beam becomes the standard structure with bilateral constraints of two redundant reactions, i.e. the beam is rigidly fixed at point 1 and the hinge at point 4 vanishes. Thus, we can consider the following four kinds of the system:

I elastic ($\sigma_Y \Rightarrow \infty$, $\phi_i^- = \phi_i^+ = 0$);

II slackened-elastic ($\sigma_Y \Rightarrow \infty$, $\phi_i^- \neq 0$, $\phi_i^+ \neq 0$);

III elastic-perfectly plastic ($\sigma_Y = 240$ MPa, $\phi_i^- = \phi_i^+ = 0$);

IV slackened-elastic-perfectly plastic

($\sigma_Y = 240$ MPa, $\phi_i^- \neq 0$, $\phi_i^+ \neq 0$).

The beam is subjected to varying vertical loads Q_1 and Q_2, acting at points 2 and 4, respectively. Since the presence of clearances does not affect the ultimate collapse load (cf. [10]), in Cases III and IV the loads have to be contained within the limit hexagon *CDEFGH*, presented in Fig. 2a.

It is assumed that the loads can vary inside the load polygon *b-c-d-e-f-g-h-i-j-k* (cf. Fig. 2b). The load polygon has been assumed in such a way that plastic deformations can occur. The initial elastic loci for the elastic-perfectly ("ep") and for the slackened-elastic-perfectly plastic "sep" beam are presented in Fig. 2a. It should be pointed out that, in the case of slackened beam, the elastic region is non-convex (cf. [12]).

Two types of loading are assumed:

1. Proportional loading and unloading, according to the paths: *a-ba*, *a-c-a*,..., *a-k-a*.
2. Cyclic loading, according to the path:
   a-b-c-d-e-f-g-h-i-j-k-b-a.

Four kinds of the system and two types of loading generate at each point of the load polygon the following six cases of the beam behaviour, namely:

e = elastic,
se = slackened-elastic,
ehp = elastic-holonomic perfectly plastic,
sehp = slackened-elastic-holonomic plastic,
eip = elastic-"incremental" perfectly plastic,
seip = slackened-elastic-"incremental" perfectly plastic.

It can be easily shown that the first four cases correspond to the path-independent solutions, whereas the remaining cases, where irreversible plastic deformations are observed, correspond to the path-dependent solutions.

Additionally, in order to illustrate the problem of unloading, the beam has been previously loaded according to three different paths of loading up to point "*e*" at the load polygon. Path I corresponds to the proportional loading *a-e-a*. Path 2 and Path 3 correspond to the following load programs: "*a-b-c-d-e-a*" and "*a-m-n-f-e-a*", respectively, see Fig. 2b.

http://rcin.org.pl

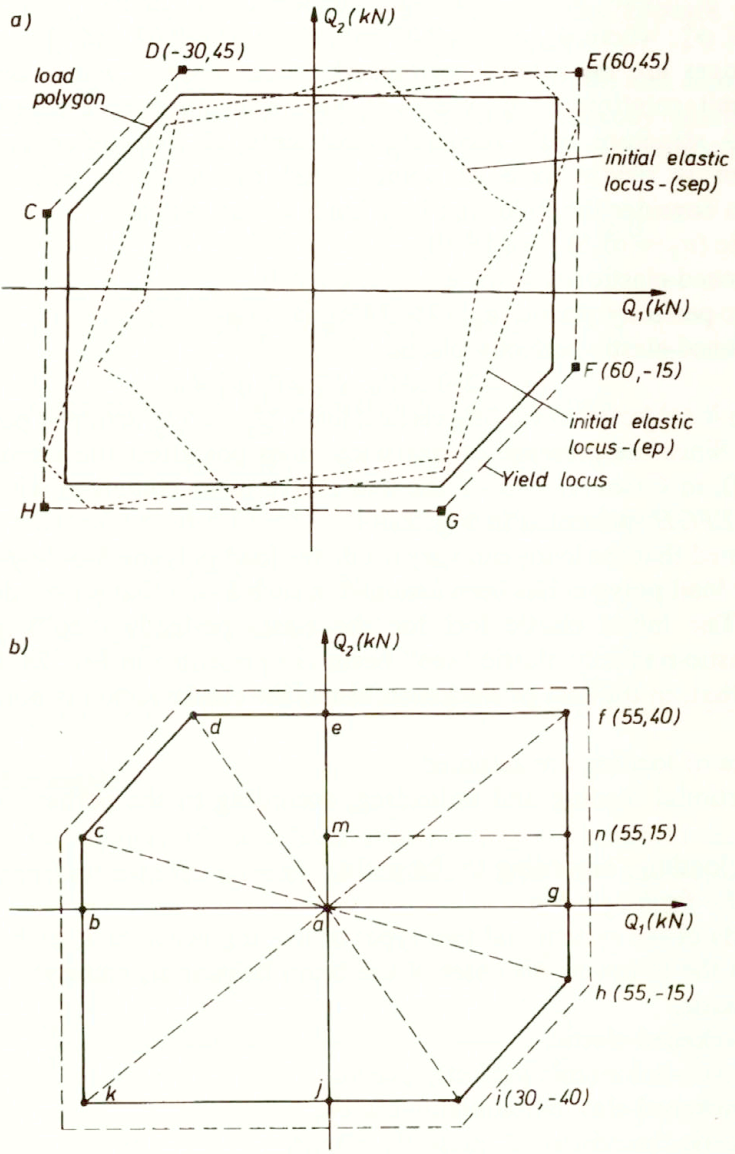

FIG. 2. Space of external loads, a) yield locus, initial elastic loci and load polygon, b) yield locus, load polygon and paths of loading.

Final results are gathered in Table 1, Table 2 and Table 3. Table 1 contains all current elastic energies at the particular points of the load polygon. Similar specification for the complementary energy is shown in Table 2. It can be seen that the results presented confirm the validity of the bounding theorems derived in the work. For instance, all the values in columns 2–6 in Table 1 are not less than those in

http://rcin.org.pl

Table 1. Elastic energy for various cases of system behaviour, W_E [kNm].

Point of load	e 1	ehp 2	eip 3	se 4	sehp 5	seip 6
a	0.0000	0.0000	0.0000	0.0000	0.0000	0.0000
b	0.3602	0.4000	0.4000	0.4458	0.4000	0.4000
c	0.4995	0.6250	0.6250	0.5852	0.6250	0.6250
d	0.5976	0.6500	0.6500	0.6833	0.7000	0.6500
e	0.3619	0.3667	0.4144	0.4208	0.4208	0.4144
f	0.4864	0.4864	0.4890	0.6578	0.5000	0.5000
g	0.3602	0.4000	0.4000	0.4458	0.4000	0.4000
h	0.4995	0.6250	0.6250	0.5852	0.6250	0.6250
i	0.5976	0.6500	0.6500	0.6833	0.7000	0.6500
j	0.3619	0.3667	0.4144	0.4208	0.4208	0.4144
k	0.4864	0.4864	0.4891	0.6578	0.5000	0.5000
b	0.3602	0.4000	0.4000	0.4458	0.4000	0.4000
a	0.0000	0.0000	0.0399	0.0000	0.0000	0.0315

Table 2. Complementary energy for various cases of system behaviour, W_σ [kNm].

Point of load	e 1	ehp 2	eip 3	se 4	sehp 5	seip 6
a	0.0000	0.0000	0.0000	0.0000	0.0000	0.0000
b	0.3601	0.4000	0.4000	0.7458	0.9000	0.9000
c	0.4994	0.6250	0.6250	1.1530	1.4249	1.4250
d	0.5976	0.6500	0.4833	1.4833	1.5000	1.2833
e	0.3619	0.3667	−0.8596	0.9958	0.9958	−0.6595
f	0.4863	0.4863	−2.7257	1.0935	1.2000	−3.2000
g	0.3601	0.4000	−5.0628	0.7458	0.9000	−5.9334
h	0.4994	0.6250	−5.6878	1.1530	1.4249	−6.2584
i	0.5976	0.6500	−6.3086	1.4833	1.5000	−7.7334
j	0.3619	0.3667	−6.5265	0.9958	0.9958	−9.5762
k	0.4863	0.4863	−6.3299	1.0935	1.2000	−11.9334
b	0.3601	0.4000	−6.4001	0.7458	0.9000	−12.4000
a	0.0000	0.0000	−7.6900	0.0000	0.0000	−14.7815

Table 3. Elastic-perfectly plastic beam. Elastic energy for loading (up to point "*e*") and unloading, W_E [kNm].

Point of load	Path 1	Point of load	Path 2	Point of load	Path 3
a	0.0000	*a*	0.0000	*a*	0.0000
—	—	*b*	0.4000	*m*	0.0509
—	—	*c*	0.6250	*n*	0.3250
—	—	*d*	0.6500	*f*	0.4875
e	0.3667	*e*	0.4144	*e*	0.3672
a	0.0048	*a*	0.0524	*a*	0.0053

http://rcin.org.pl

column 1 for each point of load polygon (Theorem 1). According to Theorem 2, the values of columns 3, 5, 6 are greater or equal to the corresponding values of column 2. Similarly, in Table 2 the values in column 6 are not less than those in column 2 (Theorem 4), the values of column 2 appear to be the upper bounds on those of column 3 (P.G. Hodge's Theorem), whereas, according to (4.22), the column 1 is the lower bound on the corresponding values of column 4. We can also see that values of columns 2, 3 and 4 in Table 1 and values of the corresponding number of columns in Table 2 satisfy inequalities $(4.27)_1$, $(4.28)_2$ and $(4.29)_2$.

In Table 3 the current elastic energies in the elastic-perfectly plastic beam are presented for three paths of loading up to point "e" ($Q_1=0$, $Q_2=40$ kN) and unloading point "a", where $Q_1=Q_2=0$. It is clearly seen that the lowest residual elastic energy corresponds to the proportional (holonomic) loading (Path I). The results obtained here do not confirm the conclusion formulated in [19].

4. Final remarks

Inequalities (2.9) derived in the paper are of a general character and of a relatively wide range of applicability. These inequalities, related to the current elastic energy estimates, have been obtained using the distortional approach. Particular attention has been paid to time-independent materials and systems. Besides the elastic and plastic strains, the clearance (gap) strains are taken into consideration, which can be also treated as elastic distortions. It should be noted that in the case of time-dependent materials, some valuable results have been already obtained using the distortional approach (cf. [20]). The specific form of inequalities (2.9) allowed us to derive several bounding theorems to the elastic and complementary energies as well as to formulate some conclusions connected with the problem of elastic energy due to the presence of residual stresses in elastic-perfectly plastic systems. The results obtained in the paper presented can also be applied in damage mechanics, where the elastic energy evaluation plays a very important role. In some particular cases, inequalities (2.9), when applied to the energy in deformable systems, lead to results known in the literature of the subject (e.g. Hodge's Theorem, the elastic energy in elastic-cracking bodies).

The results of the work presented can be numerically applied to some insufficiently recognized problems, where some intuitively acceptable assumptions are introduced and no proofs of uniqueness of the solution exist. In such cases inequalities (2.9) can be used to check the correctness of computer calculations.

The example presented in Sec. 5 referes to the simple case of a beam. However, the FEM-oriented description used in the work allows us to consider much more complex structures, including also 3D systems. The results obtained in the example confirm all the theorems and essential conclusions that follow from the theoretical considerations. The author believes that similar results, certainly more general, can be obtained using the classical continuum description. On the other hand, the matrix description is very consistent and convenient to show the construction of the theory as well as allows us to derive important conclusions in a relatively simple way. It should be pointed out that all

http://rcin.org.pl

the problems, which can be met in practical appliations, have to be at least approximated by means of a suitable discretization in the subspace of finite dimensions.

Finally, it should be noted that many problems of energy in deformable systems remain to be solved, especially in the cases of slackened systems, cracking and time-dependent materials. Further research in this domain is being planned.

References

1. A. GAWĘCKI, *Bounding energy relations for deformable bodies* (in Polish), Seminar of Polish Association of Theoretical and Applied Mechanics, Poznań, 26-th February, 1989.
2. G. MAIER, *Mathematical programming methods in analysis of elastic-plastic structures* (in Polish), Arch. Inż. Ląd., **31**, 3, 387–411, 1975.
3. A. BORKOWSKI, *Analysis of skeletal structural systems in the elastic and elastic-plastic ranges*, PWN – Elsevier, 1988.
4. J.A. KÖNIG, *Shakedown of elastic-plastic structures*, PWN – Elsevier, Warszawa 1987.
5. W.N. MAJZEL, *Temperature problems in the theory of elasticity* (in Russian), Izd. UAN, Kijev 1951.
6. W. NOWACKI, *Thermal stresses in anisotropic bodies* (in Polish), Arch. Mech. Stos. (Arch. Mech.), **3**, 6, 1954.
7. E. BETTI, *Teoria della elasticita*, Il Nuovo Cimento, **2**, 6–10, 1872.
8. G. COLONNETTI, *Sul principio di reciprocita*, Rend. Lincei, **21**, 5, 1, 393–398, 1912.
9. A. GAWĘCKI, *Elastic-plastic-slackened structures* (in Polish), Rozprawy nr 185, Techn. Univ. Poznań, Poznań 1987.
10. A. GAWĘCKI, *On plastic flow mechanisms in the perfectly plastic-slackened structures*, Arch.Mech., **40**, 5/6, 653–663, 1988.
11. A. GAWĘCKI, *Matrix theory of elastic-plastic-slackened structures*, Bull. Acad. Polon. Sci., Série Sci. Techn., **37**, 3–4, 141–148, 1989.
12. A. GAWĘCKI, *Elasto-plasticity of slackened systems*, Arch. Mech., **40**, 4, 363–390, 1992.
13. A. HAAR, T. KÁRMÁN, *Zur Theorie der Spannungzustände in plastischen und sandartigen Medien*, Göttinger Nachr.Math.Phys.Klasse, **2**, 204–218, 1909.
14. J.B. MARTIN, *Plasticity. Fundamentals and general results*, MIT Press 1975.
15. P.G. HODGE, *A deformation bounding theorem for flow-law plasticity*, Quart. Appl. Math., **24**, 171–174, 1966.
16. A. GAWĘCKI, *Holonomic behaviour of elastic-perfectly plastic-slackened structures*, Techn. Univ. Poznań Reports Zesz. Nauk. Pol. Poznań. Bud. Ląd., nr 31, 33–41, 1988.
17. A. GAWĘCKI, T. ŁODYGOWSKI, *Cracking as a problem of elastic distortions*, 28-th Polish Solid Mechanics Conference, 4–8 Sept. 1990, Kozubnik.
18. R. HILL, *The mathematical theory of plasticity*, Oxford Univ. Press, Oxford 1950.
19. N. ARAVAS, K.S. KIM and F.A. LECKIE, *On the calculations of the stored energy of cold work*, Trans. ASME, J. Engng. Mater. and Techn., **112**, 465–470, 1990.
20. J. HOLNICKI-SZULC, *Analysis of prestressed visco-elastic structures by the virtual distortion method*, Engng. Trans., **40**, 1, 133–144, 1993.

POZNAŃ UNIVERSITY OF TECHNOLOGY
INSTITUTE OF BUILDING STRUCTURES, POZNAŃ.

Received August 20, 1992, *new version July* 14, 1993.

http://rcin.org.pl

Arch.Mech., 45, 4, pp. 457–470, Warszawa 1993

Delayed die swell as a problem of instability

S. ZAHORSKI (WARSZAWA)

THE DELAYED viscoelastic die-swell phenomenon, i.e. an experimentally observed change of curvature (an inflection point) in the jet profile is treated as a problem of "instability" caused by disturbed boundary conditions at the exit. The conditions of the delayed die swell in the form of inequalities satisfied by the corresponding increments of forces and velocities are considered. Axial and radial viscosity variations implied by admissible temperature distributions are also taken into account. Effects of inertial and air-drag forces on the delayed die swell are discussed in greater detail.

1. Introduction

THE DIE-SWELL PHENOMENON, i.e. an expansion of viscoelastic as well as viscous jets during extrusion processes was widely studied in the past, both theoretically and experimentally. For details, the interested readers are directed to abundant references which can be found elsewhere (cf. e.g. [1, 2, 3, 4, 5, 6, 7]). We should stress, however, that although various possible mechanisms of the phenomenon, e.g. elastic recovery, relaxation processes, stream-line rearrangements etc. were discussed exhaustively, there still exists some doubt whether the dynamics of die swell is well understood (cf. [8]).

Recently, JOSEPH *et al.* [8] widely reported on the so-called delayed die swell phenomenon appearing as a change of curvature (a point of inflection) in the expanded jet shape. According to experimental observations, at low rates of extension the swell starts at the pipe exit. At higher rates, when the extrusion velocity is raised above a critical value, the tendency of the jet to swell at the exit is suppressed and there is a delay in the swell. This phenomenon may be associated with a change from the pre-critical to post-critical flow, i.e. the change of type of the corresponding partial differential equations governed by the vorticity behaviour (cf. [9, 10]). Referring for more details to the paper of JOSEPH *et al.* [8], we should emphasize the fact that GIESEKUS [11] was the first to note that the delayed die swell is a critical phenomenon(1).

Another very interesting paper on the numerical simulation of delayed die swell was presented by DELVAUX and CROCHET [12]. Determining a set of material and flow parameters under which it is possible to simulate delayed die swell, the authors proved a critical character of the phenomenon and emphasized the role played by the viscoelastic Mach number and/or the elasticity number. They also showed that the effect of inertia is to retard the swelling over a distance of some radii from the die exit.

In the present paper we discuss the appearance of the delayed die-swell phenomenon as an instability problem depending on disturbances of the relevant

(1) Confirmation that delayed die swell is a hyperbolic transition can be found in the recent paper [21].

http://rcin.org.pl

boundary conditions at the pipe exit. To this end we apply the concept of flows with dominating extension (FDEs) previously defined and developed in our paper [13, 14, 15]. The approach presented in the paper is based on the assumption that the die swell already exists and the corresponding balance of forces is satisfied. Proceeding in such a way we arrive at certain formal conditions necessary for appearance of an inflection point (a change of curvature) either exactly at the pipe exit or at any place along the expanding part of a jet. In our more general analysis we take into account not only temperature-dependent viscosity variations along the axis but also possible (parabolic) radial viscosity distributions in the jet cross-sections (cf. [14]).

2. Die swell as a flow with dominating extension

The flows with dominating extension as well as their various applications were defined and discussed elsewhere (cf. [13, 14, 15]). For the present purpose we quote only certain relevant assumptions and relations.

In cylindrical coordinates the velocity gradient in the expanding jet is considered in the following general form:

$$[\nabla \mathbf{V}^*] = [\nabla \mathbf{V}] + [\nabla \mathbf{v}] = \begin{bmatrix} -\frac{1}{2} & 0 & 0 \\ 0 & -\frac{1}{2} & 0 \\ 0 & 0 & 1 \end{bmatrix} V' + \begin{bmatrix} \frac{\partial u}{\partial r} & 0 & \frac{\partial u}{\partial z} \\ 0 & \frac{u}{r} & 0 \\ \frac{\partial w}{\partial r} & 0 & \frac{\partial w}{\partial z} \end{bmatrix}, \tag{2.1}$$

where, under the assumption of quasi-elongational approximation (cf. [14, 15]), the fundamental velocity field depends only on axial coordinate z, i.e. $V = V(z)$. The prime denotes differentiation with respect to z, and the radial (u) and axial (w) physical components of the additional velocity field $\mathbf{v}$ (responsible for shearing effects) depend both on r and z.

We assume, moreover, that the ratio of jet radius to its characteristic length is small, i.e. $\varepsilon = R/l \ll 1$. In many situations (especially for the delayed die swell) l may be identified with the distance s from the die exit to the place where the radius R reaches its maximum (Fig. 1). Under the above assumption we can use simplifications characteristic for thin-layer flows, taking into account that diagonal terms in the first matrix are more meaningful than terms in the second one (weak shearing effects).

The flows with dominating extension (FDEs) have been defined in [13] as such thin-layer flows for which the constitutive equations of an incompressible simple fluid (cf. [16]) can be presented in the following linearly perturbed form:

$$\mathbf{T}^* = -p\mathbf{1} + \beta_1 \mathbf{A}_1 + \beta_2 \mathbf{A}_1^2 + \beta_1 \mathbf{A}_1^+ + \beta_2 \mathbf{A}_1^2 + \beta_2 (\mathbf{A}_1^2)^+ + \frac{\partial \beta_1}{\partial V'} (V')^+ \mathbf{A}_1 + \frac{\partial \beta_2}{\partial V'} (V')^+ \mathbf{A}_1^2 + \dots, \tag{2.2}$$

http://rcin.org.pl

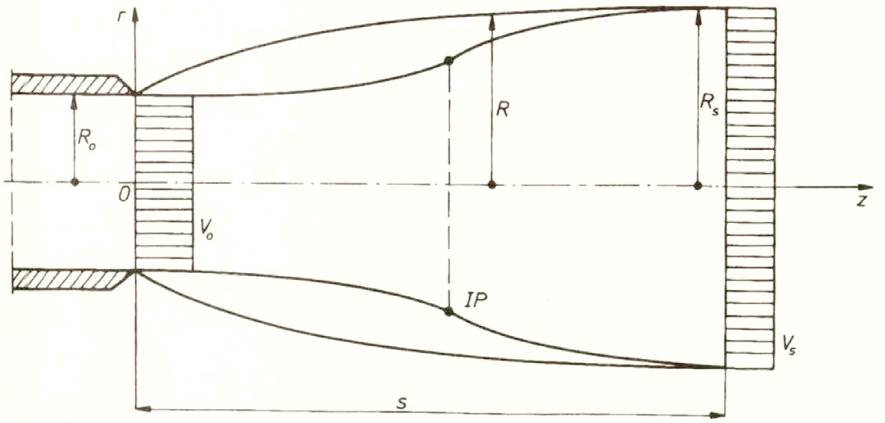

FIG. 1.

where $\mathbf{T}^*$ is the total stress tensor, p — the hydrostatic pressure, $\mathbf{A}_1$ — the first Rivlin–Ericksen kinematic tensor (cf. [16]), and β_i $(i=1, 2)$ denote the material functions depending, through the corresponding invariants, on the gradient $V'(z)$. The crosses mark linear increments which can be determined on the basis of Eq. (2.1) (cf. [14, 15]).

The elongational (longitudinal) viscosity can be defined as follows

$$\eta_E = 3\beta = 3(\beta_1 + \beta_2 V'). \tag{2.3}$$

Taking into account not only axial but also radial temperature distribution across the jet (cf. [14]), we may assume that either, in particular,

$$\beta(V'(z); r,z) = \eta(V'(z); z) f(r), \tag{2.4}$$

where $f(0) = 1$ or, in general,

$$\beta(V'(z); r,z) = \mu(V'(z); r,z)\bar{\eta}, \tag{2.5}$$

where $\bar{\eta}$ is an arbitrary constant with dimension of viscosity. Moreover, if viscosity distributions in the jet cross-section can be approximated by a parabolic function as proposed by KASE [17], we have

$$f(r) = 1 + ar^2, \qquad a > 0. \tag{2.6}$$

If in certain cases the simplified model assumption (2.4) cannot be accepted, we apply the more general assumption (2.5).

For fundamental quasi-elongational flows the corresponding constitutive equations (cf. Eq. (2.2)) lead either to

$$T^{\langle 33\rangle} - T^{\langle 11\rangle} = 3\eta V' f(r), \tag{2.7}$$

http://rcin.org.pl

if Eq. (2.2) is valid, or to

$$T^{\langle 33\rangle} - T^{\langle 11\rangle} = 3\bar{\eta} V' \mu(V'; r,z), \tag{2.8}$$

in a general case. The angle brackets denote physical components of the fundamental stress tensor.

Since the mass flow rate W is conserved along the swelling jet, we obtain

$$W = \rho \pi R^2 V = \text{const}, \tag{2.9}$$

where $R(z)$ is the outer variable radius. Similar relations are valid at the beginning and at the end, i.e. for $R(0) \equiv R_0$ and $R(s) \equiv R_s$ (Fig. 1). In the same places the following boundary conditions are satisfied:

$$V_0 = V(0), \qquad V_s = V(s), \tag{2.10}$$

where s denotes the distance between the exit and the maximum jet diameter. It also results from Eq. (2.9) that the additional velocity field does not affect the flow rate; thus, the fundamental velocity field $V(z)$ can be considered as mean velocity in any cross-section.

Integration of Eq. (2.7) over the entire cross-section

$$3\eta V' \int_0^R 2\pi r f(r)\, dr = F(z), \tag{2.11}$$

where $F(z)$ denotes the corresponding force, leads to

$$R' = -\frac{\rho R^3 F(z)}{6\eta W \varphi(z)}, \tag{2.12}$$

where the prime denotes derivative with respect to z. In deriving Eq. (2.12) we have used the differentiated form of Eq. (2.9) and the notation:

$$\varphi(z) = \int_0^R 2r f(r)\, dr, \tag{2.13}$$

where $\varphi = R^2$ for $f(r) \equiv 1$. On the other hand, integration of q. (2.7), using notation introduced in Eq. (2.5), gives

$$R' = -\frac{\rho R^3 F(z)}{6\bar{\eta} W \bar{\varphi}(z)} = -\frac{\rho F R}{6\bar{\eta} W \alpha(z)}, \tag{2.14}$$

where

$$\bar{\varphi}(z) = \int_0^R 2r\mu(V'(z); r,z)\, dr = \alpha(z) R^2. \tag{2.15}$$

It results from Eqs. (2.12), (2.14) that $F(0) = 0$, $R'(s) = 0$, i.e. for the maximum jet diameter the total force is equal to 0.

http://rcin.org.pl

3. Force and momentum balance

The balance of forces acting in the swelling jet can be presented as follows (cf. [18, 19]):

$$F(z) \equiv F_{rh}(z) = F_{rh}(0) + F_{in}(z) + F_{st}(z) + F_{ad}(z) - F_{gr}(z), \tag{3.1}$$

where the subscripts: rh, in, st, ad, and gr denote: rheological, inertial, surface-tension, air-drag and gravitational force, respectively. For $z=s$, i.e. for the maximum jet diameter, we obtain

$$F_{rh}(0) + F_{in}(s) + F_{st}(s) + F_{ad}(s) - F_{gr}(s) = 0. \tag{3.2}$$

If only rheological and inertial forces are of major importance (cf. [18]), we arrive at the following simplified relation:

$$F(z) = F_{rh}(0) + F_{in}(z) = -F_0 + W(V_0 - V) \quad \text{for} \quad 0 \leqslant z < s, \tag{3.3}$$

where $F_{rh}(0) = -F_0 = \text{const} < 0$ denotes the force at the exit. In particular, we have

$$F_0 = W(V_0 - V_s) \quad \text{for} \quad z = s, \tag{3.4}$$

and

$$F(z) = W(V - V_s) = F_0 - W(V - V_0) \quad \text{for} \quad z > s, \tag{3.5}$$

if the jet is considered beyond the point $z=s$.

Bearing in mind the momentum balance at the exit and at the maximum-diameter cross-section, we obtain (cf. [4, 20])

$$T = \int_0^{R_0} \rho 2\pi r V^2 dr - \int_0^{R_0} 2\pi r T^{\langle 33 \rangle} dr = \int_0^{R_s} \rho 2\pi r V^2 dr = \rho \pi R_s^2 V_s, \tag{3.6}$$

where T denotes the so-called jet thrust.

On defining the mean values at the exit cross-section by

$$\langle \cdot \rangle = \frac{1}{\pi R_0^2} \int_0^{R_0} 2\pi r (\cdot) dr, \tag{3.7}$$

we arrive at the RICHARDSON'S formula [4] for the die-swell ratio:

$$D^2 = R_s^2 / R_0^2 = \frac{\langle V \rangle^2}{\langle V^2 \rangle - \frac{1}{\rho} \langle T^{\langle 33 \rangle} \rangle}. \tag{3.8}$$

Since Eq. (3.7) also leads to

$$\langle V \rangle = V_0, \quad \langle V^2 \rangle = V_0^2, \quad \langle T^{\langle 33 \rangle} \rangle = \frac{F_0}{\pi R_0^2}, \tag{3.9}$$

http://rcin.org.pl

the die swell ratio (3.8) can be presented in the simplified form:

$$D^2 = \frac{V_0}{V_0 - \frac{F_0}{W}} = \frac{V_0}{V_s}. \tag{3.10}$$

The same result remains valid, if we take into consideration the total axial velocity

$$V^* = V + w, \tag{3.11}$$

assuming that w^2, where w denotes the additional axial velocity, is small enough as compared with V^2.

4. Disturbed boundary values. Conditions of existence of the delayed die swell

4.1. General case

The delayed die-swell phenomenon is characterized by a point of inflection (change of curvature) in the jet profile. For some critical velocity at the exit, the delayed swell begins at the exit ($z=0$) and next moves along the expanding part of the jet (cf. [8]). In other words, for the existence of the delayed die swell we have the following conditions:

$$R'' = 0, \quad R' \geqslant 0, \tag{4.1}$$

for such values of z for which the curvature of the jet profile changes its sign. In particular, $R''(0) = 0$ means onset of the phenomenon exactly at the exit. Therefore, the delayed part of the swelling jet corresponds to

$$R'' \geqslant 0. \tag{4.2}$$

Differentiation of Eq. (2.12) with respect to z gives for the second derivative

$$R'' = -\frac{\rho R^3 F}{6\eta W\varphi}\left\{\frac{F'}{F} - \left(\frac{\eta'}{\eta} + \frac{\varphi'}{\varphi}\right) - \frac{\rho F R^2}{2\eta W\varphi}\right\}. \tag{4.3}$$

Assuming that, at some moment, the force $F(z)$ is disturbed by the increment ΔF, Eq. (4.2) leads to the inequality:

$$\Delta F + \frac{\eta W\varphi}{\rho R^2}\left(\frac{\eta'}{\eta} + \frac{\varphi'}{\varphi}\right)\frac{\Delta F}{F} \leqslant -\frac{1}{2}F + \frac{\eta W\varphi}{\rho R^2}\left[\frac{F'}{F} - \left(\frac{\eta'}{\eta} + \frac{\varphi'}{\varphi}\right)\right], \tag{4.4}$$

where we have used the fact that $F \leqslant 0$ in the expanding jet. Similarly, differentiation of Eq. (2.14) leads to the slightly different condition

$$\Delta F + \frac{\bar{\eta} W\bar{\varphi}'}{\rho R^2}\frac{\Delta F}{F} \leqslant -\frac{1}{2}F + \frac{\bar{\eta} W\bar{\varphi}}{\rho R^2}\left[\frac{F'}{F} - \frac{\bar{\varphi}'}{\bar{\varphi}}\right]. \tag{4.5}$$

http://rcin.org.pl

In both Eqs. (4.4) and (4.5) ΔF can be treated as either sudden or periodic increment of the force F defined by Eqs. (3.1) and (3.3). If ΔF depends periodically on time, the corresponding inflection point may move forth and back along the expanding part of the jet. This type of "pumping" has been observed by JOSEPH *et al.* [8].

4.2. Inertial case

For more detailed discussion of the above results, we assume that surface-tension, air-drag and gravity effects can be neglected as compared with the inertial ones (cf. [18]).

We introduce the following new notations:

$$F(z) = \frac{6W}{\rho R^2}(KR^2 + M), \tag{4.6}$$

where K and M are constants defined through the expression

$$K = \frac{\rho}{6}\left(V_0 - \frac{F_0}{W}\right) = \frac{\rho}{6}V_s > 0, \qquad M = -\frac{W}{6\pi} = -\frac{\rho V_0 R_0^2}{6} < 0, \tag{4.7}$$

i.e. by F_0, V_0 and R_0 at the exit. It is noteworthy that the inertialess case corresponding to $K = -\rho F_0/6W$ and $M = 0$ is irrelevant for the die-swell considered (if other forces are disregarded), since then $F \equiv -F_0$ and $R'(s)$ can never vanish.

Bearing in mind simplified Eqs. (2.12), (2.6), (2.13), i.e. a parabolic distribution of radial viscosity, we arrive at

$$R' = -\frac{KR^2 + M}{\eta R\left(1 + \frac{1}{2}aR^2\right)}. \tag{4.8}$$

Integration of the above differential equation leads to

$$\left(1 - M\frac{a}{2K}\right)\ln\left(\frac{KR^2 + M}{KR_0^2 + M}\right) = -2K\int_0^z \frac{dz}{\eta} - \frac{a}{2}(R^2 - R_0^2), \tag{4.9}$$

where the constant K may be considered as a solution of the equation:

$$\left(1 - M\frac{a}{2K}\right)\ln\frac{KR_s^2 + M}{KR_0^2 + M} = -2K\int_0^s \frac{dz}{\eta} - \frac{a}{2}(R_s^2 - R_0^2). \tag{4.10}$$

This equation simplifies considerably for $a = 0$, to the following form:

$$\ln\frac{1 - D^2X}{1 - X} = D^2\,\mathrm{Re}_a, \tag{4.11}$$

http://rcin.org.pl

where

$$D^2 = \frac{R_s^2}{R_0^2}, \qquad X = -\frac{KR_0^2}{M}, \tag{4.12}$$

and

$$\mathrm{Re}_a = \frac{\rho V_0}{3} \int_0^s \frac{dz}{\eta} \tag{4.13}$$

denotes the Reynolds number averaged over the distance s. The plot of D^2 (Re_a) for several values of the parameter X is shown in Fig. 2. This parameter can vary between 0 and 1; $X=1$ characterizes the case with no swell ($D^2=1$), while $X\to 0$ denotes increasing inertia effects.

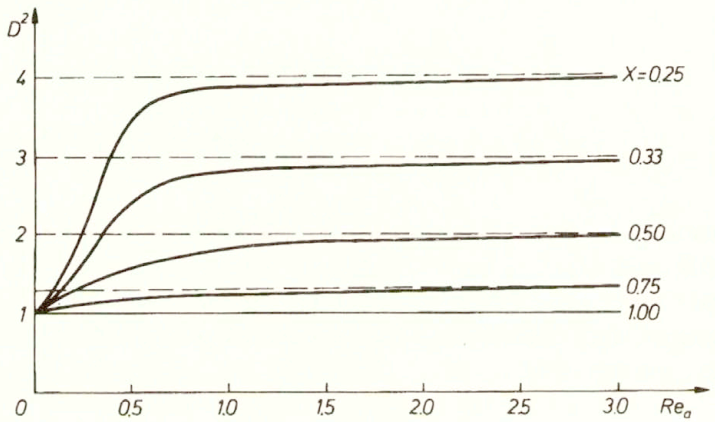

FIG. 2.

Differentiation of Eq. (4.8) with respect to z gives for the second derivative

$$R'' = \frac{KR^2+M}{\eta^2 R^3\left(1+\frac{1}{2}aR^2\right)}\left\{KR^2 - M - \frac{1}{2}aR^2(KR^2+3M) + \eta' R^2\left(1+\frac{1}{2}aR^2\right)^2\right\}. \tag{4.14}$$

It is easy to observe that for $\eta' \geqslant 0$ the above quantity is always negative and the conditions (4.1), (4.2) can never be satisfied. After introducing, however, the following increments of K and M:

$$\Delta K = \frac{\rho}{6}\left[\left(1+\frac{F_0}{WV_0}\right)\Delta V_0 - \frac{\Delta F_0}{W}\right], \qquad \Delta M = -\frac{\rho}{6} R_0^2 \Delta V_0, \tag{4.15}$$

where ΔV_0 and ΔF_0 denote possible disturbances of the velocity and force at the exit, respectively, the inequality (4.2) leads to the relations:

http://rcin.org.pl

$$\frac{\rho}{6}\left[\frac{\Delta F_0}{W}-\left(1+\frac{F_0}{WV_0}\right)\Delta V_0\right]\left(1-\frac{1}{2}aR^2\right)R^2-\frac{\rho}{6}R_0^2\left(1+\frac{3}{2}aR^2\right)\Delta V_0 \geqslant KR^2-M-\frac{1}{2}aR^2(KR^2+3M)+\eta' R^2\left(1+\frac{1}{2}aR^2\right)^2. \tag{4.16}$$

Since for $\eta' \geqslant 0$ the right-hand side of the above inequality is again positive, it may be satisfied only for non-vanishing disturbances at the exit, otherwise we have the ordinary die swell (with no changes of curvature).

In general, the increments of forces and velocities are independent of each other. In the presence of radial viscosity gradients ($a \neq 0$), however, we conclude that the following limitations are required to satisfy Eq. (4.16):

a) for $aR_0^2 \leqslant 2$

$$\begin{aligned} &\Delta V_0 \geqslant 0, \quad \text{if} \quad \frac{\Delta F_0}{F_0} \geqslant \frac{\Delta V_0}{V_0}, \\ &\Delta V_0 \leqslant 0, \quad \text{if} \quad \frac{\Delta F_0}{F_0} \leqslant \frac{\Delta V_0}{V_0}; \end{aligned} \tag{4.17}$$

b) for $aR_0^2 \geqslant 2$

$$\begin{aligned} &\Delta V_0 \geqslant 0, \quad \text{if} \quad \frac{\Delta F_0}{F_0} \leqslant \frac{\Delta V_0}{V_0}, \\ &\Delta V_0 \leqslant 0, \quad \text{if} \quad \frac{\Delta F_0}{F_0} \geqslant \frac{\Delta V_0}{V_0}. \end{aligned} \tag{4.18}$$

It is seen that for very small radial viscosity gradients, positive velocity increments are accompanied by positive force increments. On the contrary, for higher viscosity gradients, i.e. for $aR_0^2 > 2$, signs of the corresponding increments are usually opposite.

Under certain particular circumstances either force or velocity increments can be considered separately. Therefore, we obtain from Eq. (4.16):

for $\Delta F_0 = 0$

$$-\frac{\Delta V_0}{V_0} \geqslant \left[\left(1-\frac{F_0}{WV_0}\right)\frac{1-\frac{1}{2}aR^2}{1+\frac{3}{2}aR^2}+\frac{R_0^2}{R^2}\right], \tag{4.19}$$

for $\Delta V_0 = 0$

$$\frac{\Delta F_0}{W_0} \geqslant \left(V_0-\frac{F_0}{W}\right)V_0\frac{R_0^2}{R^2}\frac{1+\frac{3}{2}aR^2}{1-\frac{1}{2}aR^2}, \tag{4.20}$$

http://rcin.org.pl

where for simplicity we have omitted effects of axial viscosity gradients η'.

Being interested in the onset of the delayed die swell at the exit ($z=0$), we see that, for $a\equiv 0$, Eqs. (4.19), (4.20) reduce to the form:

for $\Delta F_0 = 0$

$$-\frac{\Delta V_0}{V_0} \geqslant \frac{V_s+V}{2V_0-V_s+V}, \tag{4.21}$$

for $\Delta V_0 = 0$

$$\frac{\Delta F_0}{W_0} \geqslant V_s+V. \tag{4.22}$$

Putting $z = 0$ ($R = R_0$), we finally arrive at the following conditions for the onset of instability:

for $\Delta F_0 = 0$

$$-\frac{\Delta V_0}{V_0} \geqslant \frac{V_0+V_s}{3V_0-V_s} = \frac{2V_0-\dfrac{F_0}{W}}{2V_0+\dfrac{F_0}{W}}, \tag{4.23}$$

for $\Delta V_0 = 0$

$$\frac{\Delta F_0}{W_0} \geqslant V_0+V_s = 2V_0-\frac{F_0}{W}. \tag{4.24}$$

It is seen that the first inequality can be satisfied for the appropriate $\Delta V_0 < 0$, while the second one cannot be satisfied at all, at least for moderate values of ΔF_0.

Up to now we have been discussing the conditions (4.16) for some particular and simplified cases. Therefore, a natural question arises how the gradients of viscosity, radially characterized by $a \neq 0$ and axially described by η', can influence the delayed die swell. This question can be answered by comparison of Eq. (4.16) for $a \neq 0$ and $a = 0$, and for $\eta' \neq 0$ and $\eta' = 0$, respectively. Such an approach leads to the conclusion that for $\eta' = 0$ non-vanishing radial velocity gradient (characterized by a) intensifies the delayed die-swell effect, if

$$aR^2 \geqslant 2-\frac{8KR^2}{KR_0^2-M} = 2-\frac{8V_s}{V_s+V}, \qquad \eta' = 0. \tag{4.25}$$

Similarly, for $\eta' \neq 0$ the effect is intensified, if

$$\eta' \leqslant 0, \qquad a \equiv 0. \tag{4.26}$$

http://rcin.org.pl

The partial derivative of viscosity $\partial\eta/\partial z$ is usually positive when temperature effects are taken into account. On the basis of Eq. (2.4), we have

$$\eta' = \frac{\partial \eta}{\partial z} + \frac{\partial \eta}{\partial V'} V'' \tag{4.27}$$

and η' for isothermal cases may be negative for negative second derivatives V'', since $\partial\eta/\partial V' \geqslant 0$ for the majority of viscoelastic fluids (cf. [16]).

5. Total velocities, stresses and forces

The constitutive equations (2.2) introduced into the equations of equilibrium lead, after retaining terms of the highest order of magnitude with respect to ε, (i.e. terms up to ε), to the nonlinear governing equations (cf. [14, 15]). In this section, omitting details of the procedure, we present only certain important results obtained under the Newtonian approximation, i.e. for viscosities independent of the gradient $V'(z)$.

Thus, we have for the total axial velocity

$$V^* = V + w = V + \frac{3}{4\eta}\frac{\partial}{\partial z}(\eta V')\left(\frac{R^2}{2} - r^2\right) = V\left[1 + \frac{3}{8}\frac{R^2}{V}\left(\frac{\eta'}{\eta}V' + V''\right)\right]\left(1 - 2\frac{r^2}{R^2}\right), \tag{5.1}$$

and

$$V^*\,|_{r=R} = V\left[1 - \frac{3}{8}\frac{R^2}{V}\left(\frac{\eta'}{\eta}V' + V''\right)\right],$$

$$V^*\,|_{r=0} = V\left[1 + \frac{3}{8}\frac{R^2}{V}\left(\frac{\eta'}{\eta}V' + V''\right)\right]. \tag{5.2}$$

The additional velocity gradient

$$\frac{\partial w}{\partial r} = -\frac{3}{2\eta}\frac{\partial}{\partial z}(\eta V') \tag{5.3}$$

introduced into the relation resulting from Eq. (2.2), viz.

$$T^{\langle 33\rangle} - T^{\langle 11\rangle} = 3\beta V' + \frac{1}{2}\left(\frac{\partial \beta_1}{\partial V'} + \frac{\partial \beta_2}{\partial V'}V'\right)\left(\frac{\partial w}{\partial r}\right) \tag{5.4}$$

leads to the following total force:

$$F^* = 3\beta V'\left[1 + \frac{3}{16}k\eta R^2\left(\frac{\eta'}{\eta} + \frac{V''}{V'}\right)^2\right]\pi R^2, \tag{5.5}$$

http://rcin.org.pl

resulting from integration over the cross-section of the jet. Here

$$k = \frac{1}{\beta}\left(\frac{\partial \beta_1}{\partial V'} + \frac{\partial \beta_2}{\partial V'}\right) V' \tag{5.6}$$

is a small parameter enabling analytic (expanded) solutions for slightly non-Newtonian fluids (cf. [14, 15]).

It is noteworthy that the force F^* differs but little from F (cf. (2.11)), since the second term in Eq. (5.5) may be small not only because of small parameter k but also for small axial viscosity gradients η' and for sufficiently small second gradients V''.

6. Air drag effects

For fibre spinning processes, surface-tension and gravity effects are usually of minor importance as compared with rheological and inertia effects (cf. [18]). The only factor which may have some meaning is the so-called air drag (skin friction) caused by a surrounding medium. These effects can easily be taken into account for the case of die swell considered, at least in an approximate manner.

According to the considerations of SANO and ORII (cf. [19]), the force resulting from air-drag contribution can be written as

$$F_{ad}(z) = c\, R^{0.2} V^{1.2} z = \bar{c}\, R^{-2.2} z \simeq \bar{c}\, R^{-2} z, \tag{6.1}$$

where c and $\bar{c}$ are constants. Replacement of $R^{-2.2}$ by R^{-2} makes the calculations much easier, and can be accepted as an approximation. Thus, the total force amounts to

$$F(z) \simeq \frac{(KR^2 + M)\, 6W}{\rho R^2} + \bar{c}\, \frac{z}{R^2}, \tag{6.2}$$

where we have used Eqs. (3.1), (4.6) and simplified Eq. (6.1). Introducing Eq. (6.2) into Eq. (4.8) (with $a \equiv 0$) we obtain

$$RR' = \frac{C}{\eta}(s - z), \qquad C = -\frac{(KR_0^2 + M)}{s}, \tag{6.3}$$

where C is a new constant and s denotes the distance from the exit to the maximum diameter.

Differentiation of Eq. (6.3) with respect to z gives for the second gradient

$$R'' = \frac{(KR_0^2 + M)}{\eta s R}\left[\left(1 + \frac{\eta'}{\eta}(s - z)\right) + \frac{(KR_0^2 + M)}{\eta s R^2}(s - z)^2\right]. \tag{6.4}$$

The condition (4.2) implies, for the corresponding increments of K and M, the following inequality:

$$(\Delta K R_0^2 + \Delta M)(s - z)^2 \geqslant sR^2[\eta + \eta'(s - z)] + (KR_0^2 + M)(s - z)^2. \tag{6.5}$$

http://rcin.org.pl

Taking into account the relation between increments in Eqs. (4.15), we arrive at

$$\frac{F_0}{W}\frac{\Delta V_0}{V_0} - \frac{\Delta F_0}{F_0} \geqslant -\frac{6}{\rho}\frac{(KR_0^2+M)}{R_0^2} + \frac{6}{\rho s}(\eta + s\eta') \tag{6.6}$$

for the onset of the delayed die swell at the exit.

After integration of Eq. (6.3), we obtain the result

$$R^2 = R_s^2 + \frac{1}{\eta}(KR_0^2+M)(s-z)^2, \tag{6.7}$$

leading, for $z = 0$, to the relation:

$$R_s^2 - R_0^2 = -\frac{1}{\eta}(KR_0^2 - M)s^2, \tag{6.8}$$

from which R_s can be related to s.

Eq. (6.8), after introducing the notations (4.12), (4.13), can be written as

$$D^2 = \frac{1}{2}\mathrm{Re}_a(1-X)+1, \tag{6.9}$$

where D^2 means the swell ratio and Re_a — the Reynolds number averaged over the distance s. Thus, the dependence $D^2(\mathrm{Re}_a)$, for various values of X between 0 and 1, is linear with the slope equal to $\frac{1}{2}$ for $X \to 0$.

7. Final remarks

On the basis of the considerations and results presented above, one may conclude that:

1. The delayed die-swell phenomenon can be treated as a problem of instability, caused by the disturbed boundary conditions expressed in terms of forces and velocities acting at the exit.

2. If the boundary conditions at the exit are undisturbed, the delayed die swell cannot occur. The curvature of the jet profile is negative everywhere and the ordinary die swell (without any point of inflection) can be observed.

3. The increments of forces and velocities at the exit are not only small but not entirely independent. They may essentially depend on radial and axial viscosity distributions. If either disturbances of forces or velocities appear separately, the former must be positive and the latter negative, to ensure existence of an inflection point, i.e. the delayed die swell.

4. The possibility of delayed die swell is greater for considerable radial viscosity gradients, i.e. for $aR^2 > 2$. On the contrary, the positive axial viscosity gradient η' implies negative effect on the delayed die swell.

http://rcin.org.pl

5. An approximate analysis of air-drag (skin-friction) effects, shows that such effects reduce the corresponding (negative) force acting on the expanding part of the jet. If $\eta' \approx 0$, the effect of air drag on the onset of instability is always positive.

6. The plots of the die-swell ratio D^2 vs. the averaged Reynolds number Re_a are monotonically increasing functions; they essentially depend on the inertia parameter. Higher inertial effects intensify the die swell phenomenon.

References

1. C. BARUS, *Isothermals, isopiestics and isometrics relative to viscosity*, American J.Sci., **45**, 87, 1893.
2. A.C. MERRINGTON, *Measurements of anomalous viscosity by the capillary tube method*, Nature, **152**, 214, 1943.
3. R.I. TANNER, *A theory of die swell*, J. Polymer Sci., **A8**, 2067, 1970.
4. S. RICHARDSON, *The die-swell phenomenon*, Rheol.Acta., **9**, 193, 1970.
5. R.I. TANNER, *Die-swell reconsidered: some numerical solutions using a finite element program*, Appl. Polymer Symp., **20**, 201, 1973.
6. J.R.A. PEARSON and R. TROTTNOW, *On die swell: some theoretical results*, J. Non-Newtonian Fluid Mech., **4**, 195, 1978.
7. R.I. TANNER, *A new inelastic theory of extrudate swell*, J. Non-Newtonian Fluid Mech., **6**, 289, 1980.
8. D.D. JOSEPH, J.E. MATTA and K. CHEN, *Delayed die swell*, J. Non-Newtonian Fluid Mech., **24**, 31, 1987.
9. D.D. JOSEPH, M. RENARDY and J.C. SAUT, *Hyperbolicity and change of type in the flow of viscoelastic fluids*, Arch. Rational Mech. Anal., **87**, 213, 1985.
10. M. AHRENS, Y.J. YOO and D.D. JOSEPH, *Hyperbolicity and change of type in the flow of viscoelastic fluids through pipes*, J. Non-Newtonian Fluid Mech., **24**, 67, 1987.
11. H. GIESEKUS, *Verschiedene Phänomene in Strömungen viskoelasticher Flüssigkeiten durch Düsen*, Rheol. Acta, **8**, 411, 1968.
12. V. DELVAUX and M.J. CROCHET, *Numerical simulation of delayed die swell*, Rheol. Acta, **29**, 1, 1990.
13. S. ZAHORSKI, *Viscoelastic flows with dominating extensions: application to squeezing flows*, Arch. Mech., **38**, 191, 1986.
14. S. ZAHORSKI, *An alternative approach to non-isothermal melt spinning with axial and radial viscosity distributions*, J. Non-Newtonian Fluid Mech., **36**, 71, 1990.
15. S. ZAHORSKI, *Fibre spinning processes as viscoelastic flows with dominating extensions*, Arch. Mech., **42**, 233, 1990.
16. S. ZAHORSKI, *Mechanics of viscoelastic fluids*, Martinus Nijhoff, The Hague, 1982.
17. S. KASE, *Studies on melt spinning. III. Velocity field within the thread*, J. Appl. Polymer Sci., **18**, 3267, 1974.
18. A. ZIABICKI, *Fundamentals of fibre formation. The science of fibre spinning and drawing*, Wiley, London, 1976.
19. *High-speed fiber spinning*, [Eds.] A. ZIABICKI and H. KAWAI, Interscience, New York, 1985.
20. J.M. DAVIES, J.F. HUTTON and K. WALTERS, *A critical reappraisal of the jet thrust technique for normal stresses with particular reference to axial velocity and stress rearrangement at the exit plane*, J. Non-Newtonian Fluid Mech., **3**, 141, 1977/78.
21. D.D. JOSEPH and C. CHRISTODOULOU, *Independent confirmation that delayed die swell is a hyperbolic transision*, J. Non-Newtonian Fluid Mech., **48**, 225, 1993.

POLISH ACADEMY OF SCIENCES
INSTITUTE OF FUNDAMENTAL TECHNOLOGICAL RESEARCH.

Received July 14, 1993.

http://rcin.org.pl

Arch.Mech., 45, 4, pp. 471–484, Warszawa 1993

Nonsimilar compressible boundary layer flow with vectored mass transfer and magnetic field

A. SAU and G. NATH (BANGALORE)

PRESENTED herein are studies of steady nonsimilar laminar compressible boundary layer flow over a flat plate of a viscous electrically conducting fluid of variable gas properties with vectored mass transfer and an applied magnetic field. The nonsimilarity is due to mass transfer at the wall, either suction or injection. Instead of being distributed so that similarity occurs, i.e. so that $(\rho v)_w \propto x^{-1/2}$, we assume that $(\rho v)_w$ is constant. This situation generally arises in practice if the wall is made of a porous material. Moreover, almost all of the analytical work deals with mass transfer that is normal to the surface. In practice, however, the surface mass transfer may include a streamwise velocity component u_w as well as a normal component v_w. This constitutes "vectored" surface mass transfer. Solutions have been obtained numerically using quasi-linearization technique in combination with an implicit finite difference scheme. It is found that both the skin friction and heat transfer coefficients respond significantly to the variation of magnetic parameter M, dissipation parameter E and the viscosity index ω.

1. Introduction

FOR HIGH VELOCITY flow of a gas past a body, the viscous heating in the boundary layer converts a large portion of kinetic energy into thermal energy which partially dissociates the gas and even produces a small, but not negligible, degree of ionization, and as a consequence, the gas becomes an electrical conductor. Studies have been made to see if the interaction of magnetic fields with these conducting gases will appreciably affect the skin friction and heat transfer in the boundary layer. Rossow [1] was the first, who studied solution to the flat plate problem considering incompressible laminar flow with constant electrical conductivity and a uniform magnetic field applied normal to the plate. Flow of a viscous incompressible electrically conducting fluid with an applied magnetic field have been investigated by GREENSPAN and CARRIER [2], DAVIES [3], GRIBBEN [4] and TAN and WANG [5]. BUSH [6] has solved compressible laminar boundary layer flow over a flat plate with an applied magnetic field fixed to the plate. Vectored mass transfer (both tangential and normal velocity components at the wall, i.e. u_w and v_w, are non-zero and subscript w denotes the condition at the wall) effects in case of adiabatic flows have been discussed by WAZZAN *et al.* [7]. NATH and MUTHANA [8] studied the effects of vectored mass transfer with variable gas properties ($\rho \propto T^{-1}$, $\mu \propto T^{\omega}$, where ω is the index in the power-law variation of viscosity) in the stagnation region of a two-dimensional axisymmetric body. INGER and SWEAN [9] have investigated the effects of vectored mass transfer on the velocity and thermal boundary layer flow (with constant gas properties and in absence of magnetic field) over a flat plate. They have

http://rcin.org.pl

assumed tangential component of velocity u_w to be constant and the normal component $v_w \propto x^{-1/2}$ (x is the streamwise coordinate), and obtained similarity solution to their problem. CHEN and SPARROW [10], in a numerical study, have investigated the same problem with the assumption that the normal component of velocity v_w at the surface is constant. In a recent study KUMAR *et al.* [11] have discussed the effect of vectored mass transfer on a two-dimensional boundary layer flow. These studies deal with self-similar flows.

The effects of vectored mass transfer, applied magnetic field and variable gas properties on the analogous steady nonsimilar case have not been reported in the literature; they may find application in aerodynamic heating which occurs in supersonic and hypersonic spacecrafts and missiles. The study of laminar compressible flow with vectored mass transfer becomes important and it has several applications such as (i) use of suction and blowing for boundary layer control on aerodynamic vehicles, (ii) film and transpiration cooling of rocket engines, turbomachinery blades and surface of high speed aerodynamic bodies, etc. Moreover, instead of fixing the magnetic field to the surface, it may be fixed with the main flow which then produces different effects in the boundary layer [12]. An example is a rotor vane moving in a fluid at rest in a passage with the magnetic field fixed to the passage.

The aim of this work is to study the vectored mass transfer on the steady nonsimilar laminar compressible boundary layer flow, over a flat plate, of a viscous electrically conducting fluid with variable gas properties, with an applied magnetic field fixed to the main flow and in the direction normal to the plate. The nonsimilar solution of the boundary layer equations has been obtained numerically using the method of quasi-linearization and an implicit finite difference scheme [13]. The particular cases of the present results have been compared with those of INGER and SWEAN [9], CHEN and SPARROW [10] and KUMAR *et al.* [11].

2. Governing equations

We consider the steady laminar compressible boundary layer flow of an electrically conducting viscous fluid with variable properties ($\rho \propto T^{-1}$, $\mu \propto T^{\omega}$, $\sigma \propto T^{n}$) over a flat plate with vectored mass transfer and an applied magnetic field B_0 perpendicular to the plate, fixed relative to the fluid. We assume that (i) the Prandtl number Pr is constant because its variation in most of the atmospheric flight problems in the boundary layer is small [14], (ii) specific heat c_p is a constant, (iii) Hall effect is negligible, (iv) magnetic Reynolds number is small, hence the induced magnetic field is negligible, (v) the high-temperature effects such as dissociation, ionization, recombination etc. have been neglected, (vi) no external electric field is applied, (vii) the velocity at the edge of the boundary layer $u_e = u_\infty$ is a constant, and (viii) the velocity of the wall $|u_w| < u_\infty$. Under the foregoing assumptions, the boundary layer equations governing the flow can be expressed as [9, 12]:

http://rcin.org.pl

$$(\rho u)_x+(\rho v)_y = 0, \tag{2.1}$$

$$\rho(uu_x+vu_y) = (\mu u_y)_y-\sigma B_0^2 u-p_x, \tag{2.2}$$

$$\rho(uh_x+vh_y) = up_x+(\mathrm{Pr}^{-1}\mu h_y)_y+\mu u_y^2+\sigma B_0^2 u^2, \tag{2.3}$$

where ρ, μ, h, B_0, σ are density, coefficient of viscosity, specific enthalpy, strength of the magnetic field and electrical conductivity, respectively. u and v are the velocity components along x and y-axis, taken in the direction of flow and perpendicular to the wall, respectively.

The boundary conditions are

$$\begin{aligned} &u(x,0) = u_w, \quad v(x,0) = v_w, \quad h(x,0) = h_w, \\ &u(x,\infty) = u_e, \quad h(x,\infty) = h_e, \end{aligned} \tag{2.4}$$

where subscripts w and e denote conditions at the wall and at the edge of the boundary layer, respectively.

Now we use the following transformations:

$$\xi=\rho_e\mu_e u_e x, \quad \eta=(2\xi)^{-1/2}u_\infty\int_0^y \rho dy, \quad \bar{x} = x/L, \quad u=u_e f'(\xi,\eta), \quad h=h_e g(\xi,\eta),$$

$$\rho=\rho_e g^{-1}, \quad \sigma=\sigma_e g^n, \quad M = \frac{\text{Ponderomotive force}}{\text{Inertia force}} = \frac{\sigma_e B_0^2 L}{\rho_e u_e}, \tag{2.5}$$

$$E = \frac{u_\infty^2}{h_e}, \quad N = \frac{\rho\mu}{\rho_e\mu_e} \quad \text{and} \quad (\,)' \equiv \partial/\partial\eta,$$

where L is the characteristic length and n is the power-law index; then the above set of equations in the dimensionless form, when the pressure gradient is replaced by its corresponding potential flow value, namely, $p_x = -\sigma_e B_0^2 u_e$ (since u_e=const), reduces to

$$(NF')'+fF'+2\bar{x}Mg(1-g^nF) = 2\bar{x}(FF_{\bar{x}}-f_{\bar{x}}F'), \tag{2.6}$$

$$(\mathrm{Pr}^{-1}Ng')'+fg'+E[NF'^2+2\bar{x}MgF(g^nF-1)] = 2\bar{x}(Fg_{\bar{x}}-f_{\bar{x}}g'), \tag{2.7}$$

where $u_e=u_\infty$ is taken to be constant and $f=\int_0^\eta F d\eta + f_w$.

The boundary conditions imposed on the set of Eqs. (2.6)–(2.7) are

$$f=f_w, \quad f'(=F) = u_w/u_e = \alpha, \quad g = g_w \quad \text{at} \quad \eta = 0, \tag{2.8}$$

and

$$F\to 1, \quad g\to 1 \quad \text{as} \quad \eta\to\infty.$$

The tangential and normal mass transfer parameters are, respectively,

http://rcin.org.pl

$$f'_w(=F_w) = u_w/u_e = \alpha = \text{const} \quad \text{and} \quad f_w = A\bar{x}^{1/2},$$

where

$$A = -(2\mathrm{Re}_L)^{1/2}(\rho v)_w/(\rho_e u_e) \quad \text{and} \quad \mathrm{Re}_L = u_\infty L/\nu_e.$$

We have taken v_w=const so that A is a const. When $\alpha>0$, $A>0$, it refers to downstream vectored suction and $\alpha>0$, $A<0$ corresponds to downstream vectored injection. Similarly $\alpha<0$, $A>0$ refers to upstream vectored suction and $\alpha<0$, $A<0$ pertains to upstream vectored injection. We have taken the gas with variable properties modeled realistically, that is [15, 16]

$$\rho\propto h^{-1}, \quad \mu\propto h^{\omega}, \quad N=\frac{\rho\mu}{\rho_e\mu_e}=(h/h_e)^{\omega-1}, \quad \sigma\propto h^n, \quad \rho_e/\rho=h/h_e=g, \quad \sigma/\sigma_e=(h/h_e)^n=g^n,$$

where $\omega=0.5$ represents conditions encountered in hypersonic flight [15], $\omega=0.7$ corresponds closely to the low temperature flows and $\omega=1$ represents the familiar constant density viscosity product for simplification.

The quantities of physical interest are the skin friction coefficient C_f and the Stanton number St defined by

$$C_f = 2\left(\mu\frac{\partial u}{\partial y}\right)_w \Big/ \rho_e u_e^2, \qquad \mathrm{St} = \mathrm{Pr}^{-1}\left(\mu\frac{\partial h}{\partial y}\right)_w \Big/ [(h_e-h_w)\rho_e u_e].$$

These can readily be related to the solution variables via the expressions

$$\bar{C}_f \equiv C_f(\mathrm{Re}_x)^{1/2}/\sqrt{2} = F'_w N_w, \qquad H_t \equiv \mathrm{St}\,(2\mathrm{Re}_x)^{1/2} = \mathrm{Pr}^{-1}(1-g_w)^{-1}N_w g'_w,$$

where $\mathrm{Re}_x = u_\infty x/\nu_e$ is the Reynolds number.

3. Results and discussion

Equations (2.6) and (2.7) with boundary conditions (2.8) have been solved numerically using quasi-linearization technique and an implicit finite difference scheme. Since the method has been described in detail in [12], its description is omitted here. The nonlinear partial differential Eqs. (2.6) and (2.7) were first linearized using quasi-linearization method, and then the resulting linear partial differential equations were expressed in difference form by using central difference scheme in η-direction and backward difference scheme in $\bar{x}$-direction. Finally, the system of equations was reduced to a linear algebraic system with a block tri-diagonal structure which is solved using Varga algorithm [17]. To ensure the convergence of the quasilinear finite-difference scheme to the true solution, the step-sizes $\Delta\eta$ and $\Delta\bar{x}$ have been optimized to $\Delta\eta=0.05$ and $\Delta\bar{x}=0.025$ and the results presented here are independent of step-sizes at least up to the fourth decimal place. The computations have been carried

http://rcin.org.pl

out for various values of $A(-0.5 \leqslant A \leqslant 0.5)$, $\alpha(-0.3 \leqslant \alpha \leqslant 1.0)$, $M(5 \leqslant M \leqslant 20)$, $g_w(0.2 \leqslant g_w \leqslant 0.6)$, $\omega(0.5 \leqslant \omega \leqslant 1.0)$, $n(1 \leqslant n \leqslant 5)$, and $E(0.0 \leqslant E \leqslant 1.0)$. In all numerical computations Pr have been taken 0.72 and η_∞, the edge value of the boundary layer is taken between 6 and 8 depending on the values of various parameters.

It may be remarked that Eqs. (2.6) and (2.7) were solved numerically for $M=0$, $\omega=1$, $E=0$ and $\bar{x}=0$ by INGER and SWEAN [9] using shooting method and for $M=0$, $\omega=1$ and $E=0$ by CHEN and SPARROW [10] when $2\bar{x}$ is replaced by $\bar{x}$ in Eqs. (2.6) and (2.7) using local nonsimilarity method. In order to assess the accuracy of the method, we have compared our results with those of Refs. [9–11] and they are found to be in excellent agreement (see Figs. 1–2 and Table 1).

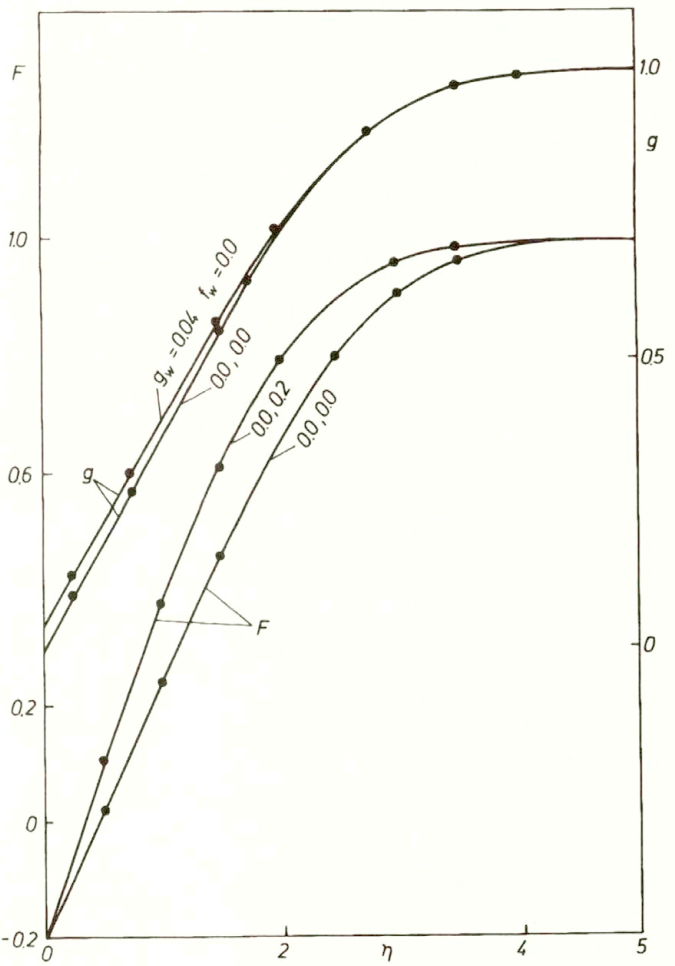

FIG. 1. Comparison of velocity (F) and enthalpy (g) profiles for $\bar{x}=0.0$, $\alpha=-0.2$, Pr=1.0, $\omega=1.0$, $E=n=M=0.0$, ——— present calculation; • INGER and SWEAN [9].

http://rcin.org.pl

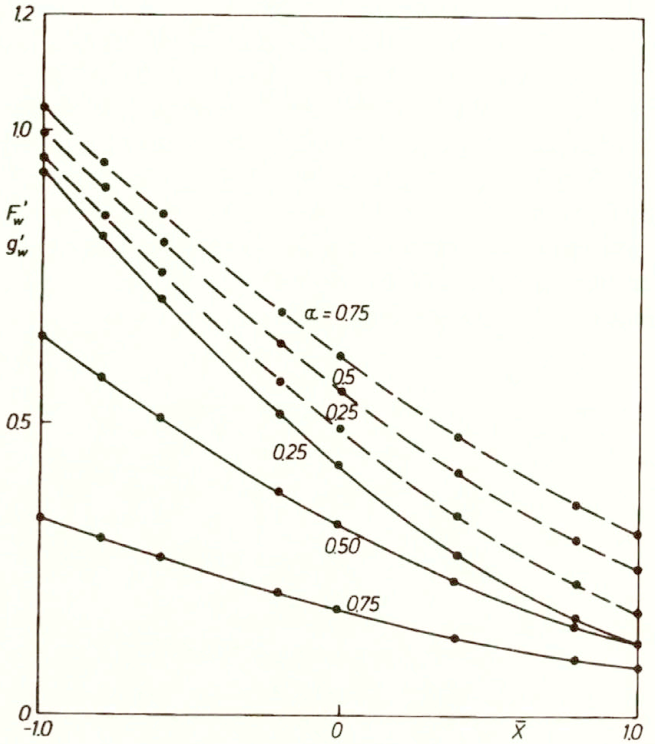

FIG. 2. Comparison of skin friction (F'_w) and heat transfer (g'_w) parameters for Pr = 0.7, $\omega = 1.0$, $E = M = 0.0$, $f_w = -\bar{x}/2$, ——— F'_w (present calculation); – – – g'_w (present calculation); • CHEN and SPARROW [10].

Table 1. Comparison of the skin friction parameter (F'_w) with INGER and SWEAN [9] and KUMAR *et al.* [11] for Pr = 1, $\omega = 1$, $M = 0$, $\bar{x} = 0$ and $E = 0$.

f_w	F_w (= α)	F'_w		
		INGER and SWEAN	KUMAR *et al.*	Present results
0.5	0.4	0.5914	0.59135	0.59137
0.2	0.6	0.3292	0.32922	0.32921
−0.2	0.2	0.3381	0.33811	0.33813
−0.5	0.4	0.1977	0.19775	0.19772
−0.8	0.8	0.0631	0.06310	0.06311

The effect of vectored mass transfer (i.e. effect of A and α) on the skin friction and heat transfer coefficients ($\bar{C}_f$, H_t) is shown in Fig. 3. Both the skin friction ($\bar{C}_f$) and heat transfer (H_t) coefficients decrease with the increase of normal injection (A) in the case of downstream vectoring ($A < 0$, $\alpha > 0$). But in case of upstream vectoring ($A > 0$, $\alpha < 0$) both skin friction ($\bar{C}_f$) and heat transfer (H_t) coefficients are found to increase as tangential injection (α) increases. For the sake of clarity we also present some of the

http://rcin.org.pl

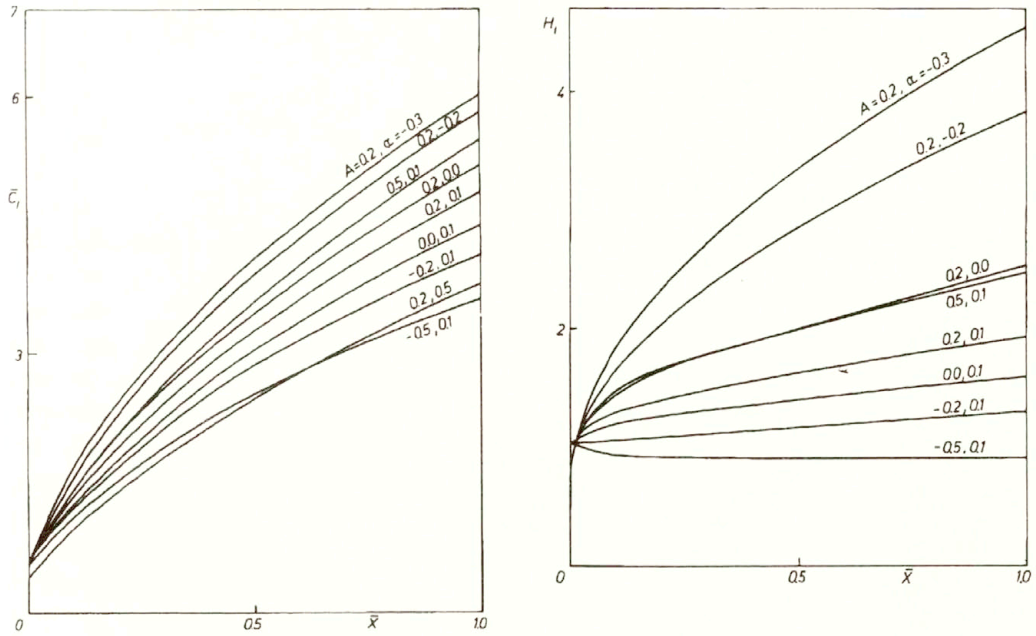

FIG. 3. Effect of vectored mass transfer (A, α) on the skin friction ($\bar{C}_f$) and heat transfer (H_t) for $g_w=0.2$, $E=1.0$, $\omega=0.5$, $M=10$ and $n=1.0$.

results quantitatively. In case of downstream vectoring ($\alpha=0.1$), as the normal injection parameter A varies from 0 to -0.5, the skin friction ($\bar{C}_f$) and the heat transfer (H_t) at $\bar{x}=1$ decrease approximately by an amount of 18% and 42%, respectively, when other parameters remain fixed. On the other hand, in case of upstream vectoring, the percentage increase in skin friction ($\bar{C}_f$) and heat transfer (H_t) coefficients at $\bar{x}=1.0$ is about 15% and 80%, respectively, as the tangential mass transfer parameter α changes from 0 to -0.3. Thus the effect of vectored mass transfer is more pronounced on the heat transfer coefficient than on the skin friction coefficient. In the case of injection, the fluid is carried away from the surface causing reduction in the skin friction parameter (F'_w), hence in $\bar{C}_f$, as it tries to maintain the same F over a very small region near the surface and this effect is reversed in the case of suction.

The effects of the magnetic parameter M, the wall enthalpy g_w and the viscosity index parameter ω on the skin friction and heat transfer coefficients ($\bar{C}_f$, H_t) are displayed in Fig. 4 in case of zero tangential mass transfer ($\alpha=0$), and it is observed that both the skin friction and heat transfer respond significantly to the variation of magnetic parameter M, and they increase as M increases. As wall enthalpy g_w increases, the skin friction coefficient increases whereas the heat transfer decreases. But both the skin friction and heat transfer coefficients decrease as ω increase from 0.5 to 1.0.

http://rcin.org.pl

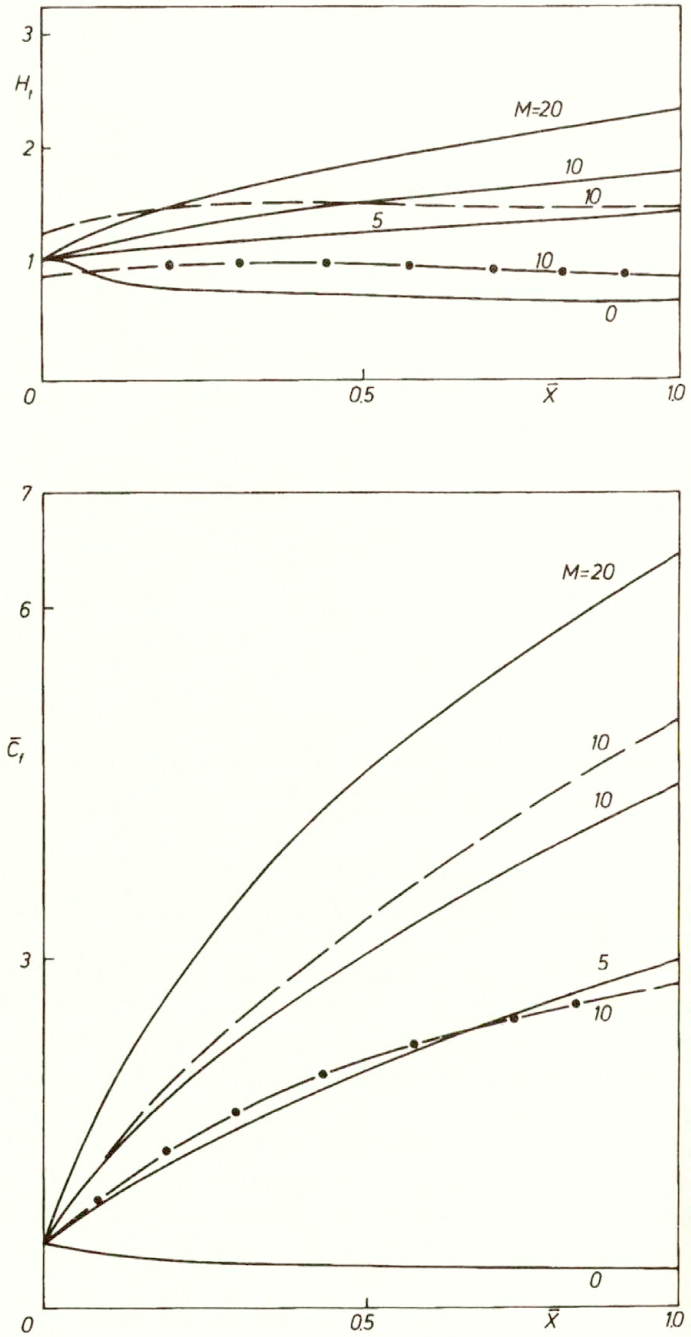

FIG. 4. Effects of magnetic parameter M, viscosity index ω and wall enthalpy g_w on skin friction and heat transfer ($\bar{C}_f$, H_t) for $A=-0.2$, $\alpha=0.0$, $E=1.0$ and $n=1.0$, ——— $g_w=0.2$, $\omega=0.5$; – – – $g_w=0.6$, $\omega=0.5$; – · – · – $g_w=0.2$, $\omega=1.0$.

http://rcin.org.pl

More explicitly, in absence of tangential mass transfer ($\alpha=0$) and at $\bar{x}=1$, the skin friction and heat transfer coefficients increase approximately by an amount of 50% and 26% respectively, as the magnetic parameter M increases from 5 to 10, when other parameters remain fixed. As the wall enthalpy g_w increases from 0.2 to 0.6, the skin friction coefficient increases by 12%, whereas heat transfer coefficient decreases by 26% at $\bar{x}=1$. The variation of ω from 0.5 to 1.0 shows that both the skin friction and heat transfer coefficients decrease approximately by an amount 38% and 51%, respectively, when other parameters remain fixed. Thus, from the above analysis it is clear that the magnetic parameter M and the parameter ω have significant effect on skin friction and heat transfer. The reason for increase in the skin friction and heat transfer coefficients ($\bar{C}_f$ and H_t) with M is due to the fact that the velocity and temperature gradients at the wall increase with the increase in M, since the velocity and thermal boundary layer thickness decrease. This increase in velocity and temperature gradients enhances the skin friction and heat transfer.

The effects of dissipation parameter E and n (the index in the power-law of electrical conductivity) on the skin friction and heat transfer ($\bar{C}_f$ and H_t) coefficients are shown in Fig. 5. As E increases from 0 to 1, both the skin friction and heat transfer

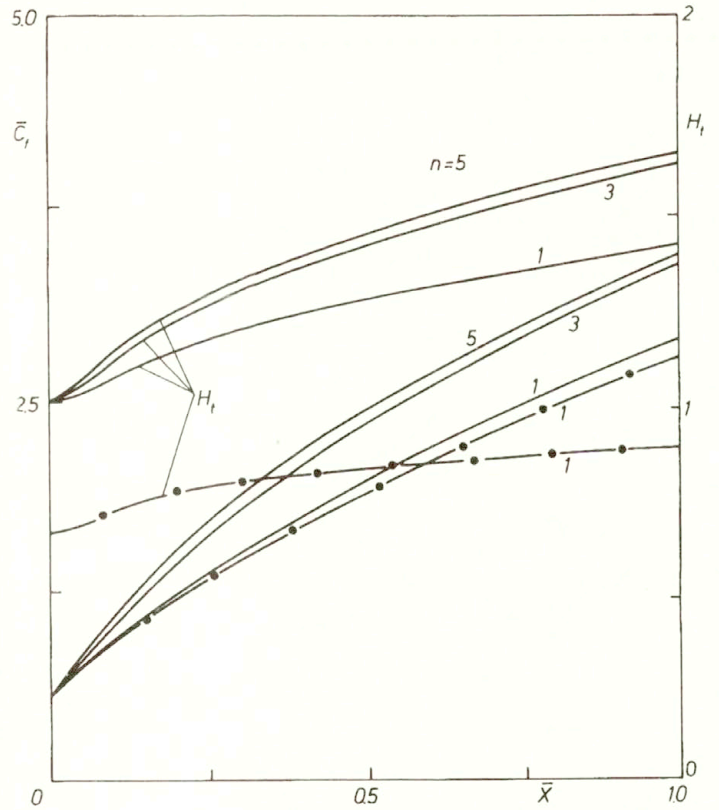

FIG. 5. Effects of viscous dissipation E and the parameter n on the skin friction and heat transfer ($\bar{C}_f$, H_t) for $g_w=0.2$, $M=5.0$, $\omega=0.5$, $A=-0.2$ and $\alpha=0.0$, ——— $E=1.0$; — · — · — $E=0.0$.

http://rcin.org.pl

coefficients increase and the effect is more significant on the heat transfer coefficient than on the skin friction coefficient. This behaviour is in support of the known fact that the viscous dissipation affects the thermal boundary layer more than the momentum boundary layer. Both the skin friction and heat transfer coefficients increase with n.

In Fig. 6 the skin friction and heat transfer coefficients ($\bar{C}_f$ and H_t) are plotted as functions of the tangential surface velocity α with the normal velocity at the surface f_w (depending on A) and M as parameters. At $\bar{x}=0$ both skin friction and heat transfer coefficients decrease for negative α (upstream vectoring) and the skin friction coefficient increases for small-to-moderate positive α (downstream vectoring) and ultimately vanishes at $\alpha=1$, whereas heat transfer increases with positive wall velocity α. For $\bar{x}>0$, the skin friction coefficient increases with M and with suction ($A>0$), but with injection ($A<0$) it shows the opposite effect.

Figures 7–8 show the effect of magnetic interaction parameter M and viscosity index ω on the velocity and enthalpy profiles (F, g). Both the velocity and enthalpy

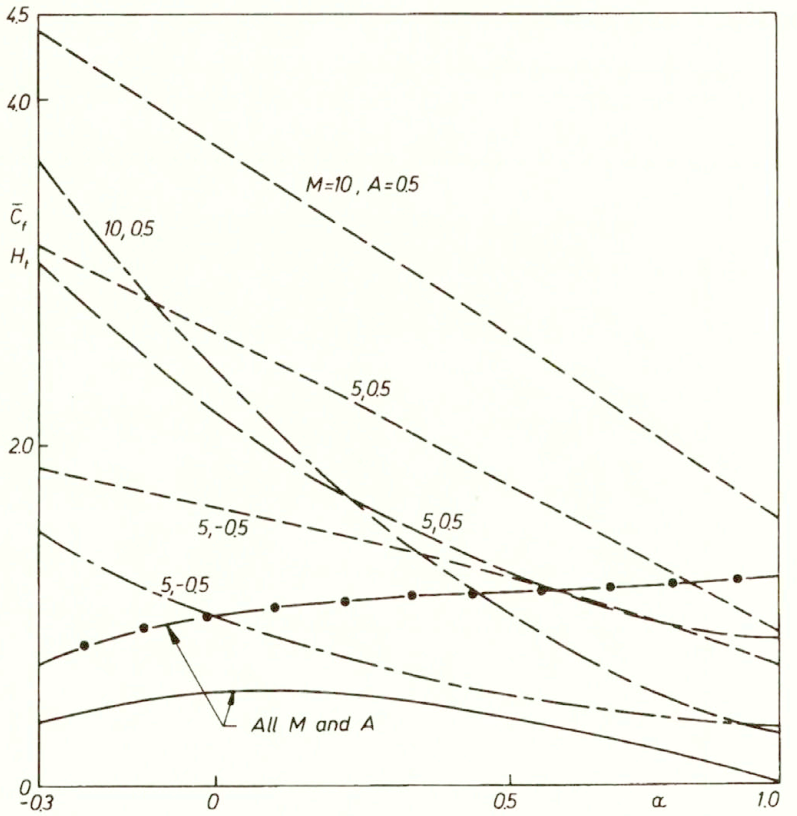

FIG. 6. Mass transfer vectoring effect and effect of M on the skin friction and heat transfer ($\bar{C}_f$, H_t) for $g_w=0.1$, $E=1.0$, $\omega=0.5$ and $n=1.0$, ——— $\bar{C}_f$, $\bar{x}=0.0$; – – – $\bar{C}_f$, $\bar{x}=0.5$; – · – · – H_t, $\bar{x}=0.0$; — — — H_t, $\bar{x}=0.5$.

http://rcin.org.pl

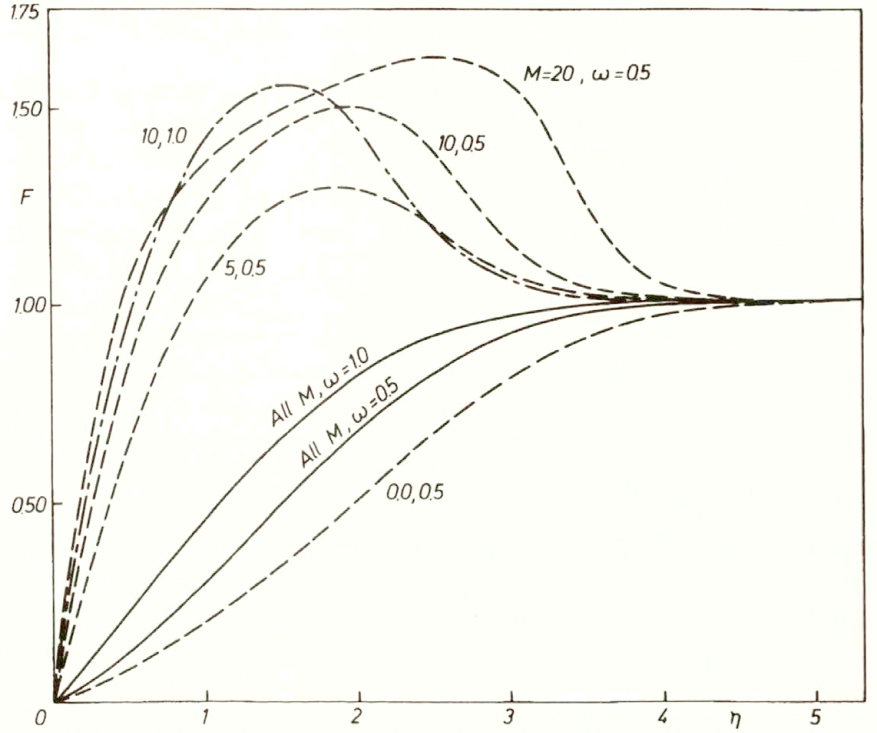

FIG. 7. Effect of magnetic parameter M and viscosity index ω on the velocity profiles (F) for $g_w=0.2$, $A=-0.2$, $\alpha=0.0$, $E=1.0$ and $n=1.0$, ——— $\bar{x}=0.0$; – – – $\bar{x}=1.0$.

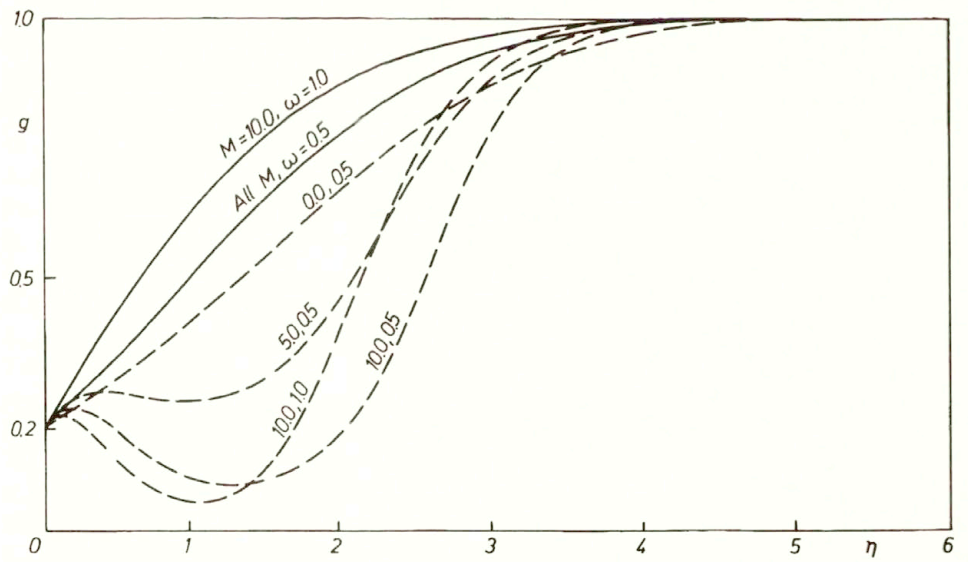

FIG. 8. Effect of magnetic parameter M and viscosity index ω on the enthalpy profiles (g) for $g_w=0.2$, $A=-0.2$, $\alpha=0.0$, $E=1.0$ and $n=1.0$, ——— $\bar{x}=0.0$; – – – $\bar{x}=1.0$.

http://rcin.org.pl

profiles are unaffected by M at $\bar{x}=0$ (obvious from the governing Eqs. (2.6) and (2.7)), whereas for $\bar{x}>0$ the profiles are different and we have observed significant overshoot in the velocity profile (F) (for $g_w<1$ velocity overshoot occurs when $Mn>1$ [18] and its magnitude increases with M, so that there is a point of inflection in the velocity profile). As ω increases from 0.5 to 1.0, the velocity and enthalpy profiles reach their free-stream value faster and hence the boundary layer thickness decreases, but the velocity overshoot increases.

The reason for the overshoot in velocity F and for increase in magnetic field when $\bar{x}>0$ may be due to the competition among inertia, pressure gradient and shear stress effects through the thickness of the boundary layer. The flow in the boundary layer and the flow in the free stream are subjected to the same longitudinal pressure gradient given by the equation $\partial p/\partial x = -\sigma_e B_0^2 u_e$ (as u_e=constant), which increases with magnetic parameter M. However, in the boundary layer, viscous effects reduce the tangential velocity. Consequently the longitudinal pressure gradient impressed on the boundary layer can cause a higher longitudinal flow acceleration to occur in the boundary layer than that present without the tangential velocity, even though shear stress also tends to balance the longitudinal pressure gradient near the surface. Quantitatively, as M increases from 5 to 10, the overshoot in velocity F at $\bar{x}=1$ increases approximately from 29% to 50% for fixed values of other parameters. Thus, velocity overshoot depends significantly on the magnetic parameter M.

Typical boundary layer velocity (F) and enthalpy (g) profiles pertaining to both upstream and downstream vectoring are shown in Fig. 9 for a fixed normal mass transfer (A). As expected, upstream tangential injection increases the boundary layer thickness whereas downstream tangential injection has the opposite effect.

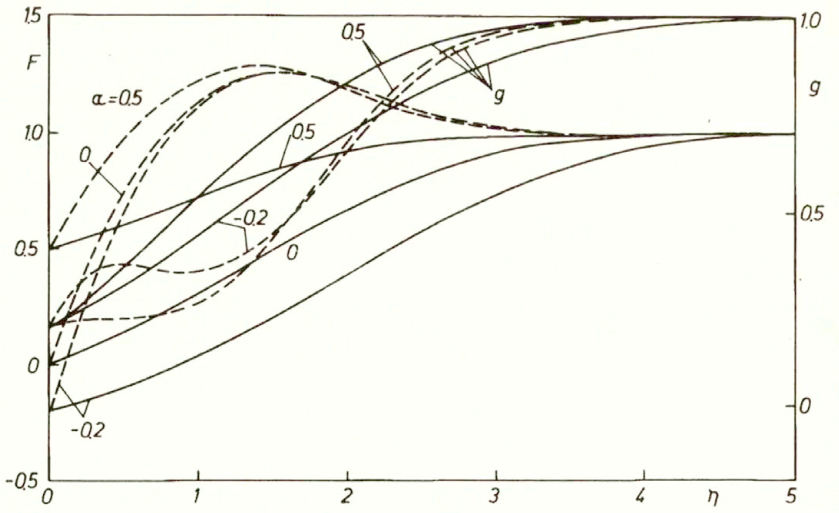

FIG. 9. Upstream and downstream vectoring effect on the velocity (F) and enthalpy (g) profiles for $g_w=0.2$, $M=5.0$, $E=1.0$, $\omega=0.5$, $A=0.2$ and $n=1.0$, ——— $\bar{x}=0.0$; – – – $\bar{x}=1.0$.

http://rcin.org.pl

4. Conclusion

The results indicate that both the skin friction and heat transfer coefficients respond significantly to the variation of magnetic parameter M, dissipation parameter E, viscosity index ω and the mass transfer parameters A and α. As the magnetic parameter M and the dissipation parameter E increase both the skin friction and heat transfer coefficients increase both the skin friction and heat transfer coefficients increase whereas viscosity index ω shows the reverse effect. The vectored mass injection is found to be more effective in reducing the skin friction and heat transfer compared to the injection applied normal to the surface. In the presence of a magnetic field, the velocity profile exhibits overshoot in certain region within the boundary layer. The boundary layer thickness increases as the tangential injection increases.

References

1. V.J. ROSSOW, *On flow of electrically conducting fluids over a flat plate in the presence of a transverse magnetic field*, NACA TN 3971, 1957.
2. H.P. GREENSPAN and G.F. CARRIER, *The magnetohydrodynamic flow past a flat plate*, J. Fluid Mech., **6**, 77–96, 1959.
3. T.V. DAVIES, *The magneto-hydrodynamic boundary layer in the two-dimensional steady flow past a semi-infinite flat plate III. The influence of an adverse magneto-dynamic pressure gradient*, Proc. Roy. Soc., **A 273**, 518–537, 1963.
4. R.J. GRIBBEN, *The magneto-hydrodynamic boundary layer in the presence of a pressure gradient*, Proc. Roy. Soc., **A 287**, 123–141, 1965.
5. C.W. TAN and C.C.T. WANG, *Heat transfer in aligned-field magnetohydrodynamic flow past a flat plate*, Int. J. Heat Mass Transfer, **11**, 319–329, 1968.
6. W.B. BUSH, *Compressible flat-plate boundary-layer with an applied magnetic field*, J. Aerospace Sci., **27**, 49–58, 1960.
7. A.R. WAZZAN, R.C. LIND and C.Y. LIU, *Laminar boundary layer with mass transfer and slip*, Phys. Fluids, **11**, 1271–1277, 1968.
8. G. NATH and M. MUTHANA, *Laminar compressible boundary layer with vectored mass transfer*, AIAA J., **14**, 1127–1130, 1976.
9. G.R. INGER and T.F. SWEAN, *Vectored injection into laminar boundary layers with heat transfer*, AIAA J., **13**, 616–622, 1975.
10. T.S. CHEN and E.M. SPARROW, *Flow and heat transfer over a flat plate with uniformly distributed vectored surface mass transfer*, Trans. ASME, J. Heat Transfer, **98**, 674–678, 1976.
11. P. KUMAR, P.S. NARAYANAN and R. SARBESWAR, *Laminar boundary layers with vectored mass transfer*, Int. J. Engng. Sci., **25**, 1503–1509, 1987.
12. K.R. CRAMER and S.I. PAI, *Magneto-fluid dynamics for engineers and applied physicts*, McGraw–Hill, New York 1973.
13. K. INOUYE and A. TATE, *Finite difference version of quasi-linearization applied to boundary layer equations*, AIAA J., **12**, 558–560, 1974.
14. A. WORTMAN, H. ZIEGLER and G. SOO-HOO, *Convective heat transfer at general three-dimensiona stagnation points*, Int. J. Heat Mass Transfer, **14**, 149–152, 1971.
15. H. SCHLICHTING, *Boundary layer theory*, McGraw–Hill, New York, 1979.

http://rcin.org.pl

16. J.F. GROSS and C.F. DEWEY [in:] Fluid Dynamics Transactions, [Ed.] W. FISZDON, Vol. II, Pergamon Press, Oxford 1965.
17. R.S. VARGA, *Matrix iterative analysis*, Prentice–Hall, New York 1962.
18. P.S. LYKOUDIS, *Velocity overshoot in magnetic boundary layers*, J. Aerospace Sci., **28**, 896–897, 1961.

DEPARTMENT OF MATHEMATICS
INDIAN INSTITUTE OF SCIENCE, BANGALORE, INDIA.

Received July 16, 1993.

http://rcin.org.pl

Arch.Mech., 45, 4, pp. 485–492, Warszawa 1993

Two widely-spaced spheres in a polar fluid

H. RAMKISSOON (ST. AUGUSTINE)

THE PROBLEM of hydrodynamic forces acting on two spheres immersed in a polar fluid and subject to a Stokes-type flow is considered in the paper. In order to describe the hydrodynamic interactions of two bodies, the method of reflections is used; the method is known from the literature concerning flows occurring in Newtonian fluids. The Eq. (3.15) derived in the paper presents the hydrodynamic drag exerted on the sphere as a function of mutual position, radii and velocities of the spheres, taking into account the material constants of the polar fluid considered. Two particular cases are concerned, when two identical spheres move at identical speeds in the directions which are parallel or perpendicular to the line connecting the centres of the spheres. Value of the drag is shown to increase with increasing values of the material constant k characterizing the fluid.

1. Introduction

THE MOTION of particles at small Reynolds numbers through an unbounded fluid finds application in the fields of meteorology, colloid chemistry, rheology and in the sedimentation of dilute suspensions. Of particular significance is the magnitude of the interaction which will be governed by such variables as the shapes and sizes of the particles, the distance between them, their orientations with respect to each other and their velocities and spins relative to the fluid.

In this short paper we consider the special case of two widely spaced rigid spheres translating in an otherwise unbounded micropolar fluid medium [1, 2] which is at rest at infinity. Applications of such fluids are well-known [3–6]. Our main objective is to obtain the force exerted on each sphere and this is achieved by utilizing the method of reflections. Two special cases are then deduced including the known classical result.

2. Preliminaries

Micropolar fluid theory was introduced by ERINGEN [1] in 1966. Basically, these fluids can support couple stress and body couples, and exhibit micro-rotational effects. Fluid points contained in a small volume element, in addition to their usual rigid motion, now possess the ability to rotate about the centroid of the volume element in an average sense described by the skew-symmetric gyration tensor $\mathbf{v}$ which is independent of the velocity field $\mathbf{u}$. In the case of slow steady incompressible flow in the absence of body forces and couples, the field equations are [1]:

$$
\begin{aligned}
&(\mu+\kappa)\,\nabla^2\mathbf{u} + \kappa\nabla\times\mathbf{v} - \nabla p = 0,\\
&(\alpha+\beta+\gamma)\,\nabla\nabla\cdot\mathbf{v} - \gamma\nabla\times\nabla\times\mathbf{v} + k\nabla\times\mathbf{u} - 2k\mathbf{v} = 0,\\
&\nabla\cdot\mathbf{u} = 0,
\end{aligned}
\tag{2.1}
$$

where $(\alpha, \beta, \gamma, \mu, \kappa)$ are material coefficients.

http://rcin.org.pl

In the case of a sphere of radius a translating with uniform speed U in an unbounded micropolar fluid being at rest at infinity, and whose field equations are given by Eq. (2.1), RAMKISSOON and MAJUMDAR [7] have determined the flow field and the drag F experienced by the sphere. Working in spherical polar coordinates (r, θ, Φ) with $\theta=0$ axis being the direction of motion of the sphere; they have shown that in this case [7],

$$\psi = \frac{U}{2}\sin^2\theta\left[\frac{A_1}{r} + B_1 r + B_2\left(\lambda+\frac{1}{r}\right)e^{-\lambda r}\right],$$

(2.2)

$$v = \frac{U\sin\theta}{2r}\left[B_2\frac{(u+k)}{k}\lambda^2\left(\lambda+\frac{1}{r}\right)e^{-\lambda r} - \frac{B_1}{r}\right],$$

$$F = -Uk_a,$$

where

$$k_a = \frac{6\Pi a(2\mu+k)(\mu+k)(1+a\lambda)}{k+2\mu+2a\lambda\mu+2a\lambda k},$$

$$A_1 = \frac{3a^3}{4}\left(\frac{2}{3}+\lambda_2\right) + \frac{3a^2\lambda_2}{2\lambda^2}\left(\lambda+\frac{1}{a}\right),$$

$$B_1 = \frac{-3a}{4}(2+\lambda_2), \qquad B_2 = \frac{-3a\lambda_2 e^{\lambda a}}{2\lambda^2},$$

$$\lambda^2 = \frac{k(2\mu+k)}{\gamma(\mu+k)}, \qquad \lambda_2 = \frac{2k}{k+2\mu+2a\mu\lambda+2ak\lambda}.$$

Here

$$\mathbf{u} \equiv \mathbf{u}(r,\theta) = (U_r, U_\theta, 0), \qquad \mathbf{v} \equiv \mathbf{v}(r,\theta) = (0, 0, v)$$

and the stream function ψ is given by the usual relations

$$U_r = -\frac{1}{r^2\sin\theta}\frac{\partial\psi}{\partial\theta}, \qquad U_\theta = \frac{1}{r\sin\theta}\frac{\partial\psi}{\partial r}.$$

It should be noted that the drag depends on the material coefficients, the radius of the sphere and the translational velocity. In fact, for any axially symmetric body it has been shown [7] that the drag is given by the elegant expression

$$F = 4\Pi(2\mu+k)\lim_{r\to\infty}\frac{r\psi}{R^2}.$$

The micro-rotation does not explicitly play any role and, consequently, attention will be focussed on the velocity field only.

http://rcin.org.pl

3. Statement and solution of the problem

Consider two spheres of radii a and b moving with instantaneous velocities U_a and U_b, respectively, in an otherwise unbounded micropolar fluid. The main aim of this work is to determine the force experienced by each sphere.

In order to facilitate comparison with the classical result obtained by HAPPEL and BRENNER [8], we shall as far as is possible utilize their notations. We choose one axis of the reference system of coordinates (x, y, z) along the line joining the centres of the spheres which we assume to move in a plane. This is taken as the xz-plane (see Fig. 1).

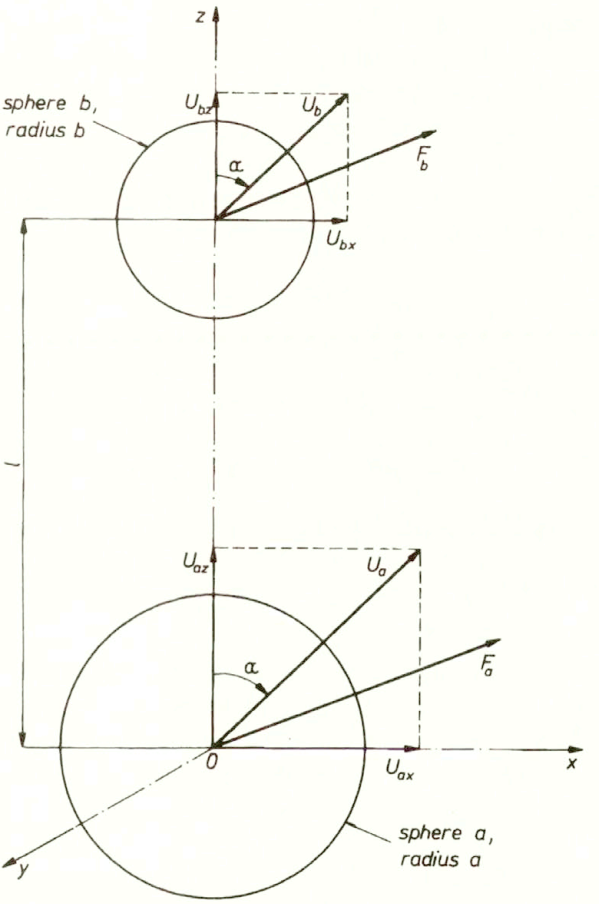

FIG. 1. Coordinate system for two-particle interactions.

We need to solve the system of Eqs. (2.1) subject to the conditions

$$\mathbf{u} = \mathbf{U}_a, \quad \mathbf{v} = 0 \quad \text{on} \quad S_a,$$
$$\mathbf{u} = \mathbf{U}_b, \quad \mathbf{v} = 0 \quad \text{on} \quad S_b, \tag{3.1}$$

http://rcin.org.pl

and $U, \mathbf{v} \to 0$ as $r \to \infty$, where S_a, S_b are the spheres of radii a and b, respectively. Since the system (2.1) and the boundary conditions (3.1) are linear, we may decompose the unknown field parameters as follows:

$$\mathbf{u} = \mathbf{u}^{(0)} + \mathbf{u}^{(1)} + \mathbf{u}^{(2)} + \dots,$$

$$\mathbf{v} = \mathbf{v}^{(0)} + \mathbf{v}^{(1)} + \mathbf{v}^{(2)} + \dots,$$

$$p = p^{(0)} + p^{(1)} + p^{(2)} + \dots,$$

where each $(\mathbf{u}^{(i)}, \mathbf{v}^{(i)}, p^{(i)})$ satisfies Eq. (2.1) and vanishes at inifinity. However, for the reason mentioned earlier, attention will be focussed on the velocity field only. We now apply the method of reflections which provides a systematic scheme of successive iterations, whereby the above boundary-value problem may be solved to any degree of approximation by considering boundary conditions associated with one particle at a time. This method was introduced by SMOLUCHOWSKI [9] and applied successfully and extensively by others [8, 10, 11, 12]. According to this method, details of which are given in HAPPEL and BRENNER [8]

$$\mathbf{u}^{(0)} = \mathbf{u}_a \quad \text{on } S_a, \tag{3.2}$$

$$\mathbf{u}^{(1)} = -\mathbf{u}^{(0)} + \mathbf{U}_b \quad \text{on } S_b, \tag{3.3}$$

$$\mathbf{u}^{(2)} = -\mathbf{u}^{(1)} \quad \text{on } S_a, \tag{3.4}$$

$$\mathbf{u}^{(3)} = -\mathbf{u}^{(2)} \quad \text{on } S_b \text{ etc.}, \tag{3.5}$$

where $\mathbf{u}^{(i)}$ is the i-th reflection. If $\mathbf{F}_a$ is the force exerted on S_a by the fluid, it has been shown [8] that

$$\mathbf{F}_a = \mathbf{F}_a^{(0)} + \mathbf{F}_a^{(2)} + \mathbf{F}_a^{(4)} + \dots, \tag{3.6}$$

where $\mathbf{F}_a^{(i)}$ is the force on S_a associated with the i-th reflection. A similar result with b replacing a, holds for $\mathbf{F}_b$, the drag force experienced by S_b.

The zeroth reflection is the solution given by Eqs. (2.2) for translation of a single sphere in an unbounded medium. If we take the velocity of this sphere of radius a to be $\mathbf{U}_a$ and write

$$\mathbf{U}_a = U_{ax}\hat{i} + U_{az}\hat{k}, \quad \mathbf{u}^{(0)} = u_x^{(0)}\hat{i} + u_z^{(0)}\hat{k},$$

then it can be shown from Eqs. (2.2) that

$$u_\alpha^{(0)} = U_{a\alpha}\left[-\frac{B_1}{2r} + \frac{A_1}{2r^3} - \frac{\alpha^2}{2}\left(\frac{B_1}{r^3} + \frac{3A_1}{r^5}\right) - B_2 e^{-\lambda r}\left\{\frac{\alpha^2}{2}\left(\frac{3}{r^5} + \frac{3\lambda}{r^4} + \frac{\lambda^2}{r^3}\right) - \frac{1}{2r}\left(\frac{1}{r^2} + \frac{\lambda}{r} + \lambda^2\right)\right\}\right], \tag{3.7}$$

where $\alpha = x$ or z, and

http://rcin.org.pl

$$\mathbf{F}_a^{(0)} = -k_a \mathbf{U}_a = -k_a (U_{ax}\hat{i} + U_{az}\hat{k}). \tag{3.8}$$

We now proceed to determine $\mathbf{F}_a^{(2)}$. From Eq. (3.7) $\mathbf{u}^{(0)}$ evaluated at the center of S_b ($x = 0$, $z = l$) is given by

$$\mathbf{u}^{(0)}|_{S_b} = \hat{i}\, d_1 U_{ax} + \hat{k}\, d_2 U_{az}, \tag{3.9}$$

where

$$d_1 = -\frac{B}{2l} + \frac{A_1}{2l^3} + \frac{B_2 e^{-\lambda l}}{2}\left(\frac{1}{l^3} + \frac{\lambda}{l^2} + \frac{\lambda^2}{l}\right),$$

$$d_2 = -\frac{B_1}{l} - \frac{A_1}{l^3} - B_2 e^{-\lambda l}\left(\frac{1}{l^3} + \frac{\lambda}{l^2}\right).$$

With the aid of Eq. (3.3), the force $\mathbf{F}_b^{(1)}$ exerted on S_b is

$$\mathbf{F}_b^{(1)} = -k_b \mathbf{u}_b^{(1)} = -k_b (\mathbf{U}_b - \mathbf{u}_b^{(0)}).$$

Using Eq. (3.9) this becomes

$$F_b^{(1)} = -\hat{i} k_b [U_{bx} - d_1 U_{ax}] - \hat{k} K_b [U_{bz} - d_1 U_{az}]. \tag{3.10}$$

The velocity field $\mathbf{u}^{(1)}$ generated by the force $\mathbf{F}_b^{(1)}$ acting at the center of S_b can now be calculated using the same technique as above. However, now the origin of the coordinate system will be located at the centre of S_b. Taking this into consideration one can easily show that

$$\mathbf{u}_a^{(1)} = \hat{i}\, d_1 [U_{bx} - d_1 U_{ax}] + \hat{k}\, d_2 [U_{bz} - d_2 U_{az}]. \tag{3.11}$$

Finally, with the aid of Eq. (3.4) we obtain

$$\mathbf{F}_a^{(2)} = -k_a \mathbf{u}_a^{(2)} = k_a \mathbf{u}_a^{(1)} = k_a [\hat{i}\, d_1 (U_{bx} - d_1 U_{ax}) + \hat{k}\, d_2 (U_{bz} - d_2 U_{az})]. \tag{3.12}$$

In a similar manner

$$\mathbf{F}_a^{(4)} = \hat{i} k_a d_1^3 [U_{bx} - d_1 U_{ax}] + \hat{k} K_a d_2^3 [U_{bz} - d_2 U_{az}]. \tag{3.13}$$

Hence, substitution of Eqs. (3.8), (3.12) and (3.13) into Eq. (3.6) gives the force exerted on S_a as

$$\mathbf{F}_a = -\hat{i} k_a [U_{ax} - (U_{bx} - d_1 U_{ax})(d_1 + d_1^3 + d_1^5 + \ldots)] - \hat{k} K_a [U_{az} - (U_{bz} - d_2 U_{az})(d_2 + d_2^3 + d_2^5 + \ldots)]. \tag{3.14}$$

Noting that the above include two geometric series and assuming that l is sufficiently large to ensure $|d_i| < 1$, we get on summation our main result,

$$-\frac{\mathbf{F}_a}{K_a} = \hat{i}\, \frac{U_{ax} - d_1 U_{bx}}{1 - d_1} + \hat{k}\, \frac{U_{az} - d_2 U_{bz}}{1 - d_2}. \tag{3.15}$$

To get the force $\mathbf{F}_b$ exerted on S_b we simply interchange a and b in Eq. (3.15).

http://rcin.org.pl

4. Special cases

a. *Identical spheres.* Here we take $a=b$ in Eq. (3.15) to get

$$-\frac{\mathbf{F}}{k_a}=\frac{U_x}{1+d_1}\hat{i}+\frac{U_z}{1+d_2}\hat{k}. \tag{4.1}$$

The force exerted on each particle is the same, their motions being parallel and velocities identical.

b. *Classical fluids.* In the case of Newtonian fluids ($\varkappa=0$) we get from Eq. (4.1), the well-known classical result [8]

$$-\frac{\mathbf{F}_c}{6\Pi\mu a}=\frac{U_x}{1+\frac{3}{4}\frac{a}{l}+\frac{1}{4}\left(\frac{a}{l}\right)^3}\hat{i}+\frac{U_z}{1+\frac{3}{2}\frac{a}{l}-\frac{1}{2}\left(\frac{a}{l}\right)^3}\hat{k}. \tag{4.2}$$

Let us examine case a). Assume that U is known and makes an angle α with the line of centres of the two particles. If $\mathbf{F}_u$ and $\mathbf{F}_D$ are drag components acting on each particle in the direction of U and perpendicular to it, respectively, then

$$F_U = F_Z\cos\alpha + F_x\sin\alpha, \tag{4.3}$$

where

$$F_x=\frac{-Uk_a\sin\alpha}{1+d_1}, \qquad F_z=\frac{-Uk_a\cos\alpha}{1+d_2}. \tag{4.4}$$

From Eqs. (4.3) and (4.4), we get

$$F_u=-k_aU\left[\frac{1}{1+d_1}-\left(\frac{1}{1+d_1}-\frac{1}{1+d_2}\right)\cos^2\alpha\right]. \tag{4.5}$$

In a similar manner it can be shown that

$$F_D=-k_aU\sin\alpha\cos\alpha\left[\frac{1}{1+d_2}-\frac{1}{1+d_1}\right].$$

The corresponding classical results utilizing (4.2) are respectively given by

$$F_{uc}=-6\Pi\mu aU\left[\frac{1}{1+\frac{3}{4}\frac{a}{l}}-\left(\frac{1}{1+\frac{3}{4}\frac{a}{l}}-\frac{1}{1+\frac{3}{2}\frac{a}{l}}\right)\cos^2\alpha\right],$$

$$F_{DC}=-6\Pi\mu aU\sin\alpha\cos\alpha\left[\frac{1}{1+\frac{3}{2}\frac{a}{l}}-\frac{1}{1+\frac{3}{4}\frac{a}{l}}\right]. \tag{4.6}$$

http://rcin.org.pl

Note that in both cases of Eqs. (4.5) and (4.6), if the spheres move along the line of centres or perpendicular to it, we obtain $F_{DC} = 0$. In the former case

$$\frac{F_U}{F_{UC}} = \frac{K_a}{6\Pi\mu a} \frac{1+\frac{3}{2}\frac{a}{l}}{1+d_2}, \tag{4.7}$$

while in the latter one

$$\frac{F_U}{F_{UC}} = \frac{K_a}{6\Pi\mu a} \frac{1+\frac{3}{4}\frac{a}{l}}{1+d_1}, \tag{4.8}$$

where d_1, d_2 are given in Eq. (3.9). Thus Eq. (4.7) gives a comparison between the drag in a micropolar fluid and that in a classical fluid when the two spheres of equal sizes are moving along the line of centres. In the case when the spheres are moving in the directions perpendicular to the line of centres, the result is given in Eq. (4.8). To get an insight into these results, we sketch in Figs. 2 and 3 the variation of the non-dimensional drag F_u/F_{uc} with λ for values of $\varkappa/\mu = 0$, 1, 5, 10, and with $a = 2$, $l = 100$.

We now make a few observations:

i. For the case $\varkappa/\mu = 0$ we expect to recover the classical drag and this is supported by the graphs.

ii. In both cases — the spheres moving in directions perpendicular to and along the line of centres, the drags do not differ appreciably and this is not surprising as l is large and a is small.

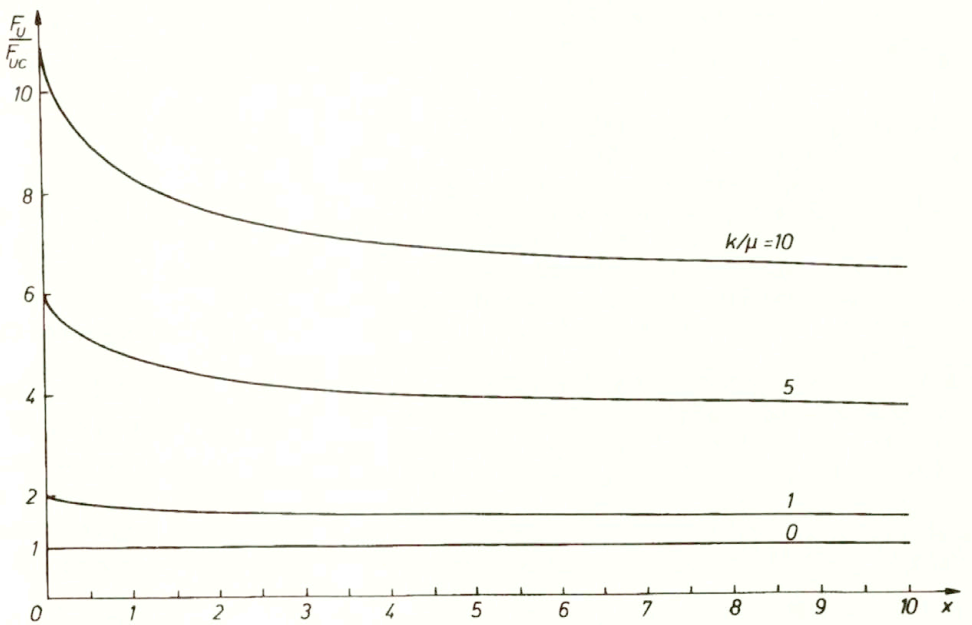

FIG. 2. Drag on spheres moving along line of centres.

http://rcin.org.pl

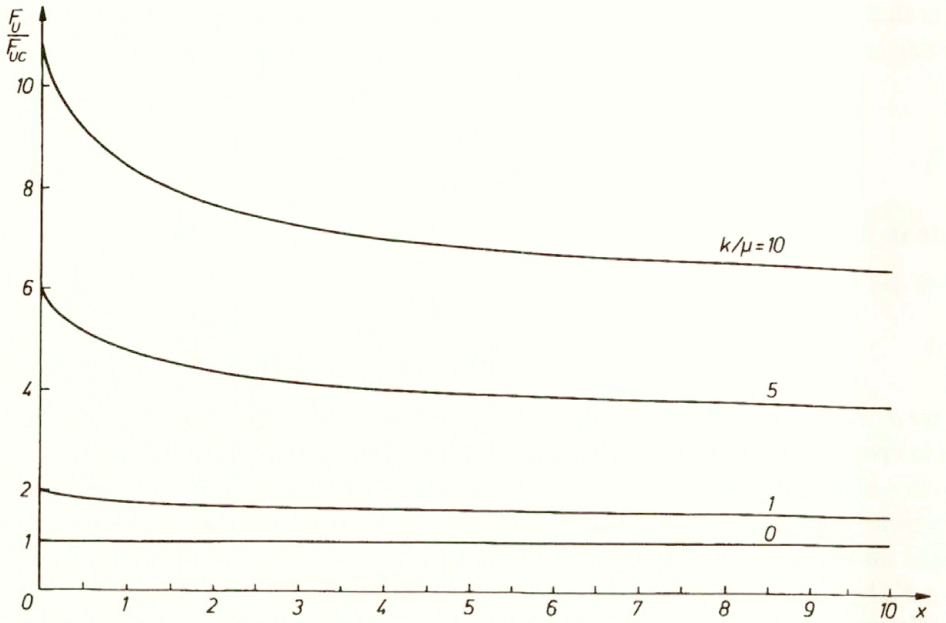

FIG. 3. Drag on spheres moving in directions perpendicular to the line of centes.

iii. $\varkappa$ is often referred to as the coupling constant and it is a measure of the strength of the "polarity" of the fluid. We see from the graphs that the drag in both cases increases with increasing $\varkappa$.

References

1. A.C. EERINGEN, J. Math. Mech., **16**, 1, 1966.
2. D.W. CONDIFF and J.S. DAHLER, Physics of Fluids, **7**, 842, 1964.
3. J. ARIMAN and A.S. CAKMAK, Physics of Fluids, **10**, 2497, 1967.
4. A.D. KIRWAN Jr. and N. NEWMAN, Int. J. Engng. Sci., 7, 833, 1969.
5. A.J. WILSON, Camb. Phil. Soc., **64**, 513, 1968.
6. H. RAMKISSOON, Int. J. Engng. Sci., **24**, 227, 1986.
7. H. RAMKISSOON and S.R. MAJUMDAR, Physics of Fluids, **19**, 16, 1976.
8. J. HAPPEL and H. BRENNER, *Low Reynolds number hydrodynamics*, Prentice–Hall, Englewood Cliffs, New Yersey 1965.
9. M. SMOLUCHOWSKI, Bull. Inter. Acad. Polonaise Sci. Lett., 1A, 28, 1911.
10. J.M. BURGERS, Proc. Koningl. Akad. Weten., Amsterdam, **44**, 1177, 1941.
11. J. HAPPEL and R. PFEFFER, A.I.Ch.E.Journal, **6**, 129, 1960.
12. J. HAPPEL and B.J. BYRNE, Ind. Eng. Chem., **49**, 1029, 1957.

DEPARTMENT OF MATHEMATICS
THE UNIVERSITY OF THE WEST INDIES, ST. AUGUSTINE, TRINIDAD, W.I.

Received July 19, 1993.

http://rcin.org.pl

Arch.Mech., 45, 4, pp. 493–498, Warszawa 1993

BRIEF NOTES

Spherical solutions to the Korteweg–de Vries equation

Y. CHEN (FAYETTEVILLE) and S-L. WEN (ATHENS)

SPHERICAL solutions for the Korteweg–de Vries equation are obtained within a reasonable approximation. They are shown to be representable as infinite sums of spherical solitons.

1. Introduction

THE SPHERICAL Korteweg–de Vries equation (referred to as KdV equation henceforth),

$$\frac{\partial u}{\partial \eta}+\frac{u}{\eta}+u\frac{\partial u}{\partial \xi}+\frac{\partial^3 u}{2\partial \xi^3}=0,$$

was first derived by MAXON and VIECELLI [1] from the study of three-dimensional, spherically symmetric acoustic wave propagating in a collisionless plasma of warm electrons and cold ions. In this equation, $u=u(\xi,\eta)$, $\eta=\varepsilon^{3/2}\omega_i t$, and $\xi=-\varepsilon^{1/2}(r/\lambda_D+\omega_i t)$, where ε is the expansion parameter, λ_D the Debye length, ω_i the ion plasma frequency, r the radial distance, and t the time. A numerical approximate solution to the equation,

$$U(\eta_0,\xi)=3\,\mathrm{sech}^2(\xi/\sqrt{2}),$$

was obtained by Maxon and Viecelli under an initial condition [1], and a solution of the form

$$U(\mu,\xi)=\delta^{-2}A(\mu)\,G\left(\frac{\xi-q(\mu)}{\delta\,\omega(\mu)}\right),$$

where $\mu=\ln(\eta_0/\eta)$ and $U=-\eta u$, was introduced by CUMBERBATCH [2].

In this paper we apply CHEN and WEN'S method [3] to the spherical KdV equation. A cnoidal wave solution is obtained and it is proved that the cnoidal wave solution can be expressed as a sum of infinite number of solitons by using Fourier series expansions and Poisson's summation formula. We have also established a criterion for the existence of a single soliton solution, it is $C>0$, where C is a constant, or $X<\dfrac{\xi}{\delta\sqrt{\eta}}$ (see Sec. 3).

http://rcin.org.pl

2. KdV equation

We start from the spherical KdV equation of the form [1]

$$\eta u_\eta + u + \eta u u_\xi + \frac{1}{2}\eta u_{\xi\xi\xi} = 0. \tag{2.1}$$

Motivated by the results obtained by CHEN and WEN in [3] and CUMBERBATCH [2], we introduce the following transformation.

Let $\tau = -\ln\eta$ and $U(\xi, \tau) = \eta u$, then

$$-U_\tau = -\eta_\tau u - \eta u_\eta \eta_\tau = \eta(u + \eta u_\eta),$$

$$UU_\xi = \eta(\eta u u_\xi),$$

and

$$\frac{1}{2}\eta U_{\xi\xi\xi} = \frac{1}{2}\eta(\eta u_{\xi\xi\xi}).$$

Therefore, Eq. (2.1) can be written as

$$-U_\tau + UU_\xi + (1/2)e^{-\tau}U_{\xi\xi\xi} = 0. \tag{2.2}$$

We are searching for real-valued solution of the form $G(X) = \delta^2 U(\xi, \tau)$ with $X = \dfrac{\xi + 2\delta^{-2}C}{\delta} e^{\tau/2}$, where C is a constant number, $\delta \ll 1$ is a small positive parameter introduced by CUMBERBATCH [2], and G is a C^3 function of its argument. Since

$$-U_\tau = -\delta^{-2}G'(X)\frac{\partial X}{\partial \tau} = -\delta^{-3}G'(X)\left\{\frac{1}{2}\xi e^{\tau/2} + \delta^{-2}Ce^{\tau/2}\right\},$$

$$UU_\xi = \delta^{-4}G(X)G'(X)\frac{\partial X}{\partial \xi} = \delta^{-5}G(X)G'(X)e^{\tau/2},$$

$$e^{-\tau}U_{\xi\xi\xi} = e^{-\tau}\delta^{-2}G'''(X)\left(\frac{\partial X}{\partial \xi}\right)^3 = e^{-\tau}\delta^{-2}G'''(X)(\delta^{-1}e^{\tau/2})^3 = \delta^{-5}G'''(X)e^{\tau/2}.$$

Then the substitution of the above results into Eq. (2.2) yields

$$-\frac{1}{2}\delta^{-3}G'(X)\xi e^{\tau/2} - \delta^{-5}CG'(X)e^{\tau/2} + \delta^{-5}e^{\tau/2}\left[G(X)G'(X) + \frac{1}{2}G'''(X)\right] = 0,$$

i.e.

$$-\frac{1}{2}\delta^2 G'(X)\xi e^{\tau/2} - \frac{1}{2}[G'''(X) + 2G(X)G'(X) - 2CG'(X)]e^{\tau/2} = 0. \tag{2.3}$$

The first term in Eq. (2.3) is of order δ^2 if $G'(X)$ and $(\xi/\sqrt{\eta}) = \xi e^{\tau/2}$ are bounded. One can argue that since in the original derivation $\xi = \varepsilon^{1/2}(r/\lambda_D - \omega_i t)$

http://rcin.org.pl

and $\eta=\varepsilon^{3/2}\omega_i t$, where ε is a small parameter, r the radial distance and t the time, it seems to be reasonable to assume $|\xi/\sqrt{\eta}|$ bounded. This is the case, in particular, when both r and t are large and of the same order, or in the domain where $|\xi/\sqrt{\eta}| \ll \delta^{-\alpha}$ with $\alpha<2$.

Therefore, a good approximation to Eq. (2.3) is:

$$G'''(X)+2G(X)G'(X)-2CG'(X)=0. \tag{2.4}$$

Integration of both sides of Eq. (2.4) leads to

$$G''(X)=-G^2(X)+2CG(X)+A/3.$$

Using the fact

$$G''(X)=\frac{1}{2}\frac{d[G'(X)]^2}{dG(X)},$$

we then have

$$\frac{1}{2}[G'(X)]^2=\frac{1}{3}[-G^3(X)+3CG^2(X)+AG(X)+B]=\frac{1}{3}F(G), \tag{2.6}$$

where A and B are two integration constants and F is the cubic function $-G^3+3CG^2+AG+B$.

3. Solitary wave solution

For a solitary wave solution we impose the boundary conditions $G, G', G'', G'''\to 0$ when $X\to\pm\infty$. These conditions imply $A=B=0$ in Eq. (2.6), and yield

$$\frac{1}{2}[G'(X)]^2=\frac{1}{3}G^2(X)[3C-G(X)]. \tag{3.1}$$

First, if $C<0$, i.e. $X>\dfrac{\xi}{\delta\sqrt{\eta}}$, we shall have the nontrivial solution

$$G(X)=3C\sec^2\left(\frac{\sqrt{-C}}{2}(X-X_0)\right),$$

where X_0 is an integration constant.

Second, if $C=0$, i.e. $X=\dfrac{\xi}{\delta\sqrt{\eta}}$, a solution to Eq. (3.1) is

$$G(X)=\frac{6}{(X-X_0)^2}.$$

http://rcin.org.pl

Because the solutions $G(X)$ in these two cases are unbounded, we are not interested in it.

If $C>0$, i.e. $X < \dfrac{\xi}{\delta\sqrt{\eta}}$, the nontrivial solution to Eq. (3.1) becomes

$$G(X) = 3C\,\mathrm{sech}^2\left[\frac{\sqrt{C}}{2}(X-X_0)\right], \tag{3.2}$$

where X_0 is an integration constant. We note that $C>0$, i.e. $X < \dfrac{\xi}{\delta\sqrt{\eta}}$ gives a condition under which a nontrivial solitary wave solution exists. In particular, if we choose $C=1$ and $X_0=0$, then from Eq. (3.2) we have

$$G(X) = 3\,\mathrm{sech}^2\left[\frac{\xi+2\delta^{-2}}{2\delta}\,e^{\tau/2}\right]. \tag{3.3}$$

4. Cnoidal wave solution

For the existence of a spherical solution, the cubic function $F(G)$ in the right-hand side of Eq. (2.6) plays an important role. Applying a similar argument as that given in Ref. [4], we can show that a cnoidal wave solution exists only if $F(G)$ has three distinct real simple zeros G_1, G_2, and G_3 such that $G_1>G_2>G_3$ and $G_2 \leqq G(X) \leqq G_1$ [4]. In this case, we have

$$\sqrt{\frac{2}{3}}\,(X_1-X) = \int_G^{G_1} \frac{dG}{\sqrt{F(G)}} = \int_G^{G_1} \frac{dG}{\sqrt{(G_1-G)(G-G_2)(G-G_3)}}, \tag{4.1}$$

where X_1 is a value at which $G(X_1) = G_1$, and the period $2T$ in X is

$$2T = \sqrt{6}\int_{G_1}^{G_2} \frac{dG}{\sqrt{(G_1-G)(G-G_2)(G-G_3)}}. \tag{4.2}$$

Equation (4.1) can be rewritten as [2]

$$\sqrt{\frac{2}{3}}\,(X_1-X) = \frac{2}{\sqrt{G_1-G_3}}\,\sin^{-1}(\sin\phi, K) = \frac{2}{\sqrt{G_1-G_3}}\,F(\phi, k), \tag{4.3}$$

where

$$\phi = \sin^{-1}\sqrt{\frac{G_1-G}{G_1-G_2}}, \qquad k^2 = \frac{G_1-G_2}{G_1-G_3},$$

and $F(\phi,k) = sn^{-1}(\sin\phi,k)$ is the normal elliptic integral of the first kind with modulus k. If we define $\upsilon = F(\phi,k)$, then

http://rcin.org.pl

$$\upsilon = \frac{1}{\sqrt{6}} \sqrt{G_1 - G_3}\,(X_1 - X),$$

and the cnoidal wave solution is obtained

$$(4.4)\quad G(X) = G_1 - (G_1 - G_2)\, sn^2(\upsilon,k) = G_2 + (G_1 - G_2)\, cn^2(\upsilon,k)$$

$$= G_3 + (G_1 - G_3)\, dn^2(\upsilon,k) = G_3 + (G_1 - G_3) dn^2\left(\frac{1}{\sqrt{6}} \sqrt{G_1 - G_3}\,(X - X_1), k\right),$$

where $sn(\upsilon,k) = \sin\phi$, $cn(\upsilon,k) = \cos\phi$ and $dn(\upsilon,k) = \sqrt{1 - k^2 \sin^2\phi}$.

It should be noted here that there is no restriction on C which can be positive, zero or negative as long as $C = \frac{1}{3}(G_1 + G_2 + G_3)$. In particular, if $X_1 = 0$, then

$$G(X) = G_2 + (G_1 - G_2)\, cn^2\left(\frac{1}{\sqrt{6}} \sqrt{G_1 - G_3}\, \frac{\xi + 2\delta^{-2} C}{\delta}\, e^{\tau/2}, k\right).$$

Using the Fourier series expansion of $dn^2(\upsilon,k)$ [6] and the Poisson summation formula [7], we obtain

$$(4.5)\qquad dn^2(\upsilon,k) = \frac{E}{K} - \frac{\pi}{2KK'} + \frac{\pi^2}{4K'^2} \sum_{m=-\infty}^{\infty} \operatorname{sech}^2\left[\frac{\pi}{2K'}(\upsilon - 2mK)\right],$$

where $K = \int_0^{\pi/2} \frac{d\theta}{\sqrt{1 - k^2 \sin^2\theta}}$ is the complete elliptic integral of the first kind with modulus k; $K' = \int_0^{\pi/2} \frac{d\theta}{\sqrt{1 - k'^2 \sin^2\theta}}$ is the complete elliptic integral of the first kind with modulus $k' = \sqrt{1 - k^2}$; $E = \int_0^{\pi/2} \sqrt{1 - k^2 \sin^2\theta}\, d\theta$ is the complete elliptic integral of the second kind with modulus k. Therefore, the cnoidal wave solution $G(X)$ in Eq. (4.4) can be written as

$$(4.6)\qquad G(X) = P + Q \sum_{m=-\infty}^{\infty} \operatorname{sech}^2 R(X - X_1 + 2mT),$$

where

$$P = G_3 + (G_1 - G_3)\left[\frac{E}{K} - \frac{\pi}{2KK'}\right],$$

$$Q = (G_1 - G_3)\, \frac{\pi^2}{4K'^2},$$

http://rcin.org.pl

$$2T = \frac{2\sqrt{6}}{\sqrt{G_1 - G_3}} F\left(\frac{\pi}{2}, k\right) = \frac{2\sqrt{6}\,K}{\sqrt{G_1 - G_3}},$$

$$R = \frac{\pi K}{2K'T},$$

where K, K' and E are defined following Eq. (4.5). In Eq. (4.6), G is clearly a periodic function of X with period $2T$. Each term in the inifinite series is a soliton. This gives a representation of a periodic function by an infinite number of solitons. It should be mentioned that the representation is valid within the order of δ^2.

References

1. S. MAXON and J. VIECELLI, *Spherical solitons*, Phys. Rev. Let., **32**, 1, 4–6, 1974.
2. E. CUMBERBATCH, *Spike solution for radially symmetric solitary waves*, Phys. Fluids, **21**, 374–376, 1978.
3. YUNKAI CHEN and SHIH–LIANG WEN, *Cylindrical wave solutions to the Korteweg–de Vries equation*, Arch. Mech., **44**, 4, 481–485, 1992.
4. YUNKAI CHEN and SHIH–LIANG WEN, *Travelling wave solutions to the two-dimensional Korteweg–de Vries equations*, J. Math. Anal. and Appl., **127**, 1, 226–236, October 1987.
5. P.F. BYRD and M.D. FRIEDMAN, *Handbook of elliptic integrals for engineers and scientists*, 2nd ed., Springer–Verlag, New York–Berlin, 1971.
6. F. OBERHETTINGER, *Fourier expansions*, Academic Press, New York–London 1973.
7. R. COURANT and D. HILBERT, *Methods of mathematical physics*, vol. 1, Interscience Publ., 1953.

DEPARTMENT OF MATHEMATICS AND COMPUTER SCIENCE
FAYETTEVILLE STATE UNIVERSITY, FAYETTEVILLE
and
DEPARTMENT OF MATHEMATICS
OHIO UNIVERSITY, ATHENS, USA.

Received February 22, 1993.

http://rcin.org.pl

Limit analysis of plates
by A. SAWCZUK and J. SOKÓŁ-SUPEL

Limit analysis, furnishing collapse loads of structures and the corresponding mechanisms of the plastic flow at collapse, represents a simple and effective tool for the security assesment, particularly for structures vulnerable to exceptional ultimate loads. It answers to one of principal limit state requirements in the European Design Codes and, therefore, is of interest both for design practice and, in educational aspects, for comprehension of the structural response.

The book is aimed at graduate and post-graduate students in structural mechanics and at structural engineers-designers. It presents basic features, methods and results of the limit analysis theory of plates. Methods for exact analysis are presented and aproximate techniques like the yield-line theory are discussed. Solutions for a broad class of plates obeying various plasticity criteria (metal and fiber-reinforced plates, both isotropic and orthotropic) are given.

The fundamental principles of perfect plasticity are briefly shown and assumptions and theorems of limit analysis are given in Chapter 2. The plate equations are analyzed in Chapter 3. Chapter 4 is concerned with circular plates under rotationally symmetric loading when ordinary differential equations govern the plastic behaviour. Analytical and numerical solutions are given. Bounding techniques that furnish estimates to the collapse load intensity are explained in Chapter 5, whereas in the next chapter orthotropic and nonhomogeneous plates are briefly considered. Chapter 8 is devoted to bending of plates of arbitrary shape. Special attention is given to plates obeying a square yield criterion in the plane of principal moments. A number of new complete solutions is presented allowing to assess the accuracy of the results furnished by the yield-line theory, which is presented in Chapter 7 and accompanied by a set of tables with specific solutions.

The text consists of about 260 pages, including 86 figures, 21 tables and 79 cross-references. In the appendix 69 complete solutions for particular cases of geometry and loading of plates are given.

The book has appeare 1992. Possible orders should be addressed to the **Editorial Office of the IFTR, Świętokrzyska 21, 00-049 Warszawa, Poland.**

http://rcin.org.pl

30th POLISH SOLID MECHANICS CONFERENCE

ogranized by

CENTER OF MECHANICS
of the INSTITUTE OF FUNDAMENTAL TECHNOLOGICAL REASEARCH
and
COMMITTEE OF MECHANICS
of the POLISH ACADEMY OF SCIENCES

Zakopane, September 5 – 9, 1994

The 30th Polish Solid Mechanics Conference will be held in Zakopane, a renowned resort at the foot of the Tatra Mountains.

Following a long tradition going back to the 1st Polish Solid Mechanics Conference in 1953, the objective of the 30th Conference is to bring together researchers engaged in all major areas of contemporary mechanics of solids and structures.

The program of the conference will include a number of general (invited) lectures and contributed papers. The contributed papers will be presented either in oral form or at poster sessions. The language of the conference will be English.

Social events and tours are planned.

Further details regarding the submission of abstracts will be announced in the first circular.

Scientific Committee

Prof. R. Bogacz
Prof. A. M. Brandt
Prof. H. Frąckiewicz
Prof. W. Gutkowski
Prof. M. Kleiber
Prof. Z. Mróz
Prof. W. K. Nowacki – chairman
Prof. Z. Peradzyński
Prof. B. Perzyna
Prof. B. Raniecki
Prof. D. Rogula
Prof. J. Sławianowski
Prof. K. Sobczyk
Prof. M. Sokołowski
Prof. W. Szczepiński
Prof. W. Szemplińska-Stupnicka
Prof. H. Zorski
Prof. M. Życzkowski

Organizing Committee

Prof. W. K. Nowacki – chairman
Dr. M. Basista
Dr. K. Doliński

Address for correspondence

Center of Mechanics – IPPT PAN

Świętokrzyska 21
00-049 Warszawa, Poland
phone: 26-88-02, fax: 269815,
telex: 825638 ippt pl
e - mail: zakopane@lksu.ippt.gov.pl

http://rcin.org.pl

First International Symposium
on
Thermal Stresses and Related Topics

THERMAL STRESSES '95

will be held at
Shizuoka University, Hamamatsu, Japan
June 5 – 7, 1995

The Symposium will be comprised of invited lectures and of the presentation and discussion of contributed papers. Ladies Program will be arranged. A post-symposium tour of Kyoto and Nara will be organized. Group flights from the United States to Japan will be planned.

Write for the First Announcement brochure to:

Richard B. Hetnarski, Chairman
International Organizing Committe
James E. Gleason Professor
of Mechanical Engineering
Rochester Institute of Technology
Rochester, NY 14623, U.S.A.

Naotake Noda, Chairman
International Organizing Committee
Dept. of Mechanical Engineering
Shizuoka University
5-1, Johoku 3 chome
Hamamatsu, 432, JAPAN

http://rcin.org.pl

11th Aachen Colloquium on Fluid Power Technology
"call for papers"

The Aachen Colloquium on Fluid Power Technology (AFK) has been established as one of the eminent international conferences for current topics from the fields of hydraulics and pneumatics during the previous two decades. The colloquium has been met with an extraordinarily good response from producers and users of fluid power technology, as well as other interested parties. Besides reports and discussions, during the three-day colloquium includes an exhibition and poster-session where exhibits from the fields of equipment, measuring systems and software are presented. At the same time, those guests who are interested in the Departament of Fluid Power Transmission and Control of the University of Technology Aachen, can take the opportunity to view the laboratories and to inform themselves on current research projects and new developments.

The main topics of the 11th AFK, which lasts from **March 8th, 1994, until March 10th, 1994,** will deal with the field of hydraulics during the first two days and with pneumatics at the final day. The main topics of the 11th AFK are as follows:

1. Improvement of the Competitivness of Fluid Power
2. Energy Saving Measures
3. New Concepts in Mobile Hydraulics
4. Hydraulics in the Plastics Industry and Metal Forming
5. Economical and Environmental Use of Pneumatics
6. New Developments of Pneumatic Components and Systems

On each of the main conference topics several lectures, which last for maximally 15 minutes, will be held.

Institut für Hydraulische und Pneumatische Antriebe und Steuerungen der RWTH Aachen, Steinbachstrasse, 53, W-5100 Aachen, Germany

http://rcin.org.pl

Guidelines for Authos

The periodical Archives of Mechanics (Archiwum Mechaniki Stosowanej) presents original papers which should not be published elsewhere.

As a rule, the volume of the paper should not exceed 40 000 typographic signs, that is about 20 type-written pages, format: 210 × 297 mm, leaded. The papers should be submitted in two copies and follow the norms outlined by the Editorial Office. The following directions are particularly important:

1. The paper submitted for publication should be written in English.

2. The title of the paper should be as short as possible. The text should be preceded by a brief introduction; it is also desirable that a list of notations used in the paper be given.

3. Short paperts should be divided into sections and subsections, long papers into sections, subsections and points. Each section, subsection or point must bear a title.

4. The formula number consists of two figures: the first represents the section number and the other the formula number under that section. Thus the division into subsections does not influence the numbering of formulae. Only such formulae should be numbered to which the author refers through out the paper. This also applies to the resulting formulae. The formula number should be written on the left-hand side of the formula (in brackets). If the author refers to formula 3 of the set (2.1), a subscript should be added to denote the formula referred to, viz. $(2.1)_3$.

5. All the notations should be written very distinctly. Special care must be taken to distinguish between small and capital letters as precisely as possible. Semi-bold type must be underlined in black pencil. Explanations should be given on the margin of the manuscript in case of special type face.

6. Vectors are to be denoted by semi-bold type, transforms of the corresponding functions by tilded symbols. Trigonometric functions are denoted by sin, cos, tg and ctg, inverse functions — by arcsin, arccos, arcctg and arctg; hyperbolic functions are denoted by sh, ch, th and cth, inverse functions — by Arsh, Arch, Arth and Arcth.

7. The figures in square brackets denote reference titles. Items appearing in the reference list shold include the initials of the author and his surname, also the full title of the paper (in the language of the original paper); moreover:

a) in the case of a book the publisher's name, the place and year of publicatoin shold be given, e.g.,
5. S. Ziemba, *Vibration analysis*, PWN, Warszawa 1980.

b) in the case of a periodical, the full title of the periodical, consecutive volume number, current issue marked in semi-bold type so as to distinguish if from the current issue number, e.g.,
6. M. Sokołowski, *A thermoelastic problem for a strip with discontinuous boundary conditions*, Arch. Mech., **13**, 3, 337–354, 1961.

8. The author should enclose a summary of the paper. The volume of the summary should not exceed 100 words.

Upon receipt of the paper, the Editorial Office forwards it to the reviewer. His opinion is the basis for the Editorial Committee to determine whether the paper is acceptable for publication or not.

Once the paper is printed, 25 copies of reprints free of charge are sent to the author.

Editorial Committee
Archives of Mechanics
(Archiwum Mechaniki Stosowanej)

http://rcin.org.pl